Università degli **S**tudi di **N**apoli **F**ederico II

Polytechnic and Basic Sciences School

Department of Earth, Environmental and Resources Science

Doctorate School of Earth, Environmental and Resources Science

Ph.D. Thesis

XXXV cycle

Plinian eruptions and their impact in urban contexts: dynamics and effects on the territory of the pyroclastic currents of the AD 79 Vesuvian eruption

Ph.D candidate: Dr. Ileana Santangelo

Matr. DR993787

Tutor: Prof. Claudio Scarpati

Co-Tutor: Prof. Lorenzo Fedele

Ph.D. coordinator: Prof. Rosa di Maio

2019/2022

TABLE OF CONTENTS

ABSTRACT

Plinian eruptions are amongst the most powerful and destructive volcanic events on Earth. These explosive eruptions generally form a sustained eruptive column which, as a result of abrupt changes in eruptive conditions can collapse producing one of the most hazardous volcanic events: pyroclastic density currents (PDCs), able to reach great distances far from the vent and entirely destroy populated areas. In this scenario, the well-documented AD 79 eruption was selected as representative case study for the current PhD research. It killed thousands of people, devastating the surrounding countryside and destroying many towns, most notably Pompeii and Herculaneum, as well as country villas, suburbs and dwellings over a radius of more than 10-18 km from the volcano. The AD 79 eruption can be said to have given birth to the science of volcanology and to have significantly advanced the science of archaeology. It was characterized by two main phases which can be summarized as follows: a Plinian sustained eruptive column emplacing a southward-distributed widespread tephra fallout concurrent with successive partial column collapses and a second phase dominated by PDCs representing the focus of the present research. Despite the large number of studies concerning the AD 79 eruption, multiple interpretations were reported in literature for the PDC deposits from this event. Therefore, with the aim of resolving the most debated topics and tentatively provide an unified view regarding the AD 79 PDC deposits and the parental PDCs emplacing them, with the current research a detailed field work was perfomed on numerous and well-exposed outcrops around Vesuvius, in the Campanian Plain and on the Lattari Mts, including several archaeological sites. 27 individual PDC stratigraphic units from the opening to the intra- and post-Plinian phases of the eruption have been documented for the first time with this research, emplaced by 16 PDCs. In order to document lateral and vertical variations in grain size, types and amount of components of the AD 79 PDC deposits, all recognized PDC stratigraphic units were carefully sampled (417 samples) with the recognition of 14 different lithofacies. A new reconstruction of the behaviour of the AD 79 PDCs has been established through the merging of all the available data. The very initial phase of the eruption is marked by the formation of a small-volume, slow-moving, ground-hugging ash flow with a limited areal distribution. For the first time, nine partial Plinian column collapses are documented representing a purely magmatic phase of the eruption. Changes in the eruptive dynamics led to the formation of post-Plinian PDCs representing the most powerful and turbulent AD 79 PDCs, even capable to overcome the barrier ridge represented by the Lattari Mountains. In addition, juvenile components (consisting of pumice clasts, both white and grey) were sampled at various stratigraphic heights and 97 of them were selected for major oxides and trace element concentrations analyses adding new information on the geochemical composition of the AD 79 PDC deposits. Finally, the detailed and well constrained stratigraphy of the AD 79

PDC deposits has been a useful tool to define the exact timing of the destruction during the intra-Plinian and post-Plinian phases of the eruption with significative implications on the risk assessment related to high-energetic volcanic events.

INTRODUCTION

Pyroclastic density currents (PDCs) represent the most hazardous events of explosive volcanism (e.g., Cas and Wright, 1987; Carey, 1991; Branney and Kokelaar, 2002) and their deposits are very abundant in the geological record. The devastating impact of the PDCs has been demonstrated by historic eruptions especially in densely populated area surrounding active volcanoes (Todesco et al., 2002; Cioni et al., 2004; Baxter et al., 2005; Gurioli et al., 2005). The AD 79 eruption represents the most famous and one of the four Plinian events occurred at Somma-Vesuvius since 22 ka BP (e.g., Andronico et al., 1995; Santacroce et al. 2008). It devasted a significant part of the perivolcanic area within 10 km from the vent (e.g., Kent et al., 1981; Sigurdsson et al, 1985; Gurioli et al. 2005a; Cioni et al., 2004; Caricchi et al., 2014), heavily damaging the Roman towns of Pompei, Herculaneum, Oplonti and Stabiae. The AD 79 eruption has been the focus of several volcanological, petrological and geochemical studies, (e.g., Lirer et al., 1973; Sigurdsson et al., 1985; Carey and Sigurdsson 1987; Cioni et al., 1990, 1992, 1995, 1996, 2000; Luongo et al., 2003a,b; Scarpati et al., 2020; Doronzo et al., 2022), representing a starting point of the modern volcanology, since the description made by Pliny the Younger (which gave the name to this type of activity) in his letters to Tacitus (e.g., Giacomelli et al., 2021). The eruption started with a weak phreatomagmatic explosion which covered the proximal area of the volcano with an ash deposit. The immediately following high Plinian column (from 14 to 32 km, Carey and Sigurdsson, 1987) emplaced a thick layer of pumice lapilli (from white to grey, indicating a change in density and chemical composition of the tapped magma, e.g., Civetta et al., 1991; Cioni et al., 1995), covering a wide area south of the volcano (e.g., Lirer et al., 1973; Sigurdsson et al., 1985). Immediately before, during and after the fallout phase of the grey pumice lapilli, several PDCs developed and spread radially around the volcano, destroying every settlement within a radius of 10-15 km (e.g., Giacomelli et al., 2003). Some structural variations in the volcanic building, such as calderic collapse and vent widening, were responsible for an increase in the mass eruptive rate during this phase, and were followed by a final phreatomagmatic phase, leading to the emplacement of ash deposits rich in accretionary lapilli. This latter phase began in the early hours of 25 August (or October). The eruption lasted at least 19 h, from 1:00 p.m. of 24 August (or October) to 8:00 a.m. of 25 August (or October).

Despite the large number of studies concerning the AD 79 eruption, several issues are still largely debated, and multiple interpretations were reported in literature for the PDC deposits from the AD 79 eruption. The basal ash layer, representing the very initial phase of the eruption, has been ascribed to a fallout (e.g., Sigurdsson et al., 1985 and Barberi et al., 1989) or a PDC origin (e.g., Lirer et al., 1993; 1997), or even to both (e.g., Cioni et al., 1992; Doronzo et al., 2022). A similar controversy exists about whether the post-Plinian accretionary lapilli-bearing deposits of the final stage of the eruption were emplaced by fallout or PDCs (e.g., Sigurdsson et al., 1985 Cioni et al., 1992; 2020; Gurioli et al., 2007; Luongo et al., 2003a; Scarpati et al., 2020 and Doronzo et al., 2022). Further, there is significant disagreement on the moment at which the transition from magmatic to phreatomagmatic activity occurred, as well as the role of magma-water interaction during the course of the eruption (e.g., Sheridan et al., 1981; Arnò et al., 1987; Barberi et al., 1989; Sigurdsson et al., 1985; Cioni et al., 1992; Lirer et al., 1993; 1997; Luongo et al., 2003a; Scarpati et al., 2020; Doronzo et al., 2022). A general agreement instead exists regarding the caldera collapse during the AD 79 eruption, but the exact timing at which the magma chamber destabilization occurred is not well-constrained on stratigraphic grounds, being inferred from different evidence by several authors (e.g., a strong enrichment in deep lithic components in some PDC units for Cioni et al., 1992; 2004). Another point of debate is the use of various and sometimes disputed correlation methods for defining the stratigraphic position of the AD 79 PDC deposits within the whole pyroclastic sequence, leading to a partly contradictory picture in which the actual number and the areal distribution of each PDC layers still remain not well defined. Finally, although many petrochemical studies on the juvenile component of the AD 79 eruption have been presented in literature (Civetta et al., 1991; Cioni et al., 1992, 1995; Mues-Schumacher et al., 1994; Redi et al., 2016; Melluso et al., 2022), petrological features of the tapped magma during the partial and total column collapse phases have been only party addressed, assuming stratigraphic schemes that appears not always well-constrained as mentioned above.

The current research focuses on the PDC deposits associated with the partial and total eruptive column collapse (i.e. intra-Plinian and post-Plinian phases) and a close-up view is provided on the very initial basal ash layer, with the aim of resolving the most debated aforementioned topics and provide an unified view of the AD 79 PDC deposits and the parental PDCs that emplaced them. In order to reconstruct the entire depositional architecture of these deposits, a detailed field analysis was perfomed on numerous outcrops around Vesuvius, in the Campanian Plain and on the Lattari Mts. Differently from the literature, where a facies analysis is reported on some specific stratigraphic units only or on the entire AD 79 PD sequence in few locations, the facies analysis approach was extended here for the first time to the whole AD 79 PDC sequence across the entire studied area. Furthermore, the stratigraphic height of the AD 79 PDC deposits was ascertained based on the recognition of distinctive, regionally-traceable interstratified fallout marker layers, applying the correlation criteria proposed by Fierstein and Hildreth (1992). In addition, with the aim to quantitatively characterize the PDC deposits and the lithofacies recognized, a total of 417 samples were collected, 344 of which were chosen for granulometric analyses. For 78 samples, characterized by an exceeding finer fraction (> 15 wt.%), particle size distribution down to 9φ (2μm) was determined by means of gravity sedimentation in water. Component analysis (juvenile clasts, lithic clasts and crystals) was performed for 264 samples down to 2φ. 104 samples with a fine fraction > 40 wt.% were examined down to 4φ. Furthermore, 4 samples were selected for density measurements and 11 for estimating the crystal enrichment factor (Walker, 1972). In addition, juvenile components (consisting of pumice clasts, both white and grey) were sampled at various stratigraphic heights and 97 of them were analysed for major oxides and trace element concentrations. The results of the analyses (sedimentological, component, petrochemical) were used to correlate the PDC deposits in the upwind sector (NW to NE of the Vesuvius vent) where the fallout deposit completely lacks. Finally, thanks to a collaboration between the Archaeological Park of Pompei and the University of Napoli Federico II, a systematic survey of numerous well-exposed outcrops along all the recent excavations, allowed to study in detail the facies variations of the PDC stratigraphic units even at small scale, investigating how their distribution is locally influenced by urban structures, and documenting their impact in an urban environment.

CHAPTER 1

1. The partial and total column collapse phases of the AD 79 Plinian Vesuvius eruption: a critical review of the previous studies

1.1 Introduction: Plinian eruptions and the case study of the AD 79 Vesuvius eruption

Plinian eruptions are powerful explosive volcanic events that impact large areas, with cubic kilometres of magma emplaced as pyroclastic material accumulated in thick blankets around the volcanic vents (e.g. Fisher and Schmincke, 1984; Sparks et al., 1997; Luongo et al., 2003a). The violence of the emplacement mechanism (i.e., fallout and/or pyroclastic density currents) and the sudden burial of the landscape make these types of eruptions extremely dangerous (Scarpati et al., 2016). These eruptions are named after the Roman statesman Pliny the Younger, who witnessed the eruption of Italy's Mount Vesuvius in AD 79, which destroyed the towns of Pompei and Herculaneum, killing thousands of people (Giacomelli et al., 2003). A Plinian eruption can last for hours or days, sustaining a giant eruptive column, but pyroclastic density currents (PDCs), often forming by partial or total column collapse, are also common. Although most of the volume of magma emitted is usually associated with the sustained column phase, the generation and propagation of PDCs causes the greatest damage to the territory and the resident population, representing the most hazardous events associated to explosive volcanism (Cas and Wright, 1987; Carey, 1991; Branney and Kokelaar, 2002; Sulpizio and Dellino, 2008). Their devastating potential has been demonstrated by historical eruptions in densely populated areas surrounding active volcanoes (Todesco et al., 2002; Cioni et al., 2004; Baxter et al., 2005; Gurioli et al., 2005). Aiming to fully understand these phenomena, an accurate reconstruction of the physical behaviour and the historical record of a volcano is a critical starting point for the assessment of volcanic hazard.

In this scenario, an excellent case is represented by the worldwide-known AD 79 Plinian Vesuvius eruption, which buried the Roman towns around the volcano under several meters of pyroclastic materials with catastrophic effects over a radius of more than 10-18 km from the vent. The huge amount of researches regarding the AD 79 Vesuvius eruption has made it possible to largely define the stratigraphy (e.g. Lirer et al., 1973, 1993; Sigurdsson et al., 1982, 1985; Arnò et al., 1987; Barberi et al., 1989; Cioni et al., 1992, 1995, 2020; Gurioli et al., 1999, 2002, 2005, 2007, 2010; Luongo et al., 2003a; Scandone et al., 2019; Scarpati et al., 2020; Doronzo et al., 2022), the distribution of the volcanic products (e.g. Cioni et al., 2020), the petrochemistry of the juvenile clasts (e.g. Di Girolamo, 1963, 1968; Barberi et al., 1981; Santacroce, 1987; Civetta et al., 1991; Cioni et al., 1992, 1995; Civetta and Santacroce, 1992; Lirer et al., 1993; Mues-Schumacher, 1994; Ayuso et al., 1998; Balcone-Boissard et al., 2008, 2011; Shea et al., 2014; Melluso et al., 2022), the eruptive dynamics, the emplacement mechanisms and the impact on the urban structures (e.g. Luongo et al., 2003a; 2003b; Gurioli et al., 2002; 2005; 2007; Mastrolorenzo et al., 2010; Dellino et al., 2021).

With my dissertation, I will investigate the pyroclastic density currents deposits associated with the partial and total column collapse during the AD 79 eruption. In this Chapter, I report the outcomes of the main volcanological and geochemical research studies about the AD 79 eruption, aimed at critically reviewing the literature concerning the PDC phases of eruption and discussing the strengths and the weaknesses of the proposed models. Chapter 1 consists of six paragraphs that, starting from a brief introduction about the volcanic and structural history of the Somma Vesuvius, provide a review of the different approaches used in literature to study the stratigraphic sequence of the AD 79 PDC deposits and their impact. This will shed light on some aspects of the eruption that are still matter of debate, such as, 1) the real number and the areal distribution of the PDCs generated during the partial and total column collapse phases, 2) the timing and the role of phreatomagmatism during the course of the eruption, and 3) the development of a "caldera-forming" phase with the possibility that this event affected the subsequent dynamic of the eruption and the nature and the behaviour of the generating PDCs.

1.2 Geological setting of Somma-Vesuvius

The Somma-Vesuvius (Fig. 1.1a), together with the Campi Flegrei Volcanic District are part of a series of active volcanic complexes developed within the extensional graben of the Campanian plain, one of the most important peri-Tyrrhenian structures of the Southern Appenines chain (e.g. Rosi and Sbrana, 1987; Sbrana et al., 2018; Peccerillo, 2017), which formed from Miocene to Pleistocene, following the opening of the Tyrrhenian basin (Peccerillo, 2017). The Somma-Vesuvius volcanic complex is made of the remnant of an older stratovolcano (Mt. Somma) cut by an eccentric, polyphasic caldera and by a stratocone (Vesuvius) grown inside the caldera after the AD 79 eruption (Cioni et al., 1999) (Fig. 1.1b).

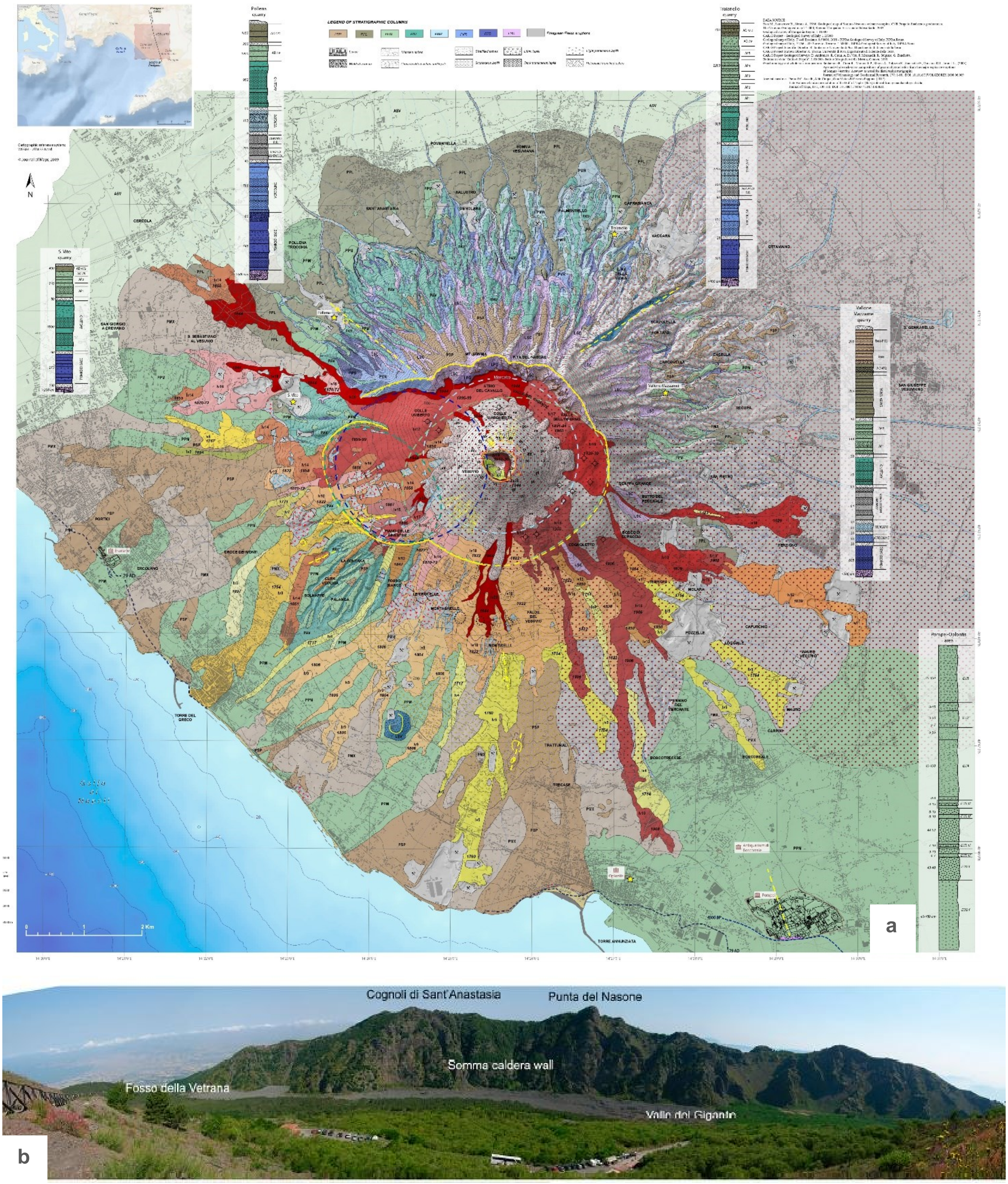

Fig. 1.1: a) Volcanological map of Somma Vesuvius, scale 1:20 000, with type stratigraphic sections (Sbrana et al., 2020). b) View from the Vesuvius cone with the inner caldera wall of Mt Somma in the background (from Sbrana et al., 2020).

The construction of the stratovolcano started after the Phlegrean eruption of the Campanian Ignimbrite eruption (39 ka; De Vivo et al., 2001; Fedele et al., 2008, 2016), as evidenced by the stratigraphy of the Trecase 1 geothermal well (Brocchini et al., 2001). The stratovolcano grew up to around 2000 m in height over a time span of ca. 20 kyr (Cioni et al., 1999, Fig. 1.2), mainly through the piling up of lava flows and spatter and loose scoria deposits (Johnston Lavis, 1884; Santacroce, 1987, Sparice et al., 2017). The deposits of four main Plinian eruptions are present in the Somma Vesuvius caldera volcanic succession: the “Pomici di Base”, the “Mercato”, the “Avellino” and the “Pompei eruptions (e.g., Santacroce, 1987; Santacroce et al., 2008).

The Pomici di Base Plinian eruption marked the onset of high-intensity explosive activity, producing the first main collapse of the caldera (Andronico et al., 1995; Bertagnini et al., 1998; Cioni et al., 1999) and the shift to a more explosive activity fed by evolved trachytic magmas (Santacroce et al., 2008). The Pomici di Base eruption was followed by effusive/mildly explosive activity from lateral vents, aligned along regional faults (San Severino, Pollena and Camaldoli eruptive fracture systems) (Fig. 1.2) and, after about 3 kyr, by the Pomici Verdoline subplinian eruption (Delibrias et al., 1979; Santacroce and Sbrana, 2003; Cioni et al., 2003), one of the higher magnitude sub-Plinian eruption of Somma-Vesuvius. The following 15 kyr were characterized by the two Plinian eruptions of Mercato (9.0 kyr BP; Mele et al., 2011) and Avellino (3.9 kyr BP; Sevink et al., 2011; Sulpizio et al., 2010a, 2010b, Fig. 1.2), separated by long periods of nearly complete quiescence. These two Plinian events produced phonolitic and phonolitic to tephriphonolitic products, respectively, culminating in phases of caldera collapse (Cioni et al., 1999).

After the Avellino eruption, the frequency of medium to high intensity eruptions increased, with at least 8 explosive events ranging from weak sub-Plinian (Cioni et al., 2008) to violent strombolian and vulcanian (Andronico and Cioni, 2002). This period of activity ended in 217-216 BC (Stothers and Rampino, 1983) preceding the AD 79 Pompei Plinian eruption. The Vesuvius cone possibly began to form after AD 79 eruption inside the Somma caldera, in coincidence with minor explosive activity described in few contemporary chronicles (Cioni et al., 2013). Its growth occurred discontinuously during periods of open conduit activity. The first period, named Santa Maria Cycle (Cioni et al., 2013), punctuated the I-III century period, preceding the sub-Plinian event of the AD 472 Pollena eruption (Sulpizio et al., 2005). Open conduit activity characterized the V–VIII and X–XII centuries (San Pietro Cycle and Villa Inglese lava flows) and preceded the AD 1631 sub-Plinian eruption (Rosi et al., 1993; Rolandi et al., 1993c; Bertagnini et al., 2006), which is regarded to as the last large explosive event occurred in the recent history of Vesuvius. The AD 1631 eruption was followed by the last period of activity (1638–1944) during which the ‘Gran Cono’ (Great Cone) of Vesuvius attained its present morphology. The eruptive activity of this period was split into 18 cycles, with summit and lateral lava effusions and semi-persistent mild explosive activity (Santacroce, 1987). Each cycle was closed by more intense effusive-explosive ‘final’ eruptions (Santacroce, 1987), the last of which occurred in 1944 (Cole and Scarpati, 2010). The Vesuvius is quiescent since March 1944 (Fig. 1.2).

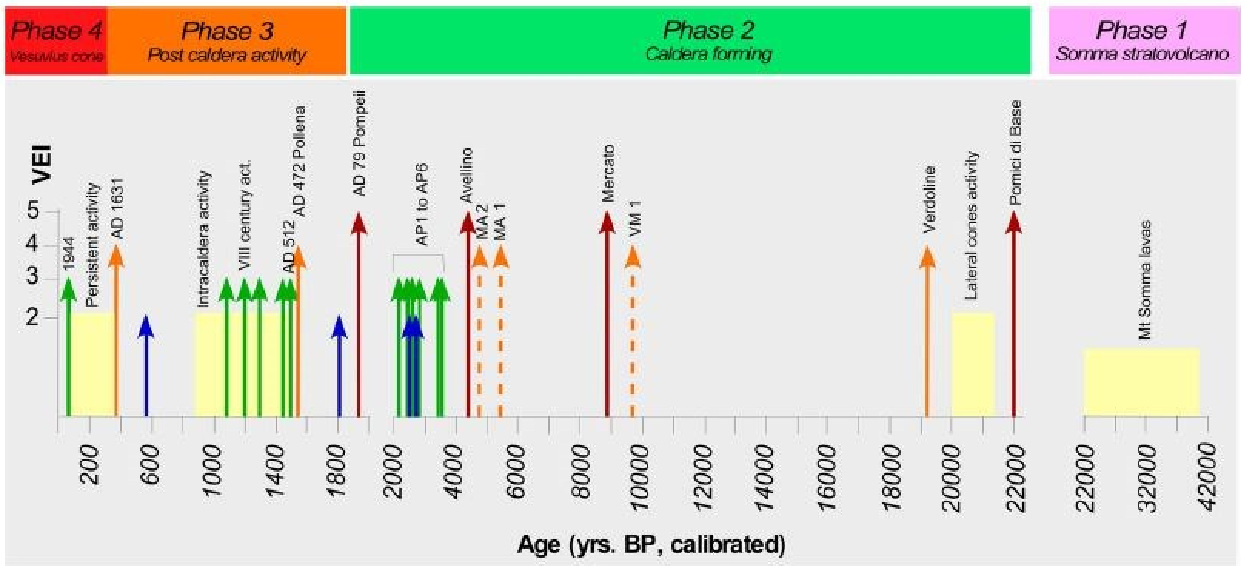

Fig. 1.2 - Chronostratigraphic scheme (not to scale) of the volcanic history of Somma-Vesuvius (from Sbrana et al., 2020). Arrows refer to explosive eruptions; the length and the colour of any arrow refer to the estimated VEI (Volcanic Explosivity Index; data from Cioni et al., 2008); dashed arrows mark eruptions of uncertain source as reported by Sbrana et al. (2020). Yellow boxes show periods of persistent strombolian and effusive activity.

1.3 The Somma-Vesuvius caldera: collapse by “caldera-forming” eruptions or “summit break-up”?

As briefly mentioned in the preceding paragraph, the Somma-Vesuvius volcanic complex is composed of a multistage older summit caldera (Mt. Somma, maximum height 1132 m above sea level, a.s.l.) and a nested younger cone (Mt. Vesuvius, 1281 m a.s.l., Cioni et al., 1999; Gurioli et al., 2010, Fig 1.1).

Over the years, different models have been proposed to explain the mechanism by which the Somma-Vesuvius caldera formed. The most relevant of these are briefly reviewed in this paragraph.

Following the pioneering models proposed by Rittmann (1964; 1967), MacDonald (1972), Bullard (1978), Williams and McBirney (1979), the Somma-Vesuvius caldera was an example of a “Krakatoan” caldera, formed by “*the foundering of the top of large composite volcanoes following explosive eruptions of siliceous pumice from one or more vents, or in some instances, from arcuate fissures on the flanks*”. The authors suggested that the events leading to the formation of the Mt. Somma caldera were associated with the AD 79 eruption, characterised by a rapid emptying of a magma chamber that finally culminated with a caldera collapse. According to Stothers and Rampino (1983), Roman paintings from Pompei and Herculaneum were evidence that, prior to AD 79 eruption the top of the volcano was asymmetrically-shaped, indicating that a Somma-type caldera was already present. In 1997, the volcanological interpretation of a Roman fresco from Pompei (Nazzaro, 1997) left few doubts about the presence of a pre-existing caldera.

On the other hand, according to other authors, the Somma-Vesuvius caldera is a multi-stage structure, resulting from several collapses. Lirer et al. (1973) first suggested that the structure could have resulted from several vertical collapses. Successively, Delibrias et al. (1979), based on the recognition of several pyroclastic sequences potentially ascribable to "caldera-forming" Plinian eruptions, proposed a poly-phased formation of the caldera, suggesting that the first collapse occurred during the "Pomici di Base" eruption.

A few years later, Walker (1984) described the Somma-Vesuvius caldera as an example of a structure formed through repeated collapses connected to the Plinian eruptions of Mercato, Avellino and Pompei. The asymmetric shape of the caldera also suggested that a lateral collapse had occurred, as Milia et al. (1998) later postulated.

The real first attempt to reconstruct in detail the multi-stage evolution of the Somma-Vesuvius caldera was made by Cioni et al. (1999). They suggested that each Plinian eruption produced a summit collapse that modified the size and the shape of Mt. Somma caldera as result of a significant emptying of shallow level, mature magma. The authors also recognized that the original apex of the older Somma stratovolcano was approximately 500 m north of the present Vesuvius crater, at 1600-1900 m a.s.l.

In disagreement with the scheme previously proposed by Scandone (1990), in which the caldera structure resulted from chaotic collapses, Cioni et al. (1999) suggested that the vertical throws (>100 m) of the Somma-Vesuvius caldera blocks, all accumulated along single faults, resulted from the morphological evolution of the rims of a multicyclic nested caldera and repeated vertical collapses.

Rolandi et al. (2004) speculated that the Somma caldera was already present prior the AD 79 and 472 AD eruptions, while the Vesuvius cone formed inside the caldera in the Middle Ages only (Rolandi et al., 1998; 2003). According to these authors, the Somma caldera was formed incrementally in time either by an "*explosive coring*" mechanism, which played a major role during the oldest Plinian eruptions of Somma volcano, and by a repeated "*flank failure*" mechanism, promoted by strong phreato-plinian events associated with the more recent Plinian eruptions of Avellino and Pompei. More specifically, the Avellino eruption would have produced volcanoclastic debris flow and base surge deposits in the W-SW area with a sector collapse. Successively, during the AD 79 eruption, the flank failure process would have extended to the SE sector of the Somma edifice. The authors also recognized large volcanoclastic debris flows, formed during the 472 AD eruption, partly breaching the northern caldera wall.

At the present, the most accepted model is that of Cioni et al. (1999), who identified and defined the chronology of the main events that recurrently induced vertical collapses based on a robust stratigraphic reconstruction.

As illustrated in Figure 1.3, the Somma-Vesuvius caldera has an evident lobate, quasi-elliptical shape with a 5-km-long, east–west major axis and it is characterized by steep walls in the northern sector and a gentle morphology in the southern one (Cioni et al., 1999).

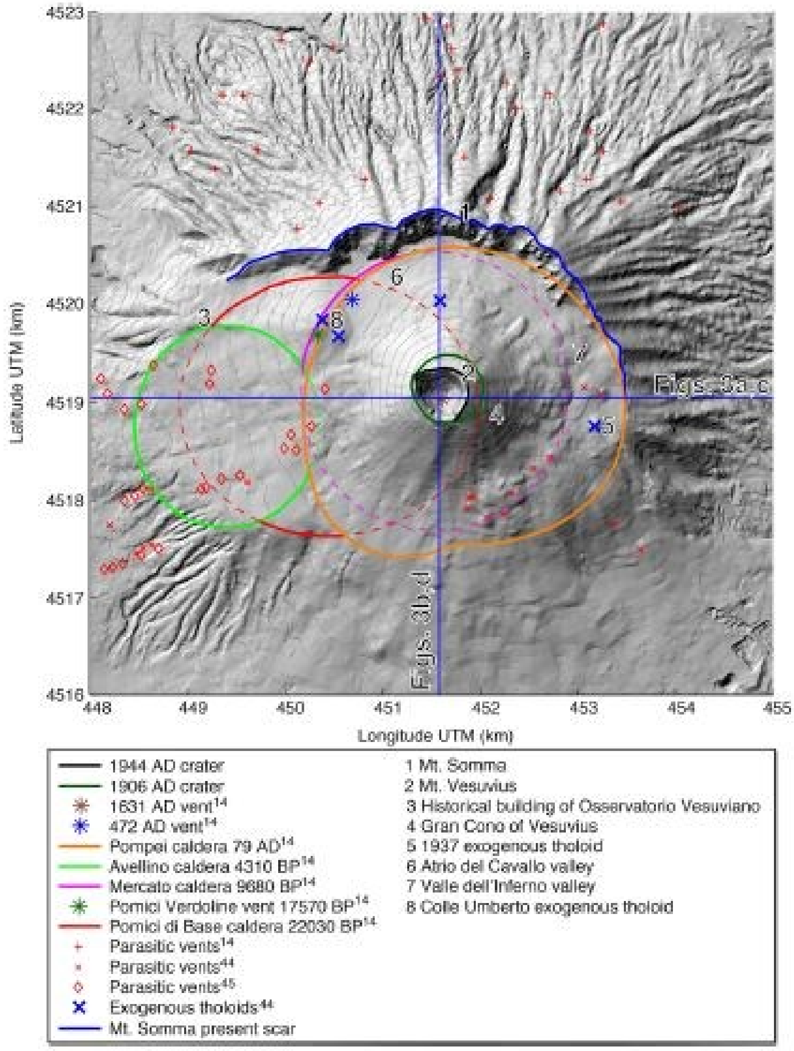

Fig. 1.3 – Digital elevation model (from Linde et al., 2017) of the Somma-Vesuvius volcanic complex with the main volcanic features (as discussed in Santacroce and Sbrana, 2003; Gurioli et al., 2010; Paolillo et al., 2016). Dashed lines refer to sectors of inferred caldera that were removed by subsequent caldera forming events. The blue lines refer to vertical sections along which 3-D density model has been performed (from Linde et al., 2017).

From the “Cognoli di Levante” in the east to “Cognoli di Giacca” in the west, the average elevation is of approximately 1000 m and two main arcuate lobes can be distinguished (Fig. 1.4). The western arc (A–B in fig 1.4), with a radius of approximately 1.5 km, delimits the “Fosso della Vetrana” to the north, and can be traced westwards down to an altitude of approximately 600 m, whereas its southward extrapolation, mantled by lava flows, intersects the Observatory

Hill (Fig. 1.4). The central portion of Mt. Somma ridge forms the main lobe of the caldera, extending from “Cognoli di Trocchia” to “Cognoli di Levante” (B–C in Fig. 1.4). There, the 150 m-high subvertical wall shows a lobate, scalloped shape due to differential erosion between dike crags (Cioni et al., 1999). A third main lobe of the caldera structure runs from the Cognoli di Levante to the south-eastern tip of Piano delle Ginestre (C–D in Fig. 1.4), with a larger radius of curvature than the B–C arc. The southern part of this lobe is well shown by a sharp increase in the slope of the mountain below an average elevation of around 600 m. There, the structure is covered by a pile of recent lava flows and pyroclastic deposits that overtopped the lowest rim of the caldera after filling the depression. The semi elliptical arc delimitating the flat morphology of Piano delle Ginestre lava field (D–E in Fig. 1.4) completes the multilobate shape of the caldera, forming an acute angle with the southern rim of the caldera. It is considered to be linked to the crescent shaped relief of the Observatory Hill, which forms the northern tip of the arc (Cioni et al., 1999). The Piano delle Ginestre therefore seems nested within the continuation of the A–B lobe of the caldera, appearing as a filled depression bounded by a “constructional” edge, which induces asymmetric growth of the volcano towards the sea (Cioni et al., 1999). The present flat morphology of the Piano delle Ginestre records the filling of the old depression by historical lava flows that overflowed the seaward rim during the 1694–1697 activity (Santacroce, 1987).

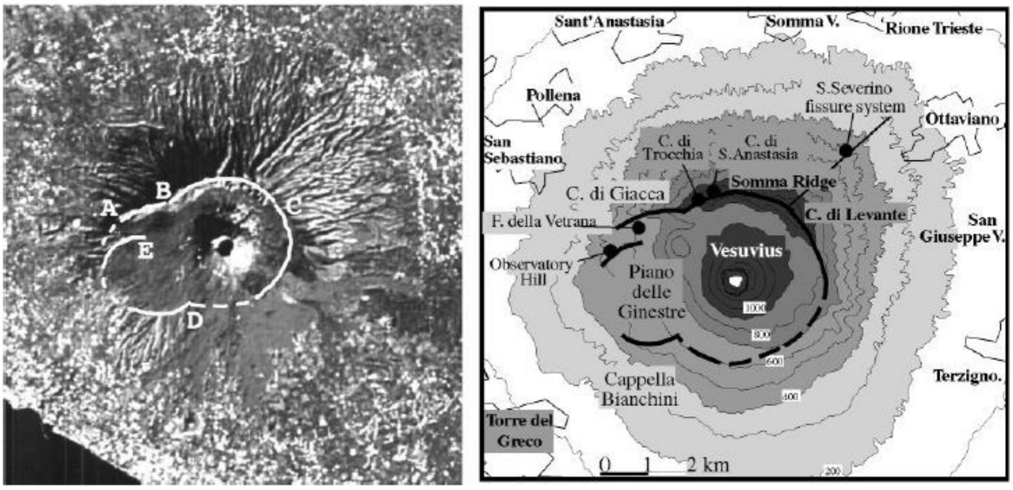

Fig. 1.4 – Satellite image of Somma Vesuvius with trace of the morphological rims of the caldera (on the left) and location map (on the right) after Cioni et al. (1999).

1.4 A look at the past: a brief summary of the studies on the AD 79 Vesuvius eruption from the 18th Century to the present

The AD 79 eruption has become famous since the historical times of Pliny the Younger who became the first eyewitness to describe a large explosive eruption. He made an accurate narrative of the main features of the eruption and of the death of his uncle, Pliny the Elder, in two letters to Tacitus (Gigante, 1989).

Although discrepancies do exist regarding some details about the stratigraphic position and the interpretation of some deposits in some specific locations, an overall agreement exists on the recognition of four main phases of the eruption (Sigurdsson et al., 1985; Cioni et al., 1990; 1992; 1999; 2004; Luongo et al., 2003a; Gurioli et al., 2007; Scandone et al., 2019; Doronzo et al., 2022):

(1) A phreatomagmatic opening phase, beginning after noon of 24 August (or October), which is thought to be related to the interaction between magma rising and overlying aquifer. This type of activity generated an ash deposit cropping out on the volcano slopes.

(2) A main Plinian phase emplacing widespread fallout products (whose juvenile fraction varies from white phonolitic pumice clasts to grey tephriphonolitic pumice clasts with increasing stratigraphic height) towards the south and south-east of the volcano, and minor pyroclastic density currents. This phase was estimated to have lasted about 18-19 hours (Sigurdsson et al., 1985; Cioni et al., 1992).

(3) A second magmatic phase, related to the collapse of the eruptive column, emplacing mainly PDCs rich in lithic fragments. Some structural variations in the volcanic building, such as calderic collapse and vent widening, were responsible for an increase in the mass eruptive rate during this phase. The phase began in the early hours of 25 August (or October).

(4) A final phreatomagmatic phase, leading to the emplacement of ash deposits rich in accretionary lapilli.

In this paragraph, I will focus on the main studies concerning the stratigraphy of the AD 79 PDCs deposits, in order to critically review the state of the art knowledges and highlight the main aspects that are still debated. This latter will be further investigated and discussed in the following chapters.
The first studies on the AD 79 Vesuvius eruption date back to the XVIII and XIX centuries, mainly resulting from archaeological findings and volcanic insights.
The first volcanological study of the products of the AD 79 Vesuvius eruption is due to Johnston-Lavis (1884) who did not recognise the presence of pyroclastic products on the external slopes of the Somma-Vesuvius. In 1908, Lacroix hypothesized that most of the pumice outcrops from the AD 79 deposits were produced by a recently discovered phenomena of the "*nuée ardent type*", eruptive phenomena previously observed during the 1902 eruption of the Pelée of Martinique (Lesser Antilles). Merril (1918; 1920) first reported that these deposits contained carbonized wood remnants, as well as partly burnt documents, suggesting the hypothesis that the city of Pompei had been inundated by burning clouds.

In the early 1950s, the archaeological excavations of Pompei and Herculaneum sparked some genuine interest in several authors. Ippolito (1950), highlighted different sedimentological characteristics of the deposits in the two archaeological sites, and proposed two different depositional mechanisms: burial by lapilli fallout from a volcanic cloud in the case of Pompei, inundation by mudflows for the city of Herculaneum.

Rittmann (1950) agreed with the models proposed to explain the burial of Pompei and Herculaneum, suggesting that the cross-bedded portions of some deposits were due to the remobilization of fallout deposits by subsequent quarrying activity.

Only in the early 1970s, the first numerical models and classifications for both the eruptive and the emplacement mechanism of explosive eruptions were starting to be proposed.

The first detailed investigations of the pyroclastic products of the eruption cropping out around the volcano were provided by the pioneering field work of Di Girolamo (1963; 1968), Lirer and Pescatore (1968) and Lirer et al. (1973). More specifically, Di Girolamo (1968) described the sequence of the AD 79 deposits outcropping along the southwestern cliff of the Torre del Greco city and inside Herculaneum excavations as composed of a “massive mudflow deposit” in the basal part, and a cross-stratified, fine-grained deposit in the upper part of the sequence. He also recognized the pyroclastic sequence on the NNE slopes of Mt. Somma and characterized the juvenile fraction on chemical, mineralogical and petrological grounds.

Lirer et al. (1973) were the first to discriminate the fallout pumice deposits erupted during the AD 79 eruption from those emplaced during the 3.9 ka Avellino eruption, the latter being dispersed toward ENE (Di Vito et al., 2009). Furthermore, they observed that the AD 79 fallout deposit display a faint stratification due to minor variations in the grain size and content of lithic fragments, and to a slight but distinct overall upward increase in the grain size. They drew the first isopach map of the AD 79 fallout deposits and estimated a total volume of emitted magma of 2.6 km^3. The authors also identified the dispersal area to the southern and south-eastern sector of Vesuvius, tracing the fallout deposit up to 72 km away from the vent. Based on the recognition of limestone lithic fragments, reaching a maximum in the upper part of the grey pumice deposit, the authors suggested a depth of 5 to 6 km for the magma chamber feeding the grey pumice, in agreement with Rittmann (1950). On the other hand, they considered that the lithic fragments (lava and limestone) in the white pumice deposits as indicative of shallower reservoir depths (i.e. about 1 km). Finally, Lirer et al. (1973) recognised an abrupt change in the colour of the pumice clasts from white to grey, which they ascribed to the existence of a compositionally zoned magma chamber (more salic at the top and mafic at the bottom and used Pliny’s letter for estimating the timing of the eruption).

In the same year, Sparks and Walker (1973) recognized the presence of primary flow deposits (ground surge layer and ignimbrite) in the AD 79 sequence.

A few years later, also Sheridan et al. (1981) and Sheridan and Wohletz (1981) recognized that the products of AD 79 eruption included pyroclastic flow and base surge deposits in the lower parts of the sequence at Herculaneum and proposed the first numerical model for the dynamics of the eruption. They related the ashy levels interlayered in the medial pumice fallout sequences to the emplacement of "hot and dry", "massive or sand-wave" pyroclastic surges generated by episodes of water access to the eruptive conduit and suggested that a collapse of the sedimentary basement was followed by the injection of external groundwater into the chamber (Fig. 1.5). According to this reconstruction, the eruption opened with a magmatic phase during which a 17 km height sustained column deposited the white pumice fallout deposit. The following emptying of the magma chamber and the rupture of the sedimentary basement caused the ingress of water into the magma chamber, with its consequent vaporization increasing the content of volatiles in the magma and the explosivity of the eruption. The eruptive column rose, emplacing the grey pumice deposit, whose juvenile clasts are denser and larger than those of the white one. The interstratified surge deposits were interpreted by the authors as related to "base surges" that represented the most energetic phase of the eruption. As the eruption continued, the activity became *hydromagmatic*, with the generation of wet surges and pyroclastic flows, followed by a purely phreatic activity when all the magma was exhausted. At the end of the eruption, some lahars were deposited around and inside the city of Herculaneum.

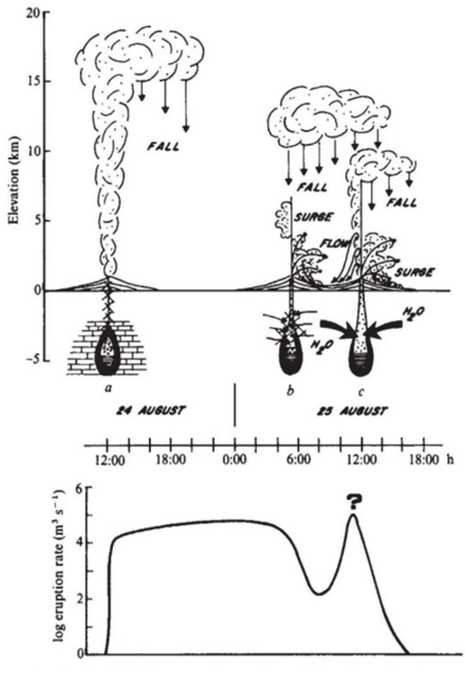

Fig. 1.5 – Model for the evolution of the AD 79 eruption as reconstructed by Sheridan et al. (1981).

In the same years, Barberi and Leoni (1980) reconstructed the structure of the magma chamber of the Somma Vesuvius based on the study of the AD 79 eruption. Based on the recognition of the carbonate lithic fragments found within the pumice fallout deposit, they calculated the depth of the (vertically zoned) magma chamber, placing it at a depth of about 2-4 km in the sedimentary basement, assuming a cylindrical shape with a height of 2 km, a diameter of 1 km and a volume of 2 km^3.

With a careful examination of Pliny the Younger's letters, Sigurdsson et al. (1982) correlated the historical and geological evidence for the first time, inferring that the AD 79 eruption consisted of two main volcanological phases. An early "Plinian" phase first affected the region to the southeast of the volcano and emplaced a 280 cm thick air fallout pumice over Pompei. Subsequently, a late "Pelean" phase began on the morning of August (or October) 25, generating "nuees ardentes" flowing down the south and west flanks of the volcano. The authors also proposed some estimates for the duration of the fallout phase (18 hours) and the sedimentation rate of the pumice lapilli at Pompei (15 cm/h).

Since the 1980s, several authors have described the stratigraphy of the AD 79 eruption from proximal archaeological sites around the volcano to medial and distal sections away from the Vesuvius vent, following different approaches and stratigraphic nomenclatures and applying different interpretative models. In Table 1, the main stratigraphic reconstructions proposed in literature are reported, referring to the articles from Sigurdsson et al. (1985), Cioni et al. (1990; 1992), Gurioli et al. (2007) and Scarpati et al. (2020).

Sigurdsson et al. (1985), based on the study of the stratigraphic sections exposed all around the volcano, used an alphanumeric and "genetic" scheme to identify the various layers of the sequence, named as "A", "S" and "F" for fallout, surge and flow emplacement mechanism, respectively. The letter "C" refers to deposits with accretionary lapilli. On the other hand, Cioni et al. (1990; 1992; 2004) and Gurioli et al. (2007), again based on the deposits cropping out around the volcano, subdivided the stratigraphic succession into 8 different Eruptive Units (EU), each characterized by different areal distribution and significant lateral variations. Eruptive Units were subdivided into sub-units in subsequent papers from the same research group (Cioni et al., 1999; 2004; 2020; Gurioli et al., 1999; 2002; 2005; 2007). Finally, Scarpati et al. (2020) used a non-genetic and descriptive nomenclature modifying the one proposed by Luongo et al. (2003a) in a study focused on the deposits cropping out in the Pompei excavations. In the following paragraphs these models will be discussed in detail along with the results from other studies which contributed to the scientific debate on the AD 79 eruption.

Sigurdsson et al. (1985)	Cioni et al. (1990; 1992; 2004) Gurioli et al. (2007)	Luongo et al. (2003a) Scarpati et al. (2020)
accretionary lapilli layers	EU8	T
accretionary lapilli layers	EU8	S
accretionary lapilli layers	EU8	R
accretionary lapilli layers	EU8	Q
accretionary lapilli layers	EU8	P
accretionary lapilli layers	EU8	O
accretionary lapilli layers	EU8	N
accretionary lapilli layers	EU8	M
accretionary lapilli layers	EU8	L
		I
	EU7pf	H
A10	EU7	G3
		G2
		G1
	EU6	
	EU5	
C1	EU4 accretionary lapilli bearing	F
F6		
S5	EU4pf/EU4b	E2
		E1
A8	EU4bl/EU4a	D
	EU3pfL	
F5		
S6	EU3pf/EU3pftot	C3
A7		B3
F4		
S4		C2
A6	EU3f	B2
F3		
S3	EU3pfiii	C1
A5	EU3f	B1
F2		
S2	EU3pfii	
A4	EU3f	B1
F1		
S1	EU3pfi	
A3	EU3f	B1
	EU2/3pf	
A2	EU2f	A
A1	EU1	

Table 1 – Comparison between the stratigraphic units recognized by Sigurdsson et al. (1985), Cioni et al. (1990; 1992), Gurioli et al. (2007), Luongo et al. (2003a) and Scarpati et al. (2020). Each stratigraphic scheme is vertically continuous but a direct correlation between the different models is not always possible. Where the cell is empty, no stratigraphic units has been described, i.e. there is not a gap in the stratigraphy but there is not a direct correlation between the several stratigraphic schemes.

1.4.1 The very initial opening phase of the eruption: a fallout or a pyroclastic density current deposit?

The nature of the very initial deposit of the AD 79 eruption, found in some proximal sites around the Vesuvius at the base of the white pumice lapilli deposit, is still largely debated. This phase was never recognized until 1985 and some authors such as Sheridan et al. (1981) proposed that the eruption opened with a magmatic phase, with the development of a sustained column from which white pumice fallout was deposited.

Only in 1985, Sigurdsson et al. (1985) presented a more detailed stratigraphic reconstruction of the AD 79 eruption in order to define the eruptive dynamics of the event. They described the ash layer A-1 at the base of the sequence (Table 1), as a greyish to pink fine ash bed with small accretionary lapilli, few centimetres thick, cropping out only to the east and to the north of the volcano (Fig. 1.6). The authors interpreted this as a fallout deposit from the first, short, explosive and phreatomagmatic phase of the eruption. They considered the presence of accretionary lapilli and the fine-grained character of this layer consistent with a "wet" low eruptive column, which dispersed easterly by low local winds, and calculated total volume of only $7*10^6$ m^3 for the deposit.

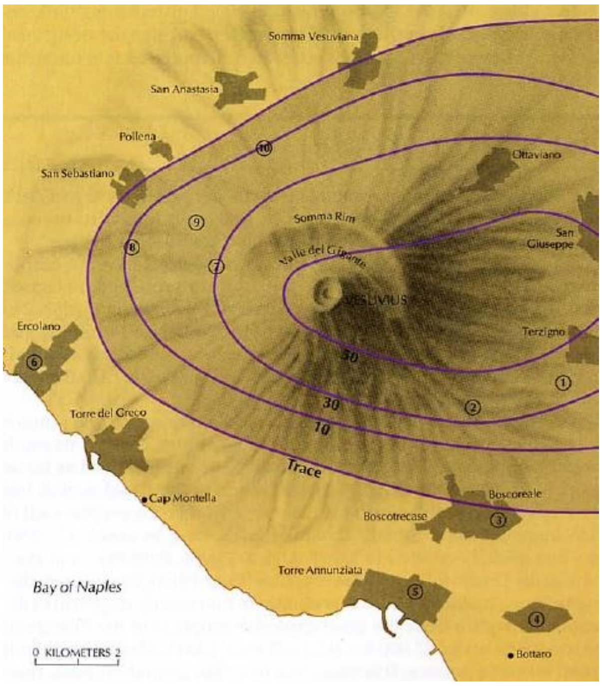

Fig. 1.6 - Isopach map for the ash fallout layer A-1 (from Sigurdsson et al., 1985). The contour lines are in millimetres. Each stratigraphic section around the volcano is numbered: 1: Terzigno; 2: Pozzelle; 3: Boscoreale; 4: Pompei; 5: Oplontis; 6: Herculaneum; 7: Observatory Hill; 8: Cava Montone; 9: Casa Baroni; 10: Monte del Vente.

Later, Barberi et al. (1989) carried out grain size and component analyses on the pyroclastic deposits of the AD 79 eruption and a review of the chronicles of the eruption, reinterpreting the overall eruptive dynamics. At the base of the AD 79 eruption, they recognized a thin coarse ash layer of constant thickness, containing accretionary lapilli and directly overlying a well-developed paleosol. In this layer, lava fragments were observed to predominate lithic fraction and carbonates are relatively abundant (8 wt.%); the absence of cumulates represents a remarkable difference with respect to the pisolitic ash of the wet final phase. Barberi et al. (1989) recognized this ash layer in most proximal sections and ascribed it to the initial fallout phase of the eruption, related to the explosive opening of the vent.

In 1990 and 1992 Cioni and coworkers provided new detailed tephrostratigraphic, sedimentological and geochemical data for the AD 79 eruption, studying 20 stratigraphic sections from the southern and eastern sectors of the volcano. In the eastern sector, they reported the occurrence of a level of light-grey ash at the base of the sequence, which they named EU1 unit (Table 1). Although the thickness of this level is variable (from 1 to 7 cm), the presence of scattered accretionary lapilli and rounded pumice lapilli led the authors to consider this ash level of fallout origin. Locally, the presence of coarser components in lentiform levels of the intermediate part of the deposit were also observed, and abundant footprints of plant remains (mostly rustles and leaves) were found in the basal part of the level. The fine grain size and the cohesive character of the ash allowed the perfect preservation of the plant footprints, suggesting a phreatomagmatic origin and low temperature emplacement conditions.

Lirer et al. (1993; 1997) used component distribution and geochemical data for the juvenile fraction to correlate the AD 79 deposits cropping out in 15 stratigraphic sections (Fig. 1.7). In the Terzigno and Pozzelle sequences, the basal ash layer was observed to display a very different component distribution, which the authors interpreted as indicating that the two deposits do not correlate with each other despite being found in the same stratigraphic position. Both deposits were considered to represent an opening eruptive phase. Their bimodal grain-size distribution, together with their very limited areal dispersion, suggested a depositional mechanism not related to a fallout origin. Furthermore, the very high fragmentation of juvenile fragments, the occurrence of accretionary lapilli and some SEM morphology were interpreted as an evidence of a slight water-magma interaction.

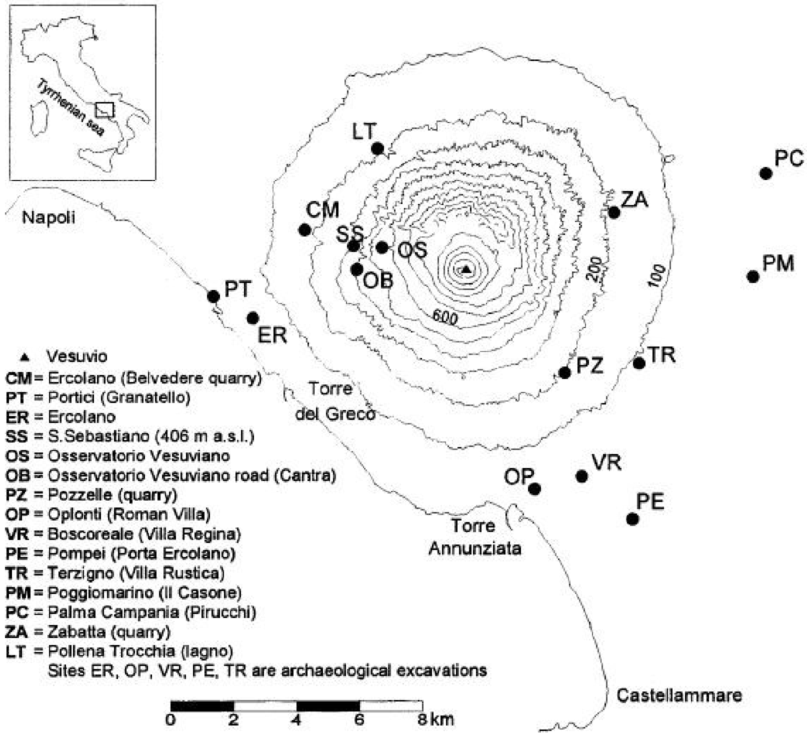

Fig. 1.7 – Location map of the stratigraphic sections investigated by Lirer et al. (1993; 1997) in the peri-volcanic area (from Lirer et al., 1997).

Recently, all authors that have studied the opening stage of the AD 79 eruption (Cioni et al., 1999; Gurioli et al., 1999; Luongo et al., 2003a; 2005; Doronzo et al., 2022) have largely agreed that the eruption started with a short-lived phreatomagmatic phase, producing an accretionary-lapilli-bearing fallout ash (up to 10 cm thick) with an eastward dispersal. Cioni et al. (1999) found this ash layer also in some sites on the western slopes of the volcano, associated with a fine grained pyroclastic current deposit. The exact timing of this opening phase (Sigurdsson et al., 1985) is not very clear, but it seems likely that it could have triggered the first plea for help to Pliny the Elder from the inhabitants of the Vesuvian area (Sigurdsson et al., 1985).

1.4.2 The intra-plinian and post-plinian ash deposits: why are their correlations are so controversial?

Pyroclastic density currents are inhomogeneous mixtures of volcanic particles and gas that flow according to their density relative to the surrounding fluid (generally the atmosphere) and due to Earth's gravity (e.g. Branney and Kokelaar, 2002). They can originate by fountain-like collapse of the whole or parts of an eruption column following explosive disintegration of magma and rock in a volcanic conduit, or from laterally inclined blasts, or even from hot avalanches derived from lava domes (e.g. Branney and Kokelaar, 2002). They can rapidly transport large volumes of hot debris for many kilometres across the ground, therefore representing a lethal and destructive volcanic hazard.

PDCs can be short-lived (highly unsteady) or relatively long-lived (sustained-unsteady to quasi-steady) phenomena driven by both magmatic or phreatomagmatic melt fragmentation (e.g. Cas and Wright, 1987; Carey, 1991; Branney and Kokelaar, 2002). Ground-hugging PDCs produce a buoyant counterpart, known as a "phoenix cloud" or "coignimbrite ash plume", (e.g. Fisher, 1966; Dade and Huppert, 1996; Baer et al., 1997; Branney and Kokelaar, 2022) which can carry ash and aerosols into the stratosphere and thus causing significant climatic perturbations. Several valuable reviews on PDC behaviour have been published in the last 30 years, with a resulting extensive, complex and sometimes contradictory literature (e.g. Carey, 1991; Druitt, 1998; Freundt and Bursik, 1998; Freundt et al., 2000; Branney and Kokelaar, 2002; Sulpizio and Dellino, 2008, Sulpizio et al., 2014). Furthermore, because most processes within PDCs cannot be observed directly, they are commonly inferred from the associated deposits, which vary from stratified to massive. Historically, the recognition of these two different lithofacies has motivated the development of two end-member models (e.g. Cas and Wright, 1987; Walker, 1983). Stratified deposits have been proposed to be the product of dilute suspensions: the so-called "pyroclastic surges", in which particles are mainly carried in turbulent suspension and in a thin flow-boundary layer. Massive deposits are instead considered to result from highly concentrated mixtures: the "pyroclastic flows", in which particle-particle interactions dominate the pyroclasts motion. More recent works (e.g. Burgissier and Bergantz, 2002; Branney and Kokelaar, 2002; Sulpizio et al., 2007; Sulpizio et al., 2014) demonstrated how these two categories are just the endmembers of a continuous spectrum, where the sedimentological characteristics of the deposit mainly depend on the interplay of particle concentration, shear rate and depositional rate over time and space.
PDC deposits from the AD 79 eruption have been the subject of multiple interpretations, based on all the models mentioned above. In the early 70s, when the first numerical models and the first classifications were proposed (McBirney, 1973; Walker, 1973; Blackburn et al., 1976; Sparks e Wilson, 1976; Wilson 1976; Sparks et al., 1977; Nairn e Self, 1978; Self e Sparks, 1978; Wilson et al., 1978; Wilson et al., 1980) and the first studies on the mechanisms of origin, transport and deposition of pyroclastic flows were carried out, the AD 79 deposits that were referred to as mudflows or reworked in previous decades, are reinterpreted as primary (Sparks and Walker, 1973). Lirer et al. (1973) described the "*dark-colored and mostly fine-grained ashes, overlaying the fallout deposit*" as associated with pyroclastic flows belonging to later phases of the AD 79 eruption, although they did not completely understand the nature of these deposits, and sometimes they still referred them as "*mudflows*".

Considering the different opinions on the stratigraphy and facies of these deposits, the result is a partly contradictory picture that I will attempt to illustrate below. A critical issue in the stratigraphic reconstructions is related to how many AD 79 PDC deposits have been recognized in the various sites that were investigated and how they have been correlated to each other.

At Oplonti (Fig. 1.8), Sheridan et al. (1981) described a "*lower group of surge beds*" and an "*uppermost part of the surge sequence made up of massive, fine ash beds full of accretionary lapilli*". "*Above the surge sequence are two pyroclastic flows: the lower one is rich in grey pumice and lacks stratification, while the upper one has numerous graded laminations, probably indicating that it is at its distal reaches. Above the pyroclastic flows is a series of wet surge deposits with planar and massive beds rich in pisolites. The overlying sequence of sandwave surge deposits is followed by another pyroclastic flow. The remainder of the section is composed of lahars*".

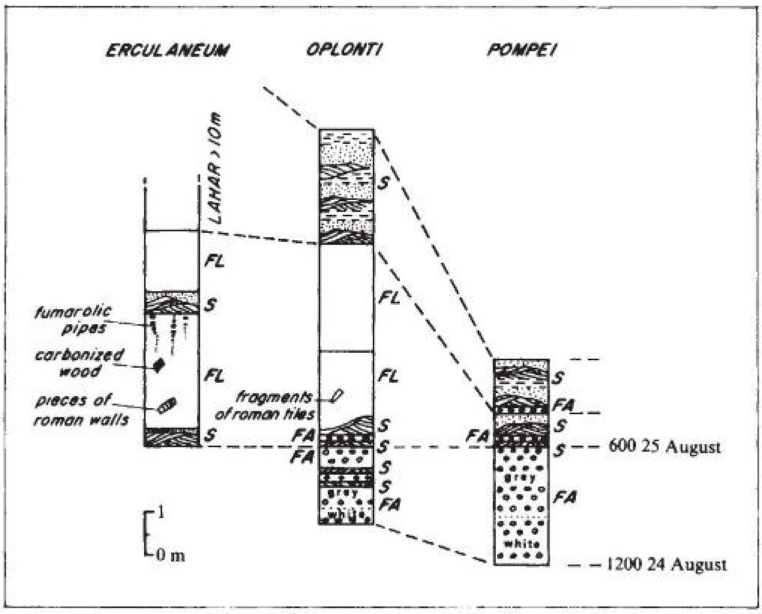

Fig. 1.8 – Representative stratigraphic sections for the AD 79 sequence cropping out in the archaeological excavations of Herculaneum, Oplonti and Pompei. FA refer to air fallout pumice, S to surge deposits and FL to pyroclastic flow, respectively (Sheridan et al., 1981).

Also in the Herculaneum excavations (Fig. 1.8), the authors recognized "*sandwave surges beds at the base of the sequence on which rests a pumice-rich pyroclastic flows containing fragments of houses, carbonized wood and fumarolic pipes toward the top*".

Sigurdsson et al. (1985) used several surge deposits interstratified with the main pumice fallout as stratigraphic *markers* in an attempt of correlating the proximal and distal sequences (Fig. 1.9). The authors correlated these surges deposits although their number, thickness and structures are different in each studied stratigraphic section, a crucial approach that will influence all their stratigraphic correlations. In fact, the use of surge deposits as stratigraphic markers is controversial due to their large facies variability and lateral discontinuity.

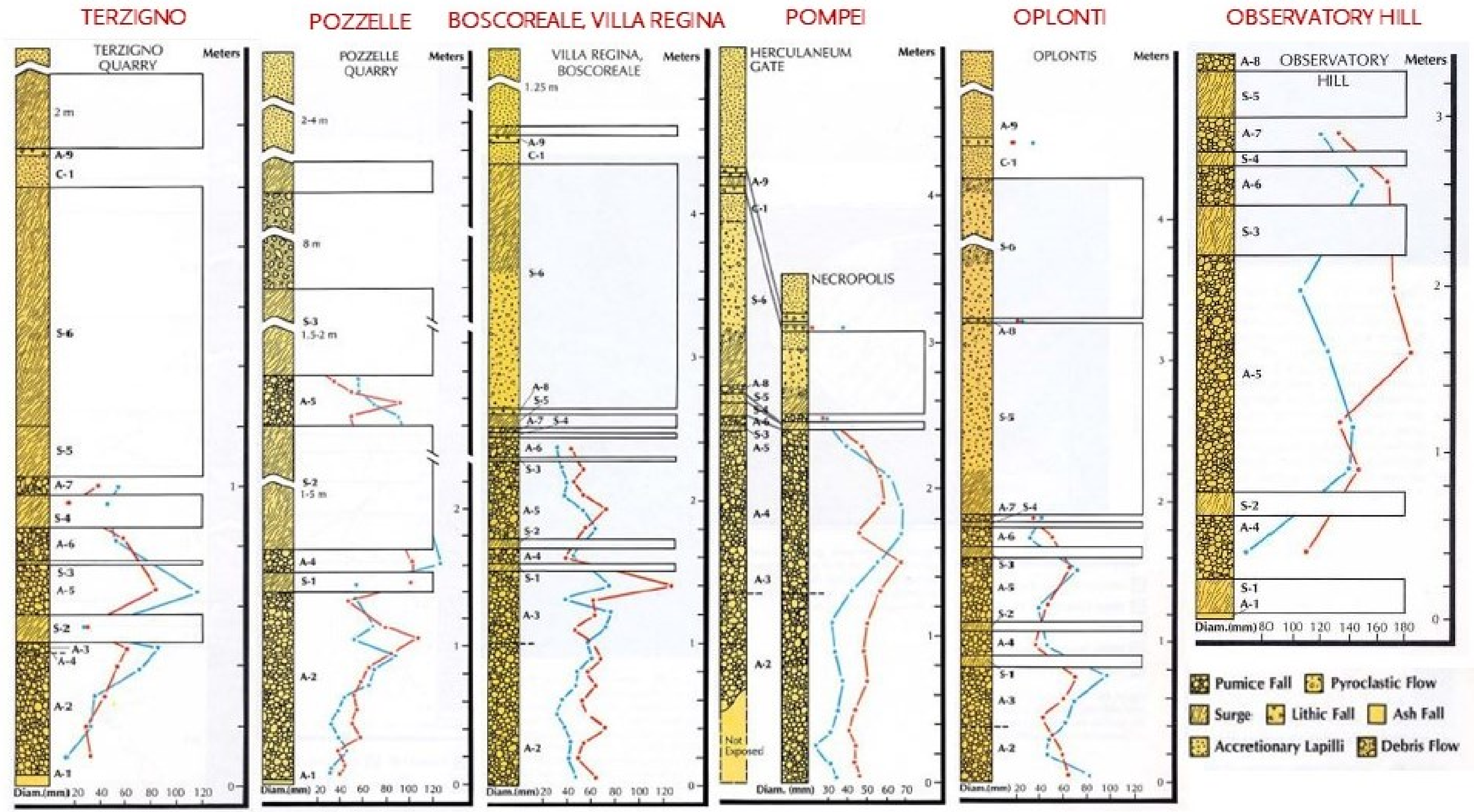

Fig. 1.9 – Stratigraphic sections of the AD 79 deposits cropping out all around the volcano according to Sigurdsson et al. (1985). In each sequence, fallout, flow and surge deposits are reported together with variations in the maximum diameter of pumice (red) and lithic clasts (blue) through the deposit.

I will not dwell on the detailed description that these authors made for each stratigraphic section but, for the purpose of this discussion, in Table 2 the main sedimentological and textural features of each surge deposit are reported.

Surge Deposits	Terzigno	Pozzelle	Boscoreale	Pompeii	Oplontis	Observatory Hill	Areal Distribution
S-6	The deposit is dark grey, sandy, lithic rich. The upper part is generally stratified and cross-bedded while the base is often massive with lenses of rounded pumice and grades locally into facies that resemble a pyroclastic flow deposit. The total thickness of S-5 and S-6 varies from60 to 140 cm.		The deposit is sandy with up to 170 cm of dune-bedded and a massive lower part.	The deposit consists of distinct lower and upper unit. The lower unit is relatively massive and flowlike, containing a higher proportion of pumice in a brown silty to sandy matrix. The upper unit is pumice poor, cross-bedded, finer grained and contains dune structure of 1.2 to 1.5 wavelenght and 10 to 30 cm amplitude.	The deposit can be sudvided into two units of equal thickness, each with a massive lower part and a cross-bedded upper part with long-wavelength dune structures. The deposit is accompanied by a pyroclastic flow deposit. The total thickness varies 2.5 to 3 m.		The unit is ubiquitous. At Pozzelle, a pyroclastic debris flow deposit is most likely contemporaneous with the surge S-6.
S-5	The deposit is dark grey, sandy, lithic rich.		The deposits is characterized by dunes with amplitudes of at least 35 cm. Where the deposit thickens up to 2 m, takes on the appearance of a pyroclastic flow.	The deposit is a cross-bedded ash. The thickness varies from 0.5 to 11 cm.	The deposit is a cross-bedded ash and lapilli with prominent alternating lenses of well-rounded pumice and sandy ash. The deposit is accompanied by a pyroclastic flow deposit, up to 110 cm thick.		The unit is ubiquitous. At Pozzelle, the deposit could have been eroded.
S-4	The deposit is sandy cross-bedded with a lower part relatively rich in rounded pumice whiche grades upward into a lithic rich top part. The thickness varies from 11 to 30 cm.						T The unit outcrops at Terzigno, Boscoreale, Pompei, Oplonti, Observatory Hill and Herculaneum. At Pozzelle, the deposit could have been eroded.
S-3	The deposit is a poorly-sorted, silty sand ash with common rounded grey pumice. The thickness varies from 1 to 6 cm. The deposit is massive.	The deposit is cross-bedded with caracteristics very similar to those of S-2. The thickness varies from 1.5 to 2 m	The deposit is massive and very thin.	The deposit is a dark grey massive ash.			The unit outcrops at Terzigno, Pozzelle, Boscoreale, Pompei, Oplonti, Observatory Hill and Herculaneum.
S-2	The deposit is a massive sandy-layer with some faint stratification and occasional dune structures. The deposit is split into two units by a 0.5 thick, sandy, well-sorted lens. The thickness varies from 7 to 24 cm.	The deposit is cross-bedded with well-developed dunes with wavelenghts of 10 to 15 m. Locally, where it is thickest, the deposit has a massive, poorly-sorted. Central unit that resembles a	The deposit is divided into two units, separated by a 1 cm well sorted pumice and lithic fall unit. It is thick up to 8 cm.			The deposit consists of two units: a lower, massive, poorly-sorted, fines-depleted unit with abundant lava and carbonate lithics up to 25 in diameter and an upper, poorly-sorted, pumice-rich, fine-grained, cross-	The unit outcrops at Terzigno, Pozzelle, Boscoreale, Oplonti, Observatory Hill, along the northern sector of Vesuvius and at Herculaneum.

Table 2 – Summary table with the main sedimentological and textural features and areal distribution of each surge deposit recognized by Sigurdsson et al. (1985).

Inside the Herculaneum excavations the AD 79 sequence consists of alternating surge and flow deposits (Fig. 1.10). The surge deposits are generally poorly sorted and poorly consolidated, silty, with massive lower and cross-bedded upper parts (surge **S-1**), faintly stratified stratification (surge **S-2**) or cross-bedded with long wavelength (surges **S-3, S-4, S-5, S-6**). On the other hand, the flow deposits are usually thick, massive (flow **F-1**) and consolidated, enriched in pumice (flow **F-2, F-4, F-5**) or lithic clasts (flow **F-3**).

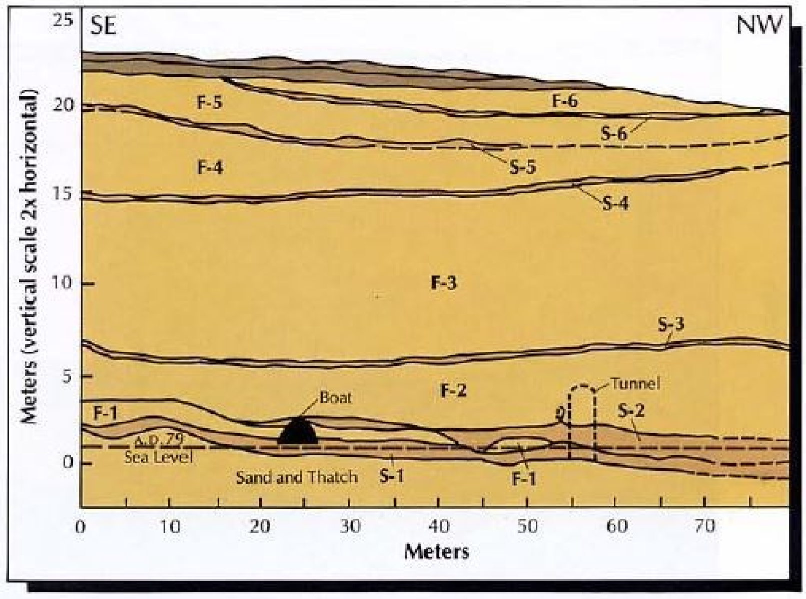

Fig. 1.10 – Stratigraphy of the AD 79 deposits at the Herculaneum beach where the sequence thicks up to 23 m (from Sigurdsson et al., 1985). Roman sea level was at 1 m. Note the alternating surge (S-1 to S-6) and flow deposits (F1 to F-6) that compose the sequence.

Sigurdsson et al. (1985) correlated six surge deposits in all studied stratigraphic sections and reconstructed their areal distribution (Fig. 1.11a) and total thickness (Fig. 1.11b) for the first time. They proposed that the shift from fallout to surge and flow activity resulted from an increasing mass eruption rate and from the tapping of a relatively volatile-depleted portion of magma, resulting in small collapses of the eruptive column.

According to their model, the first surge S-1 spread over the south and west flank of the Vesuvius, reaching Villa Regina at Boscoreale, Oplonti and all the western coast up to Herculaneum. Small tongues of this surge extended down the valley above Somma Vesuviana and Ottaviano on the northern and north-eastern flank, respectively. The second surge S-2 was three times larger than the first and spread to the north within 7 km from the crater, and to the south, destroying the villae rusticae at Terzigno, but did not reach Pompei. On the west flank, the surge S-2 reached Herculaneum where it was followed by the flow F-2. The third surge S-3 had a similar distribution to the surge S-2 but it extended even farther south, running up against the northern city wall of Pompei but not entering the city. The surge S-3 was followed by a pyroclastic flow in the northwest, flowing directly over the remains of Herculaneum. The following surge S-4 had a similar pattern to the previous surges but it spread farther south, reaching the city of Pompei. The fifth surge S-5, even larger than the S-4, was accompanied by a pyroclastic flow in many areas to the south, such as Oplonti. Finally, the sixth surge represents the largest surge over the south flank of Vesuvius, up to Stabiae. Sigurdsson et al. (1985) estimated a "Dense Rock Equivalent" (DRE) of 0.23 km^3 for all the pyroclastic surges and reported that an area of 300 km^2 around the Vesuvius was totally devastated by them.

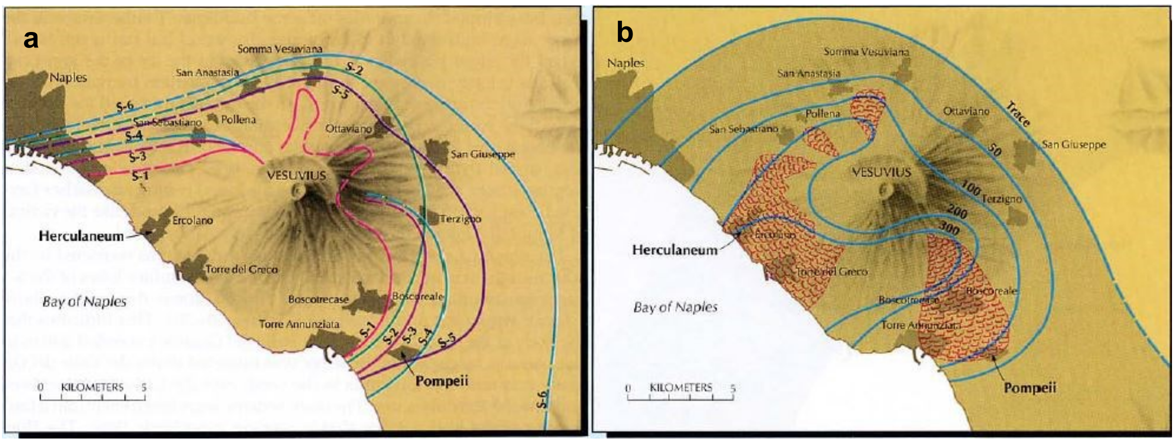

Fig. 1.11 - The six surges from the AD 79 Vesuvius eruption as reconstructed by Sigurdsson et al. (1985). a) Areal distribution around the volcano. b) The thickness of the total surge deposits (in meters) with isopaches. The red areas represent the distribution of the pyroclastic flows. Note how the surge S-6 is the largest event with the major areal distribution around the Vesuvius.

Arnò et al. (1987) studied the stratigraphy of AD 79 eruption in 7 sections around the volcano (Fig. 1.12), and described the pyroclastic sequence as composed by pumice fallout, pumice flow, ash flow, pyroclastic surge and mud deposits. They focused on the main aspects of the surge sequence and they highlighted that "*the thickest surge deposits (up to 3 m or thicker) outcrop only in the southern sectors of the volcano, extending up to more than 10 km from the vent. To the north of the caldera, these deposits are thinner and practically absent from a distance of 6 to 7 km from the caldera rim*". They were also the first to remark how the distribution of the surge deposits is significantly affected by the volcano morphology.

Furthermore, the authors provided a detailed description of the AD 79 pyroclastic flow deposits cropping out at the Pollena quarry, on the northern slopes of Vesuvius, where the sequence consists of "*a basal pumice flow and an overlying ash flow sequence composed of four flow units*". They described the pumice flow as a "*deposit of rounded pumice lapilli and larger lithic blocks supported by an ashy matrix while the four flow units are lighter in tone and are nearly 100% ash. These are separated by surge horizons that pinch and swell, ubiquitously showing dune structures*". The authors also recognised numerous lateral variations in the AD 79 flow deposits at Pollena quarry (Fig. 1.13).

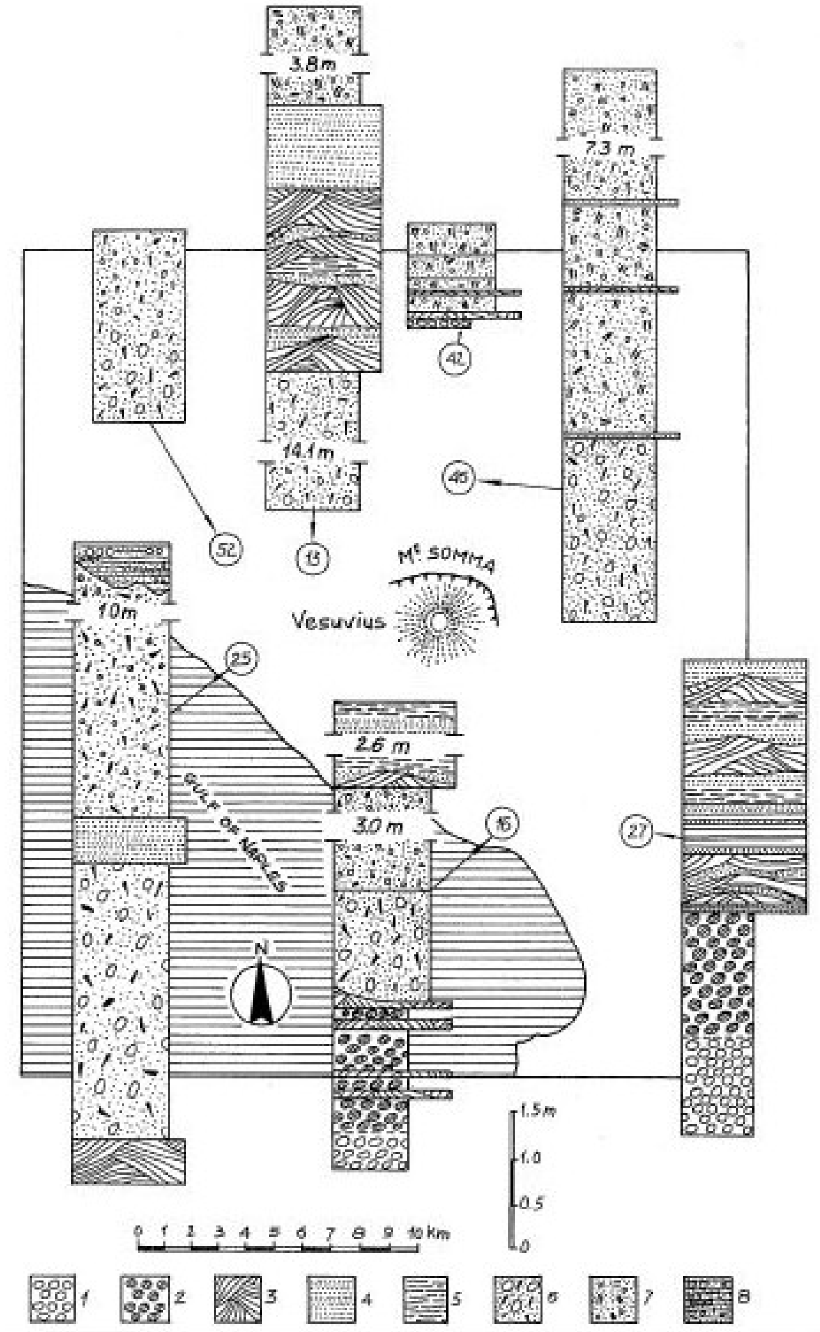

Fig. 1.12 – Representative stratigraphic sections for the AD 79 eruption, with their location on map, as reported by Arnò et al. (1987). 1= white pumice fallout deposits; 2= is for grey pumice fallout deposits 3= cross-bedded surge deposits; 4= massive ash with accretionary lapilli; 5=planar surge beds; 6= pumice flow deposits; 7=ash flow deposits; 8=mudflow deposits.

Finally, in attempt to correlate the Pollena flow sequence with the AD 79 stratigraphy observed along the other flanks of Vesuvius, Arnò et al. (1987) were also the first to discuss about the Somma caldera. They proposed that during the AD 79 eruption, "*the Somma caldera was not an absolute barrier for pyroclastic flows, but it concentrated collapsed clouds and directed their flowage outward along the opposing borders towards either Herculaneum or Oplonti*". At

Herculaneum, the authors still recognize "*mud flow deposits*" in the upper part of the AD 79 sequence and, in agreement with the previous model by Sheridan et al. (1981), they interpreted these deposits as resulting from the final wet stages of the eruption.

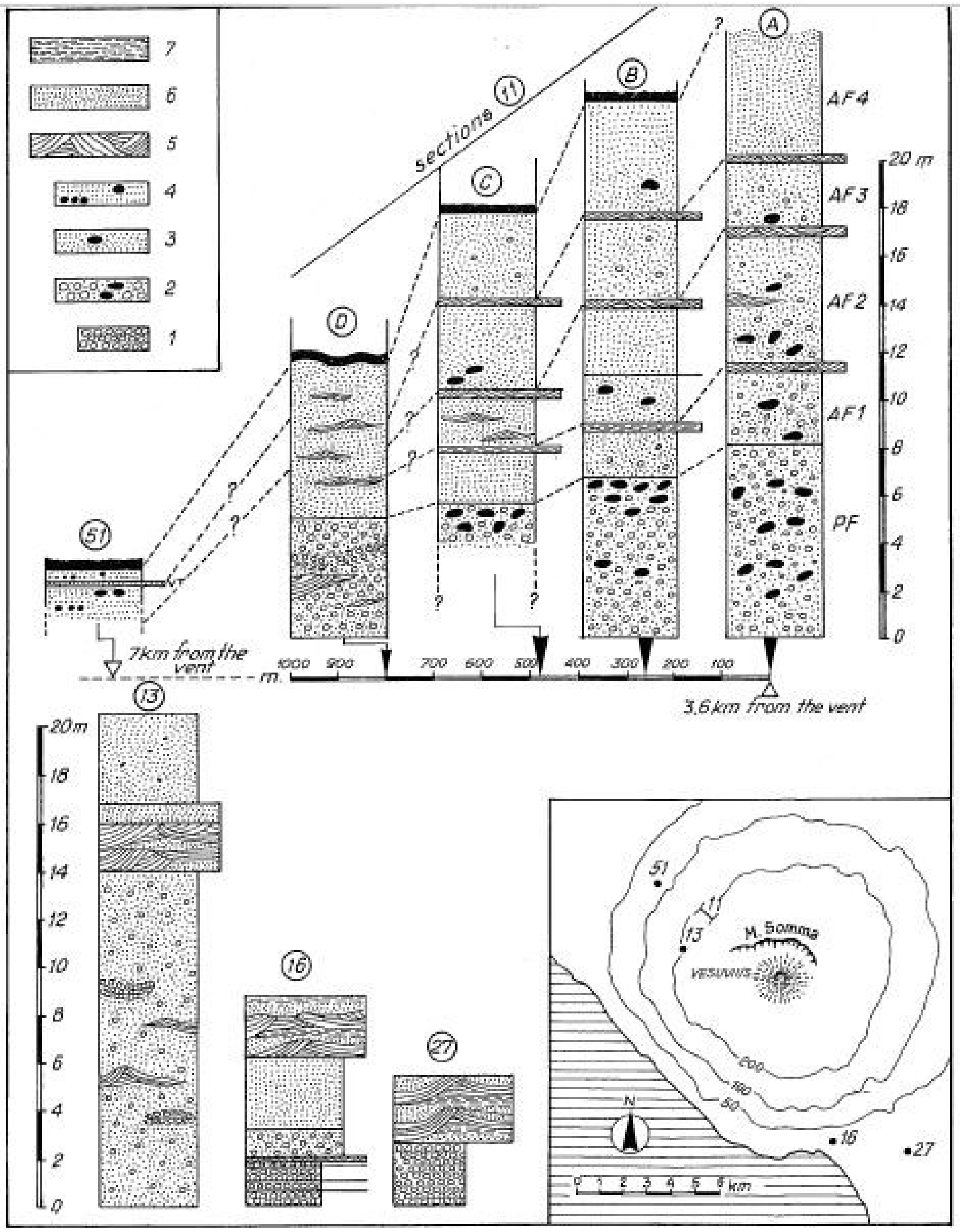

Fig. 1.13 – Lateral variations of the AD 79 pyroclastic flow deposits at the Pollena quarry, cropping out along a radial NW-SE section about 800 m long (from Arnò et al., 1987). 1= pumice fallout deposit; 2= pumice flow deposit; 3= ash flow deposit; 4= mud-flow deposit; 5= cross-bedded surge deposit; 6= massive ash deposit; 7= planar surge beds. Note that the section A, the nearest to the vent, shows the thickest pumice flow deposit. At section D, the pumice flow has developed lenses of well sorted pumice swarms and lithic and pumice stringers.

Barberi et al. (1989) carried out detailed grain size and component analyses on the AD 79 pyroclastic sequence cropping out at Pozzelle (Fig. 1.14) and re-examined the chronicles of the eruption, focusing on the onset and the crucial role of the phreatomagmatic activity (see paragraph 1.4.4).

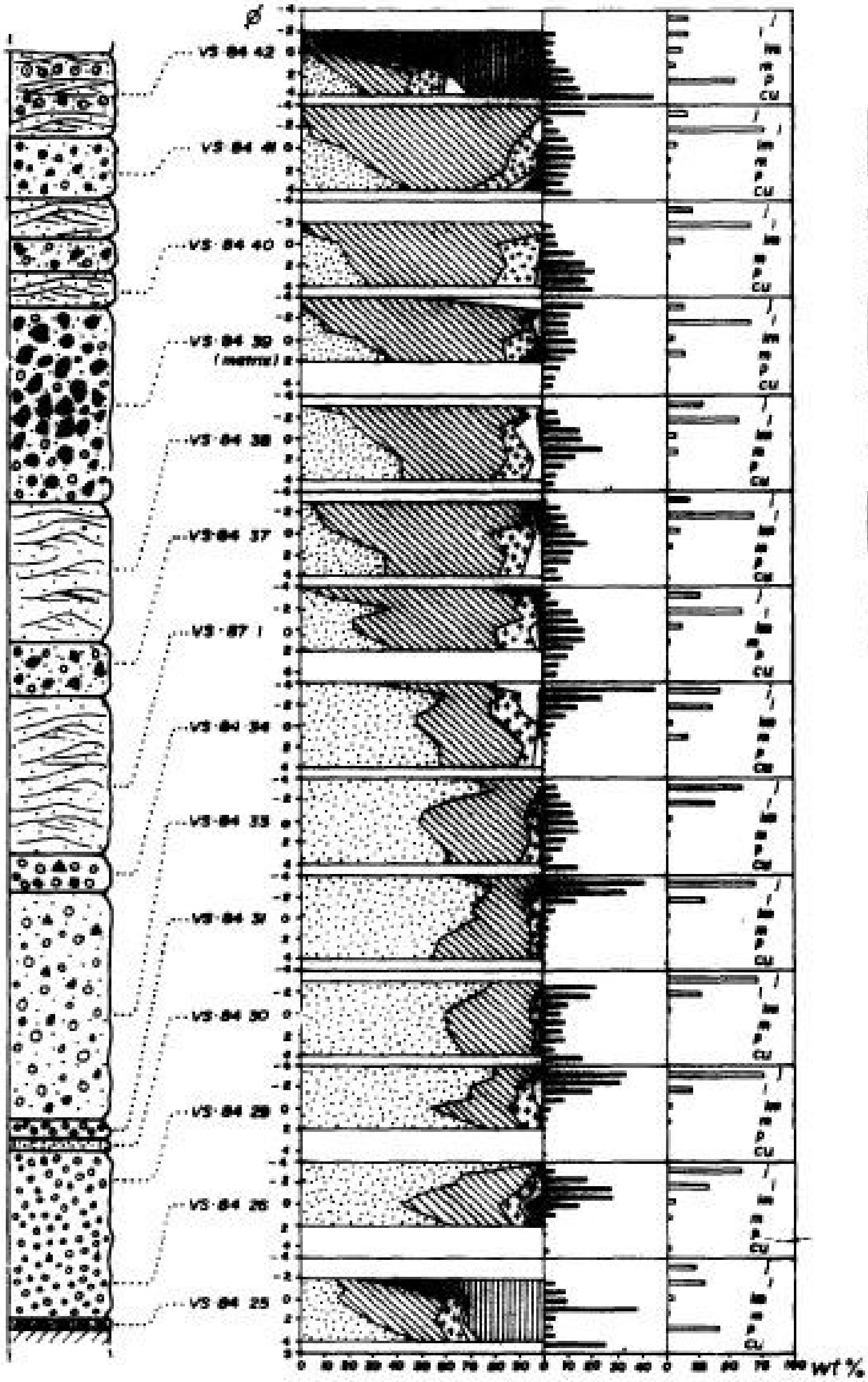

Fig. 1.14 – The AD 79 sequence cropping out at the Pozzelle quarry according to Barberi et al. (1989). From left to right, the diagrams show: the component distribution in each size class; the grain size distribution; the composition of the total sample. 1=juvenile clasts (j); 2=lavas (l); 3=limestones (lm); 4=marbles (m); 5=metasomatic and cumulitic rocks (cu); 6=pisolites (p).

In the AD 79 phreatomagmatic deposits, Cioni et al (1992) identified two *stratigraphic markers* that match the **EU4** and the **EU7** unit (Fig. 1.15), "*with some peculiar ubiquitarian features that made them a guide level in the stratigraphic sequence of the eruption"*.

The features that the authors recognized as *peculiar* and *ubiquitarian* are:

- General sequence formed by a coarse lithic-enriched grain supported basal layer, followed by a thick, generally cross-bedded coarse ash and lapilli bed, topped by pisolitic ash deposits.
- A regular fining-upward trend.
- Strong enrichment in fragments of deep-seated rocks (limestones, marbles and cumulates) in the three layers.
- Frequent occurrence of gradual transition between the layers.

The **EU4** is characterized by a basal bed (EU4a/EU4bl) with grey pumice clasts and lithic fragments made up of lavas, marbles and limestones, generally lacking in ashy matrix, massive or normally graded. Cioni et al (1992) proposed a pyroclastic flow origin for this layer but, after few years Cioni et al. (1999) revised what previously proposed, relating the basal layer (that corresponds to the **A-5** level of Sigurdsson et al., 1985, see Table 1) of the **EU4** to a fallout origin. The middle bed of the **EU4** (EU4pf/EU4b) is represented by a cross-laminated coarse ash and lapilli bed with lenses of grey and white pumice clasts. Well-developed dunes up to 5-10 m in wavelengths are also observed in this bed, which correlates with the **S-6** level of Sigurdsson et al. (1985). The upper part of the **EU4** (EU4c) is represented by pisolitic, massive or faintly laminated fine ash and corresponds to the first accretionary lapilli bearing bed **C-1** of Sigurdsson et al. (1985). Based on the recognition of an "*evident sharp increase in the lithic fragments abundance"*, Cioni et al. (1992) suggested that this eruptive unit records the transition from magmatic to phreatomagmatic activity and the onset of the "caldera-forming phase" of the eruption.

The **EU7** is considered as a *second guide level*, formed by a set of three strata consisting of: 1) a basal lapilli enriched layer with abundant lithic fragments of marbles and cumulates, followed by 2) a middle deposit of dune-bedded or massive fine ash, capped by 3) an upper pisolitic ash layer. The lower thickness and the more limited distribution of this unit was considered to suggest a minor energy of the turbulent pyroclastic flow with respect to that of the **EU4 b** unit.

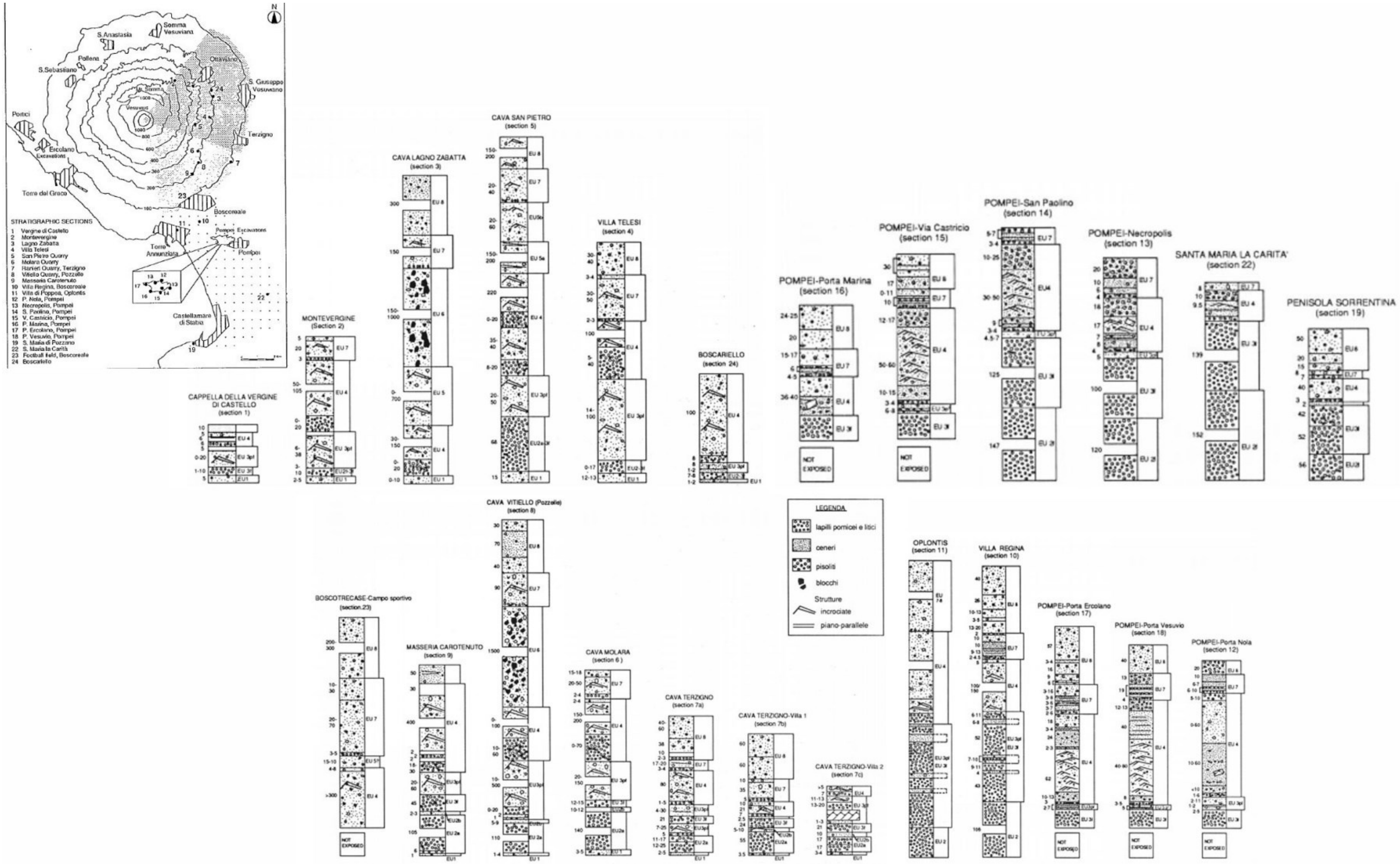

Fig. 1.15 –The AD 79 stratigraphic sections studied by Cioni et al. (1992), with their location reported in the inset at the upper right, where the southern, north-eastern and south-eastern sectors around the volcano are highlighted using different stippled patterns. In each stratigraphic section, the eruptive unit (whose thickness is reported on the left) is referred to a deposit emplaced by a single pulse or in a phase characterized by well-defined eruptive mechanisms and comprising one or more beds.

An important turning point on the discussion about the AD 79 flow deposit sequence, came in the early 1990s, when new approaches, descriptive schemes and conceptual models for enhancing the understanding of the physical behaviour of PDCs were developed (e.g., Carey, 1991; Branney and Kokelaar, 1992; Druitt, 1998; Freundt and Bursik, 1998).

In light of these novelties, Gurioli (1999) and Gurioli et al. (1999; 2005; 2007) proposed a detailed stratigraphic and sedimentological study of the lateral and vertical facies variations recognised in the EU3pf and EU4b/c units, the main AD 79 PDC deposits whose distribution has been traced over a large area around the volcano.

The EU3pf (Gurioli et al., 1999) includes several ash flow deposits sandwiched between the grey fallout deposit at the base (EU3f) and the phreatomagmatic EU4 at the top, recording the total collapse of the AD 79 Plinian column and the generation of a powerful, radially moving pyroclastic current. Over the past years, some authors (e.g. Gurioli et al., 1999; Cioni et al., 2004; 2020; Shea et al., 2011; Doronzo et al., 2022) have referred to this unit using different acronyms. These are summarised in the schematic Table 3.

Gurioli et al. (1999) Cioni et al. (2020)	**Cioni et al. (2004)**	**Gurioli et al (2007)**	**Shea et al. (2011)**	**Doronzo et al. (2022)**
Acronym EU3pf: «inlcudes several ash flow deposits sandwicheed beetween the grey fallout deposit (EU3f unit) and the phreatomagmatic EU4 unit at the top, recording the total collapse of the AD 79 Plinian eruption and the generation of a powerful, radially moving pyroclastic current».	**Acronym EU3pfi:** «some PDCs generated by the discontinous collapse of marginal portions of the convective column during the Plinian phase». **Acronym EU3pf:** «radially dispersed PDC generated by the total column collpase» **Acronym EU3pfL:** «The magmatic phase stopped with the emplacement of lithic rich deposits toward the N and the NW during collapse of the shallow magma reservoir».	**Acronym EU3pf:** «a sequence of at least 3 subunits. Subunit 1 was emplaced from the initial collapse of the column. Emplacement of the subunit II occured during the peak of the column fountaining activity. Subunit III was emplaced during the final, least energetic phase of the column collapse”.	**Acronym EU3pfi/EU3pfii/EU3pf iii:** matches the EU3pfi unit of Cioni et al. (2004) **Acronym EU3pftot**: matches the EU3pf unit of Cioni et al. (2004) **Acronym EU3pfL**: matches the EU3pfL unit of Cioni et al. (2004)	**Acronym EU3pf:** matches the EU3pfi unit of Cioni etl. (2004). **Acronym EU3pftot:** matches the EU3pf unit of Cioni et al. (2004)

Table 3 – The table schematically shows the different nomenclature used by different authors to refer to several sub-units of the same, generic EU3pf unit of Gurioli et al. (1999).

Gurioli et al. (1999) assumed that the AD 79 sequence can be correlated all around the Vesuvius and applied the concepts of “*facies variations*” and “*aggradational sedimentation*” to the deposits of the EU3pf unit for the first time, highlighting their complex vertical and lateral facies variability. Even if such lithofacies approach represented a pioneering work at that time, it remains controversial the method used by the authors for identifying the stratigraphic markers EU4 and EU7, especially on the northern (Fig. 1.16) and western slopes of the Vesuvius, where the main fallout deposits are totally missing.

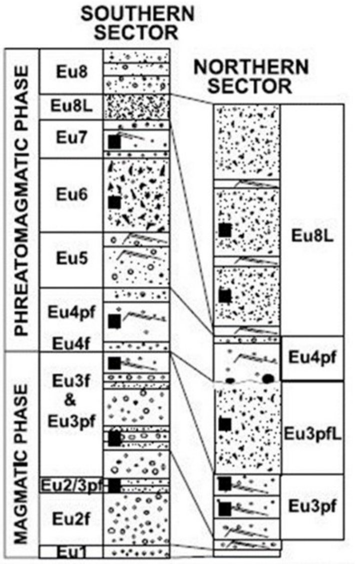

Fig. 1.16 – Schematic stratigraphy of the AD 79 deposits cropping out in the southern and northern sectors of the volcano (Cioni et al., 2004). Worth of note are the absence of any fallout layer in the northern sector and the correlations that the authors propose.

Gurioli et al. (1999) described the deposits of the EU3pf as about 1 m thick, radially dispersed up to 10 km from the vent area, and moderately controlled by local topography, resulting in a large vertical and lateral facies variability (Fig. 1.17), probably related to local variations in turbulence, concentration and stratification of the current.

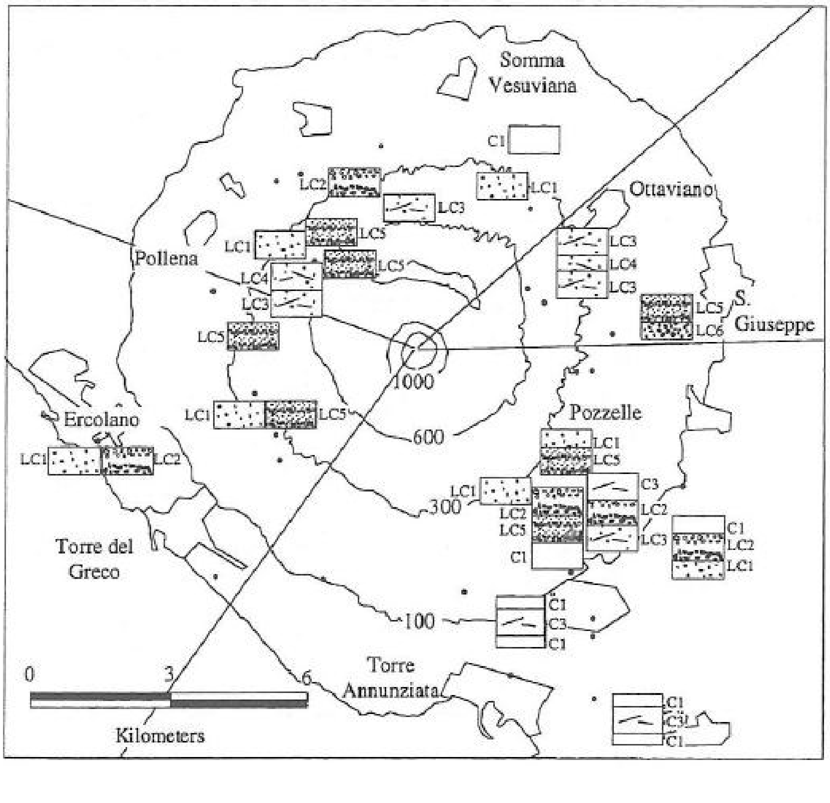

Fig. 1.17 – Distribution of the main facies observed by Gurioli et al. (1999) in the EU3pf unit around the Somma Vesuvius. The letter L indicates an abundance of lapilli between 25% and 75%, whereas the

letter C indicates an abundance of lapilli < 25%. The number 1 is for a massive facies; the number 2 for a graded density facies; the number 3 for a plane parallel to cross stratified facies; the number 4 for a regressive cross stratified facies; the number 5 for a stratified facies alternating fine and coarse beds; the number 6 for facies depleted in fine ash.

They estimated that the median clast size decreases gradually from proximal to distal locations and suggested that the coarsest deposits, generally occurring as breccia lenses in the EU3pf sequence, are located within paleodepressions.

Based on the reconstruction of the EU3pf facies variations over a regional scale, the authors proposed a model (Fig. 1.18) for the areal distribution (Fig. 1.19) and the behaviour of the intra-plinian pyroclastic currents that point out the following:

(1) In the southern part of the Somma Vesuvius area, the relatively smooth paleotopography controlled the overall deposition of this unit only at the local scale.
(2) In the eastern sector, the interaction of the current with the ridge representing the remnants of the old Mount Somma caldera possibly triggered a general increase of the current turbulence and velocity, and a more efficient air ingestion which resulted in the local deposition of a thinly stratified sequence.
(3) In the western sector, the presence of a breach in the caldera wall and of an important break in slope in the area of Piano delle Ginestre possibly increased deposition from the PDC, producing a large, several meters thick depositional fan toward the sea facing sectors (as in Herculaneum).
(4) In the northern sector, the deeply eroded paleotopography with many valleys cut on steep slopes, favoured the development of a fast moving, dense basal underflow within the current. This allowed the segregation of the coarse, lithic material, the deposition of thick lobes in the main valleys and the separation of a slower and more dilute portion travelling and depositing thin, stratified beds on morphological ridges.

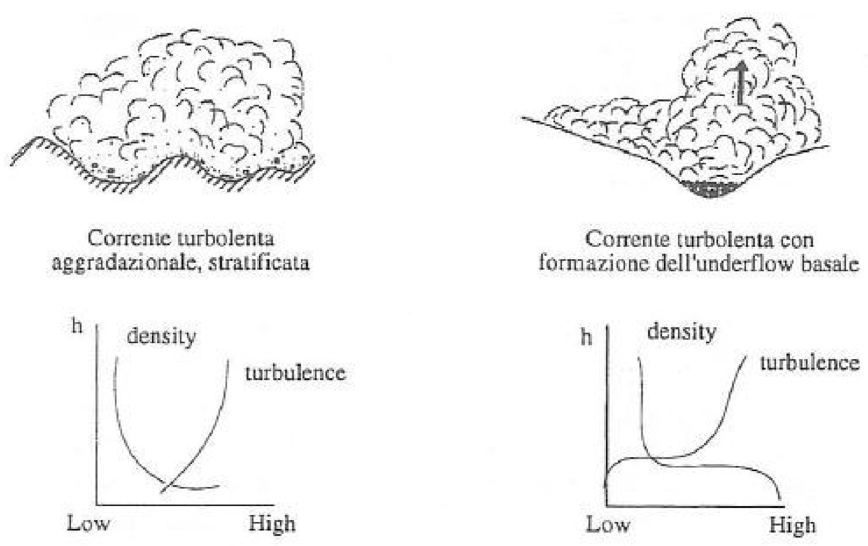

Fig. 1.18 –The pioneering model proposed by Gurioli et al. (1999) for explaining the facies variations of the EU3pf unit a) in the southern sector of Somma Vesuvius and b) in the northern sector of Somma Vesuvius. For each model, the authors report a profile of density and concentration for the current emplacing the EU3pf unit.

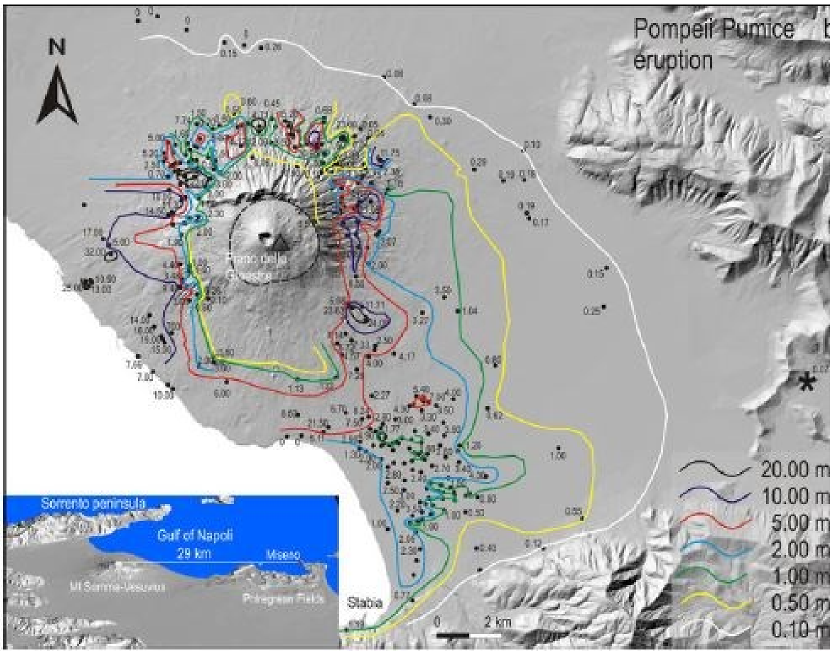

Fig. 1.19 – Dispersal areas of the AD 79 PDC deposits as reconstructed by Gurioli et al. (1999; 2010). The inset shows the Gulf of Napoli and the location from which Pliny the Younger observed the eruption. The isopachs indicate the total thickness of the PDC deposits.

In order to complete the discussion regarding the EU3pf unit, an additional noteworthy contribution was provided by the paper of the Shea et al. (2011). These authors focused on the six major PDCs generated during the magmatic phase of the eruption [designated for simplicity as P1 to P6 and corresponding to the EU2/3pf and the entire EU3pf of Cioni et al. (2004), Fig. 1.20a], exploring new insights into the eruptive dynamics of the AD 79 partial and total collapsing column. By measuring the density of 100 juvenile clasts (Fig. 1.20b) and wall-rock abundances for several fallout and magmatic PDC units and estimating some ascent parameters (such as decompression rate and the conduit radius), the authors concluded that:

1) At least four partial collapses (P1 to P4) resulted from increasing abundance of denser pumice.
2) In contrast, the total collapse (P5) probably occurred in response to an increase in the wall-rock content injected into the eruptive plume during a progressive widening of the conduit.
3) The last small-scale collapse of the magmatic phase (P6) occurred when the discharge rate was low but the extremely high clast densities combined with the enlarged conduit led to the formation of a boil-over collapse.

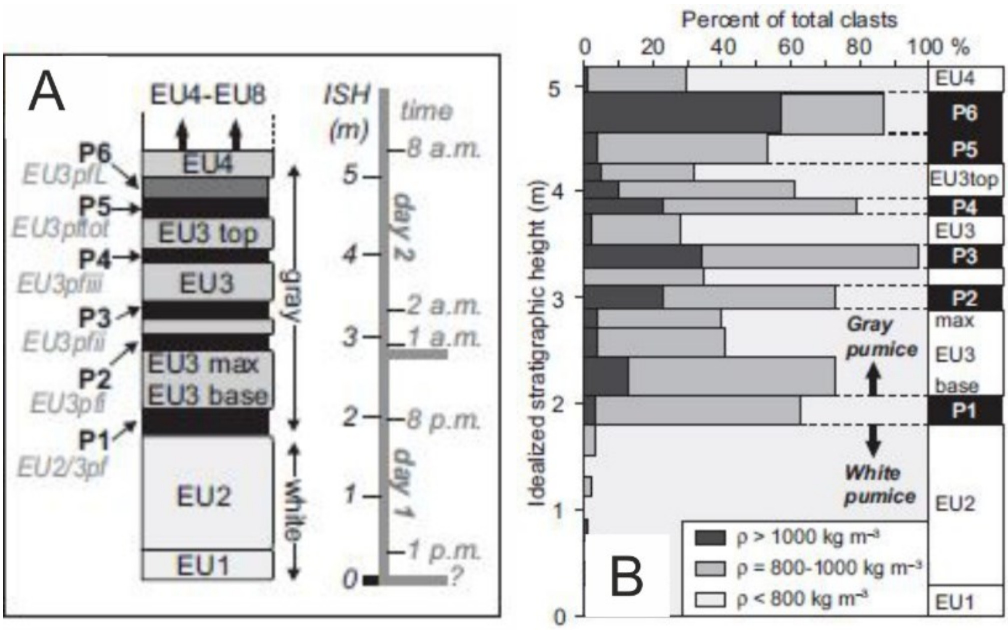

Fig. 1.20 – A) Simplified stratigraphy of the magmatic phase of the AD 79 eruption with eruption timeline according to Shea et al. (2011). Note that the authors use the stratigraphic scheme of Cioni et al. (2004) but designate the six PDCs investigated as P1 to P6 for simplicity. B) Vertical variations in density for the deposits of the magmatic phase of the AD 79 eruption (from Shea et al., 2011) displayed as intervals of low, medium and high-density pumice. Note the abrupt increase in the density of the pumice clasts in correspondence of PDC units.

In addition to the detailed reconstruction of the EU3pf unit reported above, Gurioli (1999) studied also the EU4 (Table 4) by integrating facies analysis with sedimentological data, which were also the subject of further investigations by the same research group (Gurioli et al., 2005; 2007).

Facies			
Regional scale	Local scale	Interpretation	Areal distribution
The main deposit of the EU4 unit (EU4pf unit) shows clear vertical grain size and textural variations. It is often laminated in the upper part and characterized by undulatory bedded to dune bedded deposits, with a thickness of about 4 m in the proximal part of Vesuvius, changing into deposit with massive to laminated facies at about 6-7 km from the vent and with a massive accretionary lapilli bearing facies in the distal part of the volcano. In some localities, the deposits are lithic rich (lavas, marbles, limestones, skarns and cumulites) and consist of pumice and lithic lapilli in a fine to coarse ash matrix, in which there are outsized lava and dense pumice ballistics with dimensions up to a few decimeters. The occurrence of "traction carpets" and local, extended erosion of the pumice-bearing layer of the underlying EU4a is evidence of the high shear rate exerted by the EU4pf.	Both inside and outside Pompeii, this unit is characterized by a great thickness variability and a large facies variations. The most common vertical lithofacies association varies from a basal massive ash containing rounded-pumice lapilli (and locally decimeter-sized lithic clasts and building fragments) through a crudely to diffuse stratified ash containing rounded pumice lapilli to a planar to undulated to low angle, cross stratified fine ash at the top. The thickness decreases from the north to the south of the town and is strongly affected by the urban structure. In the Herculaneum excavations, the unit is characterized by two main beds. The lower, reversely graded bed, is discontinous with a maximum thickness of 0.1 m and generally lacks fine ash and locally shows multiple reverse grading. The upper bed shows a lateral transition from coarse-tail density-graded facies to massive to crudely stratified facies and has constant thickness of 0.2-0.3 m.	The EU4pf unit can be interpreted as derived from a short-lived sustained, turbulent, unsteady, density stratified current. Inside the archaeological sites of Pompeii and Herculaneum, the EU4pf lower current seems to have been 2-4 m thick, being able to interact with obstacles of a few meters in height while, the dilute upper part of the current has been able to flow over the towns.	The EU4pf unit is distributed radially from the vent and reaches a distance of about 21 km in the southern part of the volcano while, in the norther sector, where the initial path of the PDC was possibly shielded by the high Mt. Somma scarp, the current travels not farther than 7-8 km.

Table 4 – Summary table of the main sedimentological features (at both the regional and local scale), with their interpretation and areal distribution, of the EU4 unit, distinguished into the EU4pf main deposit and the overlying EU4c unit (Gurioli, 2000; Gurioli et al., 2005; 2007; Cioni et al., 2020).

The unit marks the reappraisal of the eruption after the end of the Plinian phase and is related to the onset of the caldera collapse (Cioni et al., 1999). Gurioli (1999) argued that the EU4 includes a second fallout bed (“EU4a2”), interstratified within the EU4b unit. This fallout bed can be clearly recognized only in distal sections of the southern sector of the volcano, while in the northern and in the western ones it is represented by a discontinuous level of ballistic ejecta.

More recently, Cioni et al. (2020) have proposed that the EU4pf represents the widest distributed pyroclastic current in the entire sequence of the AD 79 eruption, covering a radial area around Vesuvius of at least 445 km^2 on land (Fig. 1.21). The PDCs from which the unit was deposited are thought to be among the ones with the greatest runout for the Somma-Vesuvius (20 km; Gurioli et al., 2010). The main sedimentological features of the EU4pf observed by various authors are summarised in Table 4, together with the proposed interpretations and areal distributions.

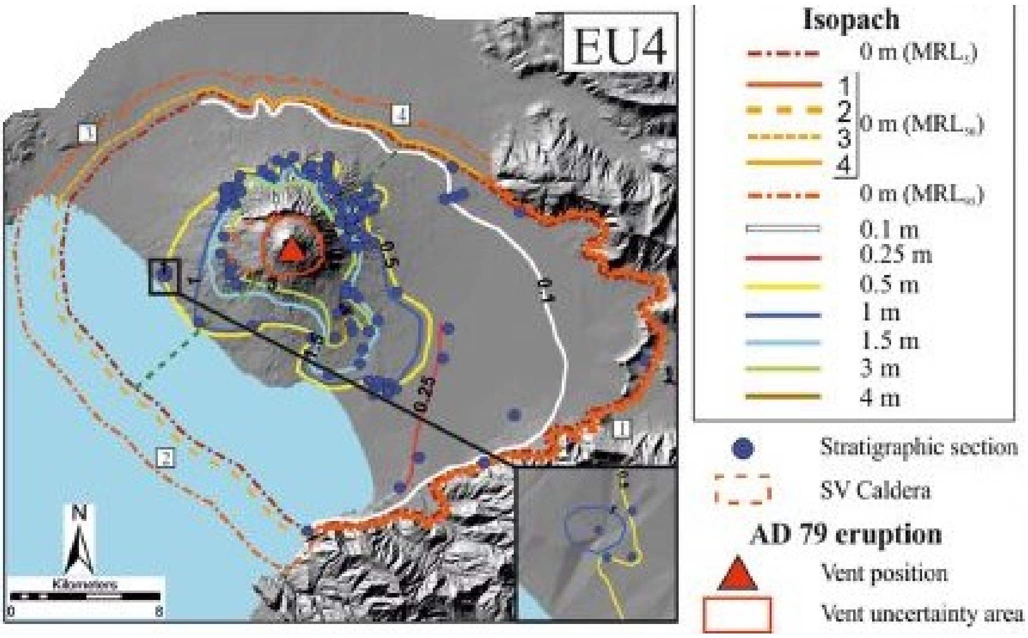

Fig. 1.21 – Maximum runout line and isopaches (in metres) related to the EU4pf unit according to Cioni et al. (2020), based on a statistical box model approach.

Gurioli et al. (2002) reported a detailed description of the AD 79 stratigraphic sequence at Herculaneum excavations and, despite the cross-wind position of the town with respect to the dispersal of the Plinian fallout deposits, they identified “*two discontinuous thin fallout layers”* and “*some distinctive stratigraphic markers(EU2pf, EU4 and EU8 units)*”, which allowed the authors to insert these layers in the framework of the stratigraphic scheme proposed by Cioni et al. (1992).

Gurioli et al. (2002) used the result of their lithofacies study (Fig. 1.22) to show how even small local irregularities of the substratum in an urban structure (e.g. buildings and steps), can affect the behaviour of the pyroclastic currents, enhancing turbulence and allowing rapid transition from non-turbulent to turbulent transport within the flow.

Key	Facies	Occurrence
MCS	Massive to crudely stratified	EU2/3pf EU3pf1 EU3pf2 EU4
CTGr	Coarse-tail density graded	EU3pf1 EU3pf2 Unit A Unit B Unit D
PPCB	Plane-parallel to low-angle cross-bedded	EU2/3pf EU8
RGr	Reversely graded	EU3pf2 EU4 Unit A
FP	Fines-poor	EU2/3pf EU3pf2
SCF	Stratified alternating coarse and fine grained layers	EU2/3pf Unit B
AL	Accretionary lapilli-bearing	EU8

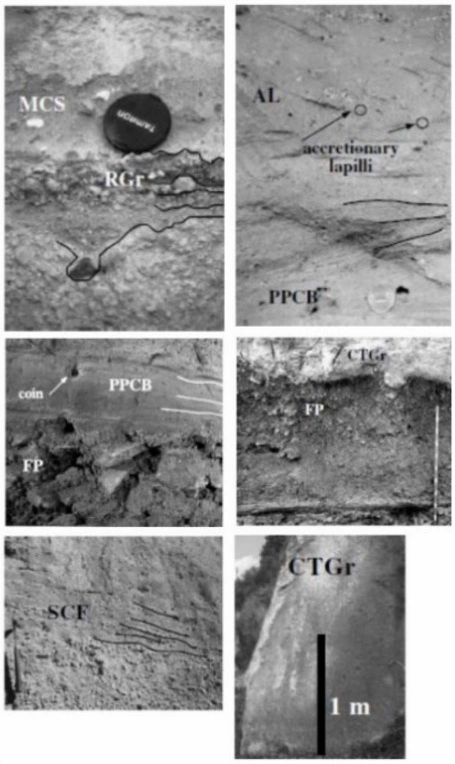

Fig. 1.22 – Schematic diagram and representative field photographs summarizing the main features of the 7 different facies recognized in the pyroclastic deposits of Herculaneum by Gurioli et al. (2002). Each eruptive unit is characterized by a distinctive facies.

Over the past 20 years, Gurioli, Cioni and coworkers (Cioni et al., 1995; Cioni et al., 1996; Cioni et al., 1999; Gurioli et al., 1999; Cioni et al., 2000; Gurioli et al., 2002; Cioni et al., 2004; Gurioli et al., 2005a; Gurioli et al., 2005b; Gurioli et al., 2007; Zanella et al., 2007; Gurioli et al., 2010; Shea et al., 2011; Aravena et al., 2019; Cioni et al., 2020, Tadini et al., 2020), have further integrated the stratigraphic database of Cioni et al. (1990; 1992) with data from new outcrops. These allowed several aspects of the eruption to be investigated, such as: a) the temperature of the AD 79 PDCs and their impact dynamics on the human settlements of Pompei and Herculaneum; b) the morphological features and the variations in crystallinity and vesicularity of the juvenile pyroclasts; c) the lithic component of the PDC deposits; d) the areal distribution of the most energetic EU3pf and EU4b/c units, which were modelized by using a statistical box-model approach.

Lirer et al. (1993; 1997) proposed a multivariate statistical analysis to correlate the AD 79 sequence outcropping in several sites in the peri-volcanic area (Fig. 1.7). They recognized 4 main *marker layers* among the fallout, the stratified surge and the pyroclastic flow deposits and their correlations only partly match the stratigraphic correlations proposed by Sigurdsson et al. (1985) and Cioni et. (1990; 1992).

Luongo et al. (2003a, 2003b), proposed a new stratigraphy for the AD 79 eruption, based on seven sections located close to the city walls of the Pompei excavations and inside the city, using a new descriptive nomenclature. At the base of the PDC succession the authors identified some very thin massive ash layers (unit **C**) with rare, rounded, fine pumice lapilli. Upwards in the sequence, above a well sorted fallout layer rich in lithic clasts (**unit D**), a matrix-supported, stratified bed rich in rounded pumice lapilli in the basal part (unit **E1**) and with numerous sedimentary structures (such as dunes and cross stratification, unit **E2**) towards the top, is observed. The uppermost part of the sequence comprises a succession of plane parallel ash layers with abundant accretionary lapilli (unit **F**, **H** and **L**), separated by three, very thin, lithic rich fallout layers (unit **G1, G3** and **I**).

Scarpati et al. (2020) observed a lower poorly sorted, ash layer (unit **C1**), up to 1.5 cm thick, 5 cm below the top of the grey pumice fallout deposit and reported a detailed description of the upper part of the sequence, documenting for the first time the occurrence of some layers that they named from M to T (Fig. 1.23). The authors recognized the presence of erosive scars and gullies (R1 and R2 unit, Fig. 1.23), filled by lenses of reworked material, at the base of the layer D for the R1 and at the base of the unit E for R2. The first erosive episode R1 occurred before the short recovery of the fallout phase that emplaced layer D, close to the outer side of the northern walls of the city. The second erosive episode R2, more widespread and intense, occurred before the PDC phase that emplaced layer E. The recognition of such erosive episodes is considered to testify for volcanic hiatuses during the AD 79 eruption.

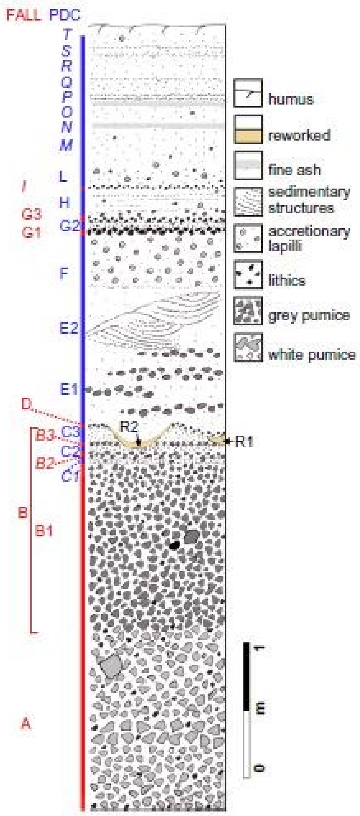

Fig. 1.23 – Composite stratigraphic section of the AD 79 deposits, according to Scarpati et al. (2020). For each unit the mechanism of emplacement is shown on the left: by fallout (in red) and by PDC (in blue). Note the presence of two erosive surfaces filled by reworked material composed of white and grey pumice clasts with a variable abundance of lithic clasts and shells of gastropods, under the fallout layer D (R1) and the PDC layer E (R2). New levels reported in the stratigraphy of the AD 79 eruption by Scarpati et al. (2020) are in italics.

1.4.3 The post-Plinian accretionary lapilli bearing layers: fallout or pyroclastic density current deposits?

Although an overall consensus exists about the AD 79 eruptive dynamics (Sigurdsson et al., 1985; Cioni et al., 1990; 1992; 1999; 2004; Luongo et al., 2003a; Gurioli et al., 2007; Scandone et al., 2019; Doronzo et al., 2022), whether the post-Plinian accretionary lapilli bearing deposits (C1 - Sigurdsson et al., 1985; EU4c and EU8 – Cioni et al., 1992; 2004; F to T – Luongo et al., 2003a; 2003b) were emplaced by fallout or PDCs, is still controversial. All these deposits have been found in several proximal sites around the Vesuvius, up to distal sites about 15 km away from the vent. The main interpretations proposed for these deposits are summarised in Table 5.

Authors	Nomenclature	Description	Fallout/Pyroclastic density current
Sigurdsson et al. (1985)	C1	Dark grey ash with common accretionary lapilli. In all the studied sections, the thickness is relatively uniform.	The deposit represents the transition to the phreatomagmatic phase of the eruption and it is associated with a fallout emplacement.
	Accretionary lapilli layers	The uppermost layers of the AD 79 sequence are undifferentiated dark gray, silty-sandy and pumice-free beds, characterized by abundant accretionary lapilli with cross-bedding and dune structures. The thickness varies from a minimum value 0f 60 cm at Pompeii to a maximum value of 200 cm at Oplontis.	These layers can be interpreted as related to small phreatic and phreatomagmatic explosions which lasted for days or weeks and generated ash fall and wet surges up to 10 km away from the Vesuvius.
Cioni et al. (1990; 1992; 2004) Gurioli et al. (2007)	EU4c	The unit is massive to faintly-laminated, poorly-sorted, accretionary lapilli bearing and matrix-supported ash layer with an uniform thickness (up to 20 cm).	The deposit is a product of the convective co-ignimbritic plume dispersed from the prevailing winds in a south-eastern direction, mainly derived by ash elutration from the current depositing the EU4pf unit.
	EU8	The unit consists of a thick sequence of stratified, phreatomagmatic ash beds, strongly enriched in accretionary lapilli and always characterized by the presence of wet textural features. This unit occurs with variable thicknesses all around the Vesuvius, and, following the topography in the northern and western sectors, the deposit is lithic rich (EU8L) with fresh lava fragments and slightly lithified while in the southern part of the volcano, it shows more evidently ash and flow alternation.	In the southern sector, the unit has been interpreted as deposited from low concentration, turbulent currents in which the accretionary lapilli bearing layers were derived from settling of particles from the trailing ash clouds. In the northern and western sector, the correlated EU8L unit has been interpreted as emplaced from topographically controlled, not turbulent, low velocityand lithic rich pyroclastic currents.
Lirer et al. (1993; 1997)	-	-	The third and last phase of the eruption, pyroclastic flows and surges, associated with phreatomagmatic activity, were the main lithotypes. These products accumalted in the whole perivolcanic area with an elliptical distribution.
Luongo et al. (2003) Scarpati et al. (2020)	F unit	Massive to well-stratified fine-grained ash layer with accretionary lapilli	The unit has been interpreted as emplaced directly from a pyroclastic current.
	L to T units	The L to T units form the upper part of the exposed AD 79 sequence at Pompeii, consisting of alternating massive and well-stratified, poorly-sorted ash deposits, some of which with diffuse accretionary lapilli and	The deposits have been interpreted as emplaced from phreatomagmatic PDCs of the final post-Plinian stage of the eruption.

Table 5 – Summary of the sedimentological descriptions and proposed interpretations for the first post-Plinian accretionary lapilli bearing deposit and the very final post-Plinian deposits of the AD 79 eruption.

The areal distribution about the very final post-Plinian deposits (Fig. 1.24) was reconstructed only by Sigurdsson et al. (1985). The authors estimated a volume of 0.16 km^3 DRE for this last phase of the eruption.

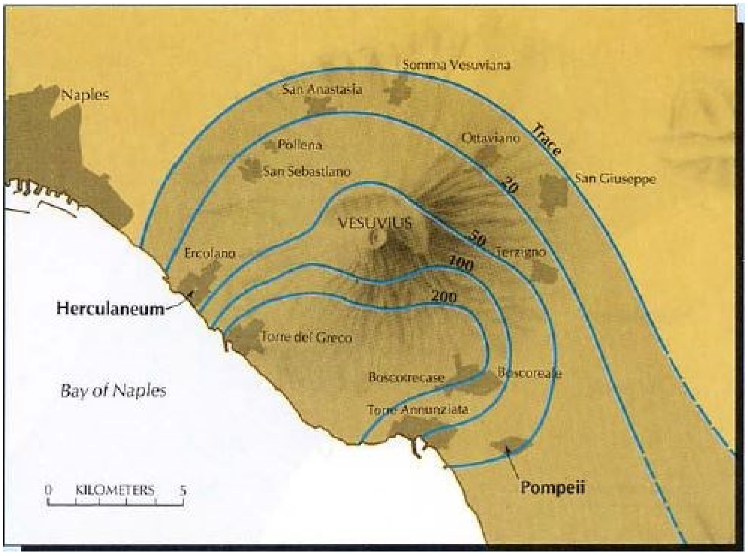

Fig. 1.24 – Areal distribution and thickness (in centimetres) of the accretionary lapilli beds (fallout and surge deposits) of the AD 79 eruption cropping out around the volcano (following Sigurdsson et al., 1985). Note that their thickness and distribution is limited compared to that of the surge deposits.

1.4.4 The role of the phreatomagmatic activity during the course of the eruption

Although there is general agreement that the AD 79 eruption was characterized by phreatomagmatic phases (e.g. Sheridan et al., 1981; Sigurdsson et al., 1985; Cioni et al., 1992; Lirer et al., 1993; Luongo et al., 2003a; Scarpati et al., 2020; Doronzo et al., 2022), the moment at which the transition from magmatic to phreatomagmatic activity occurred and the role of phreatomagmatism during the course of the eruption are still matter of debate.

Sheridan et al. (1981) distinguished "*hydromagmatic explosions*" alternated with purely magmatic activity, which dominated the late stage of the eruption. As a support to this interpretation, they report the observation of "*a sharp increase in the proportions of deep lithic inclusion type fragments such as high-grade contact metamorphic, skarns and cognate plutonic nodes*". Therefore, the authors place the beginning of the phreatomagmatic activity during the grey pumice fallout phase, when "*the eruption becomes discontinuous, with an increased explosivity which widens the vent conduit system above the magmatic chamber as result of vaporization of a small ratio of external water to magma in the chamber during the pumice fallout*". Subsequently, the activity became "*hydromagmatic*" or characterized by "*phreatic explosions*", resulting from an "*abundant source of water available to the chamber when the vent pressing drops below that of hydrostatic head (-300-500 bar)*". The authors interpreted the occurrence of surges of fine-grained ashes, widespread phreato-plinian layers, vesiculated tuffs and phreatic breccias, as a clear evidence of this kind of activity. Furthermore, the occurrence of simultaneous small pyroclastic flows at this stage of the eruption is related to a contemporaneous hydromagmatic and magmatic activity, with marginal hydromagmatic explosions (rather than column collapse) explaining the fine fragmentation typical of the last pyroclastic flows.

Sigurdsson and co-workers (Sigurdsson et al., 1982; 1985; Carey and Sigurdsson, 1987), proposed that interaction between external water and magma had occurred in the very initial phase of the eruption (with the emplacement of the basal ash fallout layer A-1) and in the last phase of the eruption (with the emplacement of a sequence of fine ash beds characterized by abundant accretionary lapilli). The generation of widespread surges and pyroclastic flows, together with an increase in lithic fragments during the final stages of the eruption, was instead interpreted as related to the column collapse due to the concomitant effect of decreasing mass discharge rate and volatile content and increasing vent diameter. Therefore, following this interpretation, the phreatomagmatic phase is confined to the very final stages of the eruption, as testified by the presence of accretionary lapilli. Lirer et al. (1993; 1997), Luongo et al. (2003°; 2003b) and Scarpati et al. (2020) are in agreement with this model.

Barberi et al. (1989) considered the presence of fine ash and the occurrence of deep lithic fragments as "*unequivocal evidence*" for supporting a phreatomagmatic character of the deposits. The component analyses they used to support their model are restricted to the Pozzelle site (Fig. 1.14), which was assumed to represent a "type-section".

The authors recognized some features indicative of a magmatic origin in the pyroclastic sequence up to the VS 84-33 pumice flow deposit [corresponding to the S-4 surge deposit of Sigurdsson et al. (1985)], clearly deviating from the grain size and component pattern of the upper VS 87-1 surge bed [S-5 of Sigurdsson et al. (1985)]. Therefore, they considered the phreatomagmatic phase to have started with the generation of the VS 84-34 coarse fallout bed [A-6 layer of Sigurdsson et al. (1985)], considering the increasing abundance of lithic clasts of deep provenance (mainly skarn, cumulites and marbles) as an evidence for magma/water interaction. Therefore, Barberi et al. (1989) propose a "*transitional phase*" between magmatic and phreatomagmatic phase, occurring in a stage of the eruption that is between those suggested by Sheridan et al. (1981) and by Sigurdsson et al. (1985).

In the following years, numerous authors, such as Cioni et al. (1990; 1992; 1996; 1999; 2000; 2004; 2020) and Gurioli et al. (1999; 2005; 2007; 2010), have largely relied on the model proposed by Barberi et al. (1989). They used "*the sharp increase in the abundance of fragments of deep provenance such as marbles, limestones and cumulates*" as "*distinctive and* *diagnostic elements*" for recognizing stratigraphic markers in the AD 79 pyroclastic sequence (Fig. 1.25).

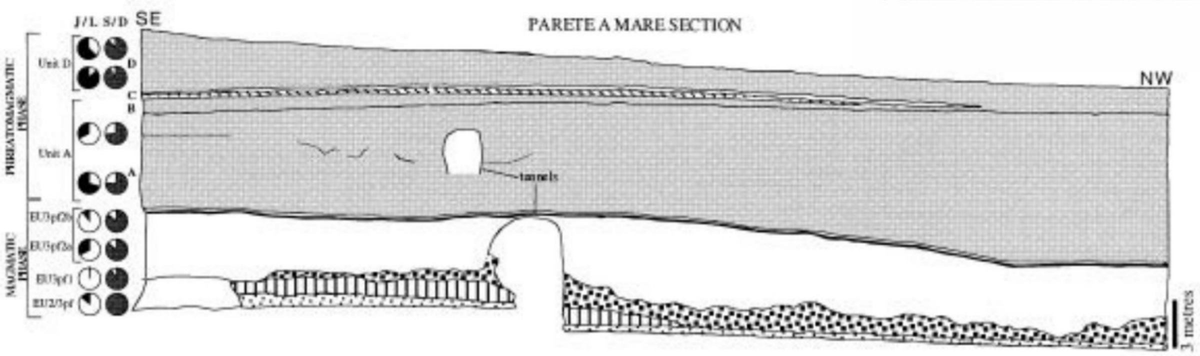

Fig. 1.25 – Stratigraphic sketch for the AD 79 deposits cropping out along the Parete a Mare walls inside the archaeological excavations of Herculaneum as reconstructed by Gurioli et al. (2002). The main eruptive units are indicated by different ornamentation. For each eruptive unit, component data are shown on the left with J/L being the ratio between juvenile (in white) and wall rock lithic fragments (in black), and S/D the ratio between shallow seated wall rock (in dark grey) and deep-seated wall rock (in white) lithic fragments.

1.4.5 Timing of the caldera collapse and its influence on magma-water interaction

Sheridan et al. (1981) first suggested that a "*rupture of the metamorphic encasament*" had occurred during the AD 79 eruption, but only a few years later Sigurdsson et al. (1985) ascribed a very thick (up to 8 m) matrix and poorly-supported deposit with abundant lava and carbonate blocks to a caldera collapse.

Cioni et al. (1990; 1992; 1999; 2004) interpreted the strong enrichment in deep lithic components (e.g. skarns and marbles from the thermometamorphic and metasomatic aureole around the magma chamber, and cumulates) as an evidence for the onset of the caldera collapse. They ascribed the EU4b unit (Fig. 1.26) to the climatic phase of the eruption, characterised by a first destabilization of the magma chamber, the onset of the caldera collapse, the interaction of the magma with external water, and the full collapse of the eruption column. According to their reconstruction, the EU5 unit, consisting of lithic rich (up to 40-50 wt.% of lithic fragments), massive to dune-bedded pyroclastic currents deposits, cropping out only on the slopes and in the main valley of Vesuvius and being completely absent in the southern medial areas, records a further destabilization of the magma chamber (Fig. 1.26). The EU6 unit, which mainly fills topographic lows in the south-eastern part of the volcano up to 6 km from the vent, instead records the climax of the caldera collapse and the final collapse of the roof of the magma chamber (Fig.1.26).

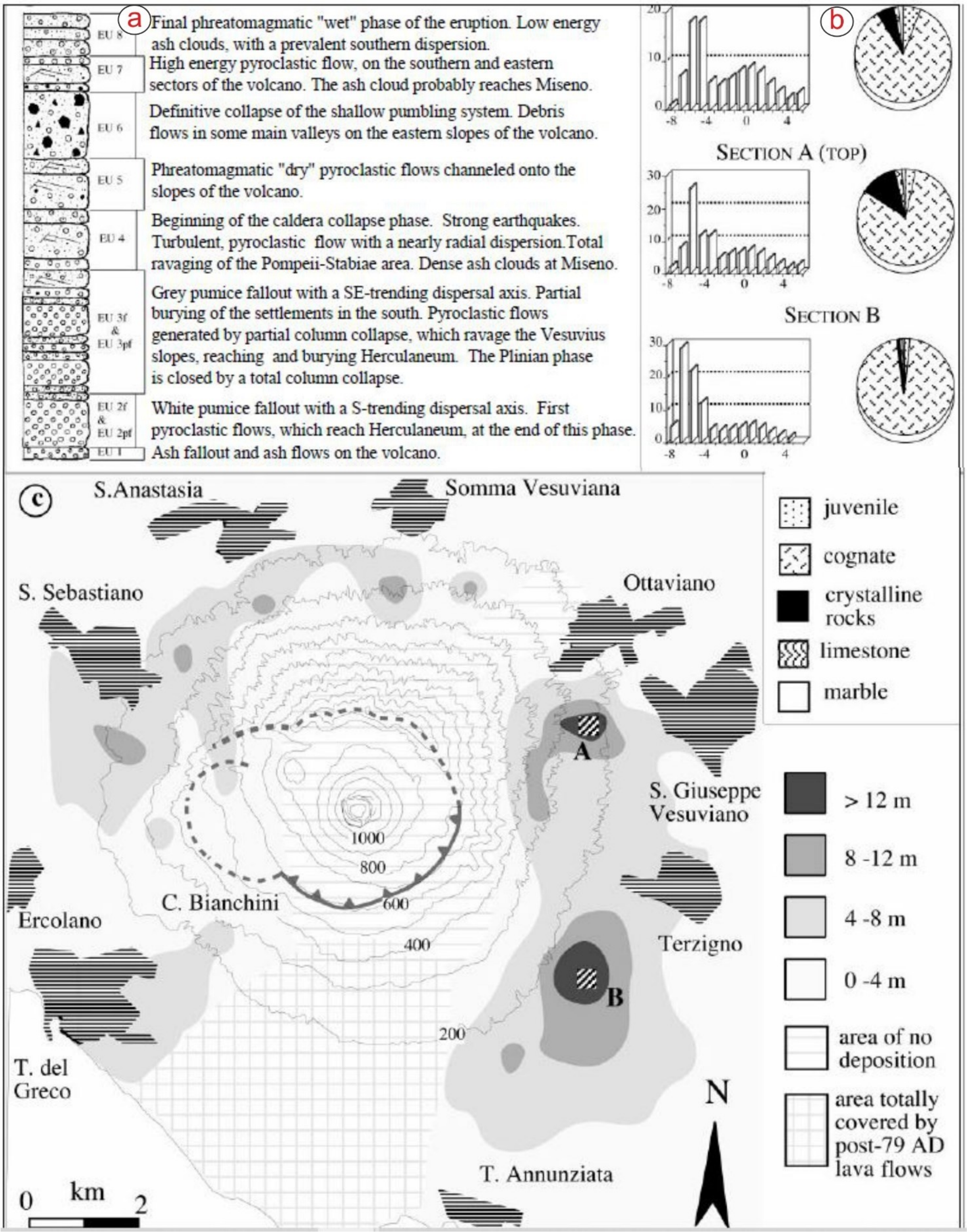

Fig. 1.26 – a) Generalized composite stratigraphic section of the AD 79 pyroclastic deposits (from Cioni et al., 1999). b) Grain size and component analyses of breccia deposits from A and B sections. c) Isopach map of the AD 79 pyroclastic flow deposits and inferred caldera rim.

1.5 Geochemical and petrological variations in the eruptive sequence of the AD 79 eruption

The magma chamber and the pre-eruptive conditions of the AD 79 eruption have been studied by integrated petrological and stratigraphic investigations. In this paragraph, dedicated to the geochemistry of the AD 79 PDC deposits, I report some of the main results and models about the processes acting within the magma chamber during the eruption. A distinctive feature in the stratigraphy of the AD 79 pyroclastic deposits is the marked change of chemical composition and particle density in the transition from white to the grey pumice clasts (Lirer et al. 1973; Barberi et al. 1981; Sheridan et al. 1981; Cornell and Sigurdsson 1984; 1987; Wolff and Storey 1984; Sigurdsson et al. 1985; 1987; 1990; Joron et al. 1987; Carey and Sigurdsson, 1987; Civetta et al., 1991; Cioni et al., 1992; 1995).

Di Girolamo (1968) analysed the pyroclastic sequence inside the Pompei excavations (Regio II and Regio III) and showed that white pumice clasts are leucitic phonolites gradually differentiating towards the top. The upper grey pumice clasts have instead a more uniform and mafic composition. The ash deposits were not considered to reflect the composition of the feeding magma but rather the product of the destruction of the top part of the volcanic edifice.

Barberi et al. (1981) and Joron et al. (1987) interpreted the compositional range of the AD 79 products in terms of fractional crystallization. In their model, a tephritic magma first entered the magma chamber with a temperature of 1200 °C. During a long period of rest (lasted for several centuries at least), the magma experienced some differentiation through crystal fractionation with removal of about 70 wt.% of a mineral assemblage mainly consisting of cpx, pl and lc (plus lesser ol and mt) producing the “grey” magma. Further differentiation through the fractionation of ~20 wt.% of cpx+lc+mt produced the phonolitic “white” magma. As a result of the interaction of the residing magma with the carbonate country rocks, contact reaction skarns were also formed, whose minerals (mainly olivine and plagioclase) were variably incorporated into the magma, modifying its composition and inducing a late precipitation of unusual phases (such as scapolite and cancrinite).

Sigurdsson et al. (1990) used the compositional variations in the juvenile clasts of the AD 79 pyroclastic deposits as indicators of pre-eruptive chemical gradients in magma chamber. The authors suggested a mixing model in which the two endmembers correspond to an evolved phonolite magma (white pumice) and a later-erupted, more primitive mafic phonolite (Fig. 1.27).

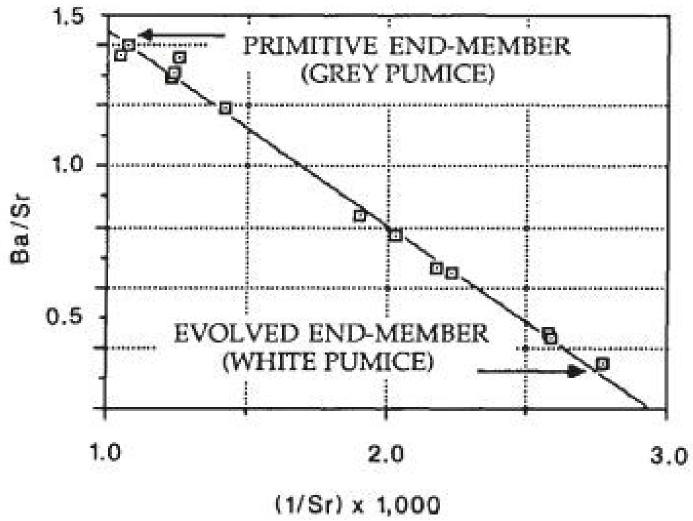

Fig. 1.27 - Plot of Ba/Sr vs. (1/Sr) x 1,000 for pumice clasts of the AD 79 fallout deposit at Pompei (from Sigurdsson et al. 1990). The compositional range covered by white and grey pumice is well represented by a two-component mixing model between the more primitive grey and the evolved white endmembers.

Sigurdsson et al. (1990) also provided an estimate of the water content in the two magma types, being respectively 4.7 and 3.5 ±0.50 wt.% for the white and grey pumice. They further suggested that the compositional trends observed in the white pumice clasts are consistent with either two end-member mixing or a slight pre-eruption chemical gradient in the white magma, proposing that some mixing should have occurred at the grey-white pumice transition. Further mixing of the two endmembers occurred after the first tapping of the grey mafic magma.

A thorough study of the geochemistry of pyroclastic deposits of the AD 79 eruption was conducted by Civetta et al. (1991), who presented isotopic data on whole rock, glass and mineral separate samples. They observed that both white and grey pumice clasts show some variability in both major and trace elements concentrations (Fig. 1.28), as well as distinct Sr and Nd isotopic compositions, interpreting these as related to a repetitive history of magma refilling within the Vesuvius shallow reservoir. In their model, Civetta et al. (1991) suggested that the magma chamber before the AD 79 eruption was characterised by a significant amount of “residual” magma, i.e. some magma that was not erupted during the previous eruption. This magma, enriched in crystals and depleted in volatiles due to degassing, was relatively basic in composition (tephritic-phonolitic). During the AD 79 eruption, new batches of magmas with different isotopic ratios entered the chamber, mixing and convecting with the less-differentiated residual magma. The mixed magma then experienced some magma chamber processes and formed a highly differentiated "white" portion capping the convective "grey" portion.

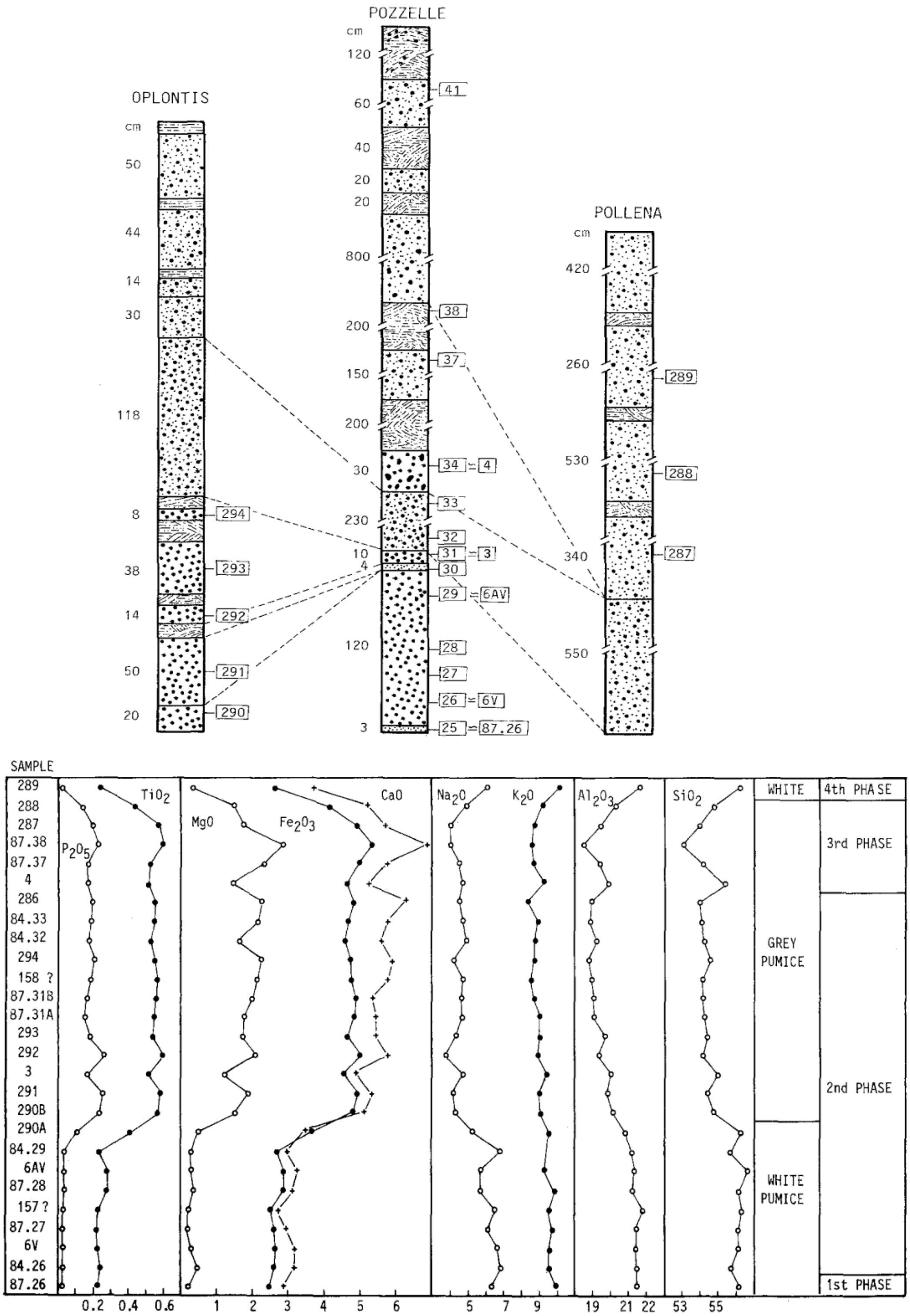

Fig. 1.28 – Vertical chemical variations for the juvenile fraction in an idealized and composite section of the AD 79 pyroclastic deposits. Samples location and numbers are reported in the stratigraphic columns on the top (from Civetta et al., 1991).

Cioni et al. (1992) observed a clear vertical compositional variation for some trace elements and major oxides in the juvenile fraction of the AD 79 eruption (Fig. 1.29). They recognized two different trends within the stratigraphic unit of the white pumice (EU2 unit), while the grey pumice clasts resulted more homogeneous, with a peak of less evolved compositions in the centre of the fallout sequence, immediately before the first deposits of partial column collapse (the EU3pf). These authors were also the first to provide new data for the third, phreatomagmatic phase of the eruption, which lead them to suggest that even less evolved phono-tephritic magmas were emitted during the EU7 phase, immediately after the caldera collapse.

More in detail, the authors highlighted that the pumice clasts from "magmatic" pyroclastic flow deposits (EU2pf and EU3pf) exhibit homogeneous composition well overlapping that of the coeval pumice fallout layer. Conversely, the pumice clasts from "phreatomagmatic" pyroclastic flow deposits (EU4, EU6, EU7) are generally heterogeneous in composition. Such difference is considered to reflect the regular withdrawal from a zoned magma body during the Plinian phase, and the extraction from a chaotically destabilized magma chamber during and after the caldera collapse, as also testified by the highly variable content of cognate material from the collapsing walls of the chamber.

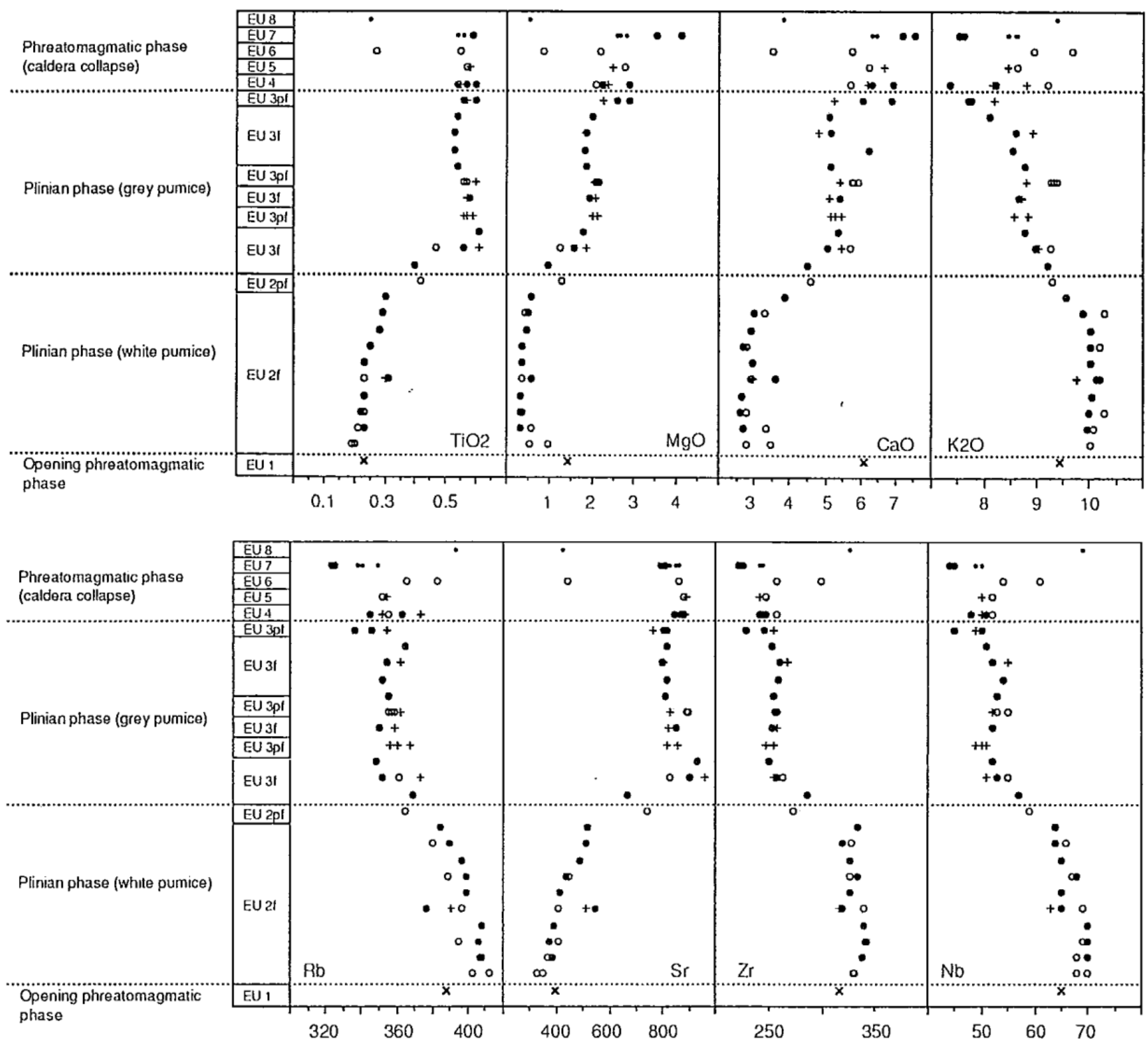

Fig. 1.29 – Some major oxides and trace elements variations in the juvenile fraction of the AD 79 deposits from the stratigraphic sections of: O, Pozzelle Quarry, •, Necropolis, . ,Terzigno Quarry, †, Oplontis, x, Villa Telesi (Cioni et al., 1992).

Cioni et al. (1995; 1999) and Gurioli et al. (1999; 2002) report the occurrence of white pumice clasts (together with grey ones) in the pyroclastic flow deposits associated with the final, phreatomagmatic phase of the eruption (EU4, EU6 and EU8), attributing them to a "*tapping of nearly pristine white magma trapped roofward in the chamber and not involved in the turbulent mixing*".

Lirer et al. (1993) used a chemostratigraphic approach to correlate several stratigraphic sequences of the AD 79 eruption. They observed a vertical variation of the CaO in the glass shards of crushed pumice fragments showing three compositional trends (Fig. 1.30). According to the authors, one represents the composition of white pumice (about 3.0 wt.% CaO) and the other two (with CaO in the ranges of 4.0-4.5 and 5.0-5.5 wt.%) represent variations of the grey pumice clasts. These two compositions often occur within the same pumice fragment.
Pumice clasts from the fallout and surge deposits directly overlying the white fallout pumice deposits yielded both phonolitic and tephritic-phonolite compositions. On the other hand, the products from the upper part of the sequences show tephriphonolitic compositions with two distinctive CaO contents (about 4.0 and 5.0 wt.%, respectively). The authors interpreted these as the result of the mixing between a salic phonolitic magma (the first erupted) and a tephritic phonolite one, producing the intermediate "mafic phonolite" composition (CaO 4.0-4.5 wt.%). They suggest that the co-existence of the two grey compositions within the same pumice clast could be explained by the syn-eruptive mingling between the endmembers consisting of tephritic phonolite and the intermediate "mafic phonolite" magma.

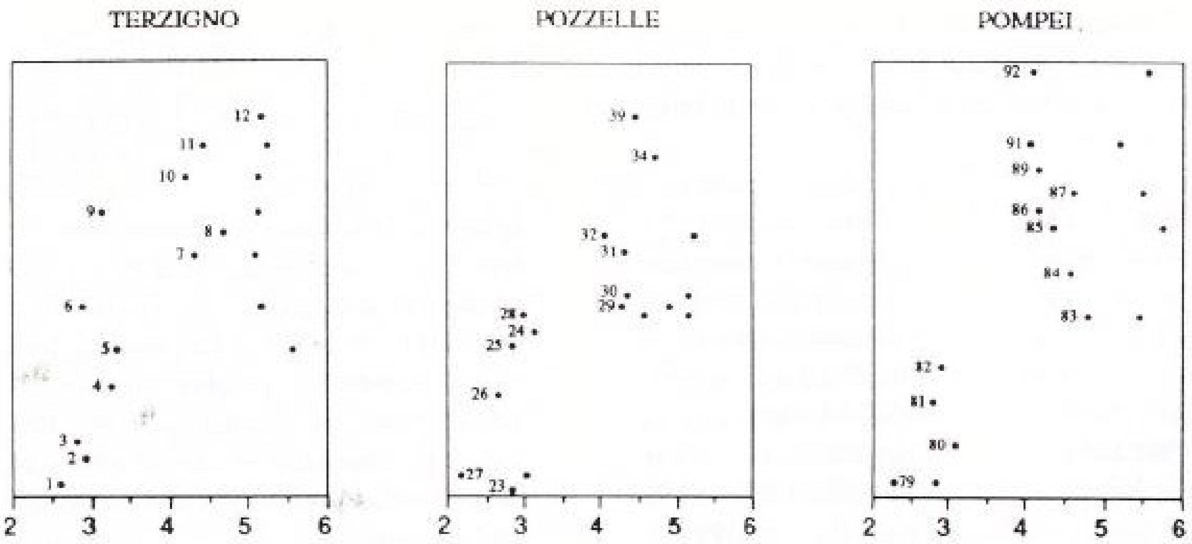

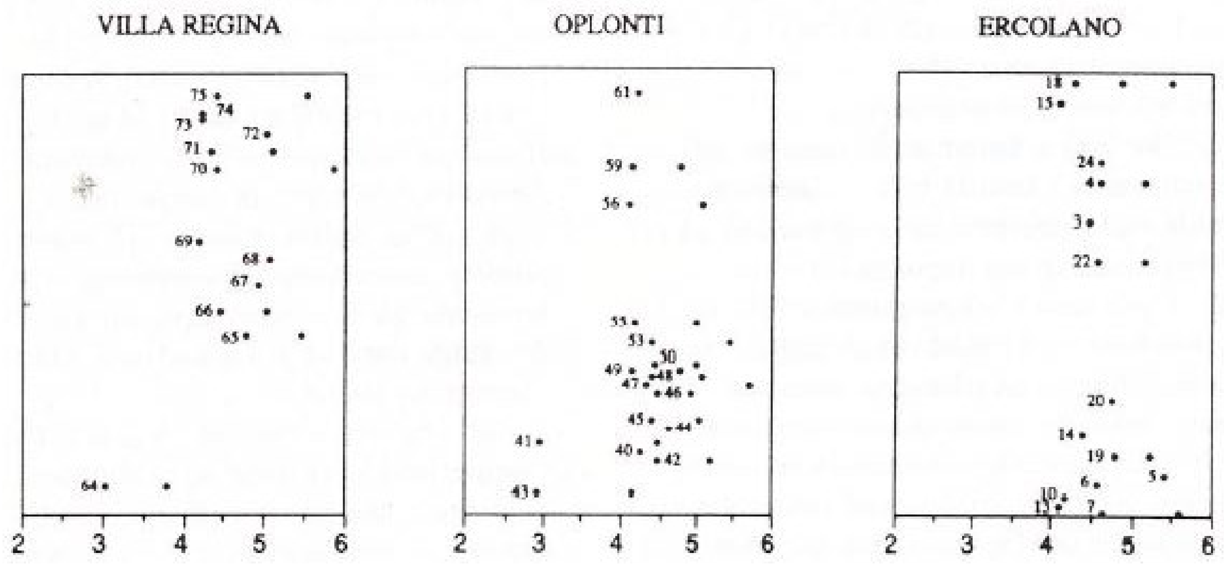

Fig. 1.30 – Vertical variation of CaO content (in wt.%) in the juvenile fraction along six investigated AD 79 sequences of Pompei (from Lirer et al., 1993). Note the three compositional trends (see text for further explanation).

Mues-Schumacher (1994) interpreted the differences between white and grey pumice clasts in terms of fractional crystallization of clinopyroxene, sanidine and leucite. According to the author, the well-developed vertical gradients observed for the white pumice clasts indicate a stable layering within the upper phonolitic magma body, originating from diffusion of highly incompatible elements. The lack of a similar stratigraphy-related zonation within the grey pumice clasts is instead taken as an evidence for a more homogeneous tephriphonolitic magma resulting from continuous convective mixing within the lower part of the magma chamber. Mues-Schumacher (1994) also reported the presence of a "*boundary zone"* at the transition from white to grey pumice, characterized by the presence of both white and grey pumice clasts and by a third type of pumice clast, "*the boundary pumice*". This pumice clast is light grey in colour and internally homogeneous, without evidence of physical mingling between "white" and "grey" magmas and displays and intermediate composition between the grey and white pumice clasts, especially evident for MgO, K_2O and Ba contents. The boundary pumice would have represented a third magma component in the magma chamber, the interface magma layer, resulting from mixing and diffusion processes across the phonolitic/tephriphonolitic magma boundary, which likely occurred prior to the eruption.

Cioni et al. (1995) conducted a very detailed study of both the pumice and the cumulate lithic fractions of the AD 79 deposits to reconstruct the thermal, compositional and isotopic pre-eruptive layering of the shallow magma chamber, investigate the syn-eruptive mixing between the different magmas occupying the chamber and recognize the variability of mafic magma batches feeding the chamber.

They suggested that during the different phases of the eruption, about ~25-30% of the magma was ejected as white K-phonolitic pumices while 70-75% as grey K-tephri-phonolitic pumices. Therefore, the white pumice clasts would have represented a magma that was produced by the differentiation of a residual aliquot of tephriphonolitic magma from the previous Plinian eruption of Avellino, leading to the development of a compositionally layered cap in the magma chamber. The early-erupted units fed by such evolved magmas (the EU1 and EU2 fallout layers) would have been therefore chemically homogeneous, with only slightly higher SiO_2, MgO and CaO and lower Al_2O_3, Na_2O, and K_2O in EU2. The grey pumice clasts would have instead resulted from syn-eruptive mixing involving three main end-members: the phonolitic "white" magma (salic end-member, **SEM**), mafic cumulates (cumulate end-member, **CEM**) and a crystal-poor grey phono-tephritic magma (mafic end-member, **MEM**), never erupted without first being mixed with the "white" magma. The grey mafic magma has a homogeneous composition and constant $^{87}Sr/^{86}Sr$ isotopic ratio, possibly because of sustained convection, high temperatures of 1000-1100 °C, a very low viscosity and relatively low densities.
Notwithstanding the chemical differences, the two main pumice types were reported to be largely similar, both including phenocrysts of kfs and cpx (plus lesser bt, lc, grt, amph, pl and sporadic ol, ap and ne), set into a glassy groundmass with microlites of lc, kfs, cpx, amph and bt. Nevertheless, the authors also reported a remarkably lower density for the white pumice clasts (600-700 kg/cm^3 vs. 800-1200 kg/cm^3). In addition, the two are also distinguished by their groundmass, with that of the white pumice clasts including colourless glass and abundant lc grains (plus lesser kfs, cpx, amph and bt), whereas that of the grey pumice clasts has a brownish glass and a higher load of generally larger crystals (mainly including lc cpx and bt).
Cioni et al. (1995) also focused on the ejecta hosted in the AD 79 deposits, mainly represented by skarn and crystalline silicate rocks. These generally represent about 1-5 wt.% of the deposit, with the peak being found in the coarse-grained basal bed of the EU4. The skarn ejecta were classically considered as the product of the thermal contact metamorphism (plus metasomatism) at the magma/carbonate country rock interface. Such magma-wall-rock interaction could have played also some role on the eruptive style, as it could have significantly increased the CO_2 content of the magma (e.g. Jolis et al., 2015). The crystalline silicate rocks were instead interpreted to represent both cumulitic rocks and metasomatic cumulitic ejecta, representative of an intermediate "assimilation zone" between the skarn shell developed around the carbonate country rocks and the cumulate rocks of the inner magma chamber walls.
In the following years, several authors further have investigated the petrology of the AD 79 deposits and the chemostratigraphic variations in the juvenile components (e.g. Ayuso et al., 1998; Cioni et al., 2000; Morgan et al., 2006; Shea et al., 2014, Melluso et al., 2022), as well as the composition of fluid (FI) and melt inclusions (MI; Marianelli et al., 1995; Cioni et al., 1998; Fulignati et al., 2004; 2011; Balcone-Boissard et al. 2008; 2011). These latter studies

have provided significant insights as to the processes of volatile accumulation and degassing in the different portions of the magma chamber allowing to unravel the factors that governed the transition from an initial phase of steady state sustained column, to a following phase of oscillatory eruptive column. Large variations in both residual volatile contents and textural features were observed between the different eruptive units and pumice types, suggesting that degassing processes were highly heterogeneous. More in detail, Balcone-Boissard et al. (2011) proposed that pre-eruptive conditions had a strongly influence on the syn-eruptive degassing processes and thus on the eruptive dynamics. The white and the upper part of the grey magmas were demonstrated to be H_2O-saturated prior to eruption. In this framework, the eruptive units fed by the "white magma" were interpreted as related with a closed-system degassing evolution. On the other hand, the first units featuring grey pumice clasts, though stored under similar pre-eruptive conditions with respect to the "white magma", followed an open-system degassing evolution, as indicated by their textural features. The oscillatory regime that dominated the later "grey magma" eruptive phase would have been related to pre-eruptive water undersaturation of most of the magma, and the associated time delays necessary for H_2O exsolution. In addition, the high residual H_2O content of the "grey magma" erupted after the renewal of Plinian activity following the first column collapse, were interpreted as related with the syn-eruptive saturation and reduced H_2O exsolution efficiency.
Additional insights on the petrology of the AD 79 juvenile products have been obtained by means of experimental investigations (Scaillet et al. 2008; Shea et al., 2009; 2014). The decompression experiments performed by Shea et al. (2009) failed to reproduce the textural features of lc crystals from the white pumice clasts, which were on the contrary well reproduced by equilibrium crystallization experiments. As the first are considered to approach conduit conditions while the seconds are in line with those of the magma chamber, the authors concluded that lc crystallisation did not occur during rapid magma ascent but rather occurred over longer time intervals of days at lower degrees of undercooling. Furthermore, the authors proposed that the "white magma" was not only compositionally- but also thermally-zoned, with upper portions feeding the EU1 reaching equilibrium at 830-840 °C, while the lower ones (EU2) formed in the 850-925 °C range (both at ~100 MPa). A similar thermal variability was previously reported for the MI hosted in the white pumice clasts analysed by Cioni et al. (1998), who obtained two clusters of homogenisation T, in the range of 800-850 °C and 900-950 °C, respectively. Shea et al. (2009) suggested that these T differences could have reflected the late arrival of a tephritic magma that mixed within the residing magma to produce the tephriphonolitic "grey magma". This is also in line with the results from Cioni et al. (1998), who found two distinct populations of homogenization temperatures in MI for the white pumice clasts, one between 800 and 850 °C (in agreement with those for EU1), the other between 900 and 950 °C (roughly in line with those for EU2). Finally, as the crystallisation experiments

performed by Scaillet et al. (2008) allowed the authors to explore the intensive parameters characterizing the magmas feeding the AD 79 eruption, which were also compared to those of other explosive Vesuvian eruptions (Mercato, Avellino and Pollena). The results indicate that pre-eruptive conditions would have been characterised by 200 MPa, 815 °C and 6 wt.% of dissolved H_2O and relatively high oxygen fugacity. In addition, comparison with experimental results obtained for other explosive Vesuvian eruptions (Mercato, Avellino and Pollena) led the authors to suggest that magma reservoirs have migrated upwards through time, from 7-8 km to 3-4 km (as in the case of the AD 79 eruption). This trend was also accompanied by an increase of MgO and T with time, based on geothermobarometric and MI data from older (the Pomici di Base) and younger (AD 1631, 1906 and 1944) eruptions.

At the end of this brief summary on the overall petrology of the AD 79 eruption, some critical points regarding the petrochemistry of the AD 79 magmatic and phreatomagmatic pyroclastic flow deposits can be highlighted:

1) the petrological and geochemical features of the magmas feeding the main fallout phase of the eruption have been extensively studied over the years, while the those regarding the magma that were tapped during the partial and total column collapse phases have been only partly addressed.
2) Civetta et al. (1991) and Cioni et al. (1992; 1995), based their geochemical correlations on an assumed stratigraphic scheme that appears not always well-constrained, in the light of more recent studies about the complex architecture of large ignimbrite deposits (e.g. Branney and Kokelaar, 2002; Brown and Branney, 2004). This is particularly true for the deposits that crop outside the dispersal area of the fallout deposits, on the northern and western sector of the volcano, as already discussed in the paragraph 1.4.2. This casts some doubts, e.g., on the correlations proposed by Cioni et al. (2004) between the deposits cropping out in the northern and southern sectors of the volcano (see Fig. 1.16) and by Civetta et al. (1991), who considered the Pollena sequence to be correlated with the AD 79 stratigraphy observed along the southern flank of Vesuvius (see Fig. 1.28).
3) The joint occurrence of both the white and the grey pumice clasts in the pyroclastic flow deposits associated with the final, phreatomagmatic phase of the eruption should be systematically studied and further discussed, because this feature is instead observed in most of the post-Plinian units (see chapter 2 and 5).

1.6 Impact of the AD 79 eruption: damages and cause of death during the partial and total column collapses

The AD 79 Vesuvius eruption buried the Roman towns around the volcano under several metres of pyroclastic materials. The destruction of these towns allowed volcanologists to build models that can provide valuable information on the extent and type of damage that a future Plinian eruption could cause in urbanized areas. Detailed descriptions of the effects of explosive eruptions on urban settlements are relatively rare. Apart from disease and starvation, the largest number of human deaths caused by explosive eruptions in the twentieth century are due to pyroclastic flows (e.g. Baxter et al., 1998; 2008; Esposti Ongaro et al., 2002).

In the following paragraph, I will summarize the main damages suffered by buildings and population during the intra-plinian and post-plinian PDC phases of the AD 79 eruption, reporting the stratigraphic height at which were recovered human bodies and crumbled walls (mainly at the Pompei and Herculaneum excavations), and focusing on some critical points such as:

a) what is the impact of the magmatic and phreatomagmatic PDCs? Is the extent of damages the same for the two phases?
b) what are the main causes of death by PDCs?
c) how does the gradually increasing distance from the vent affect the behaviour of the PDCs?

Following the early excavations, started in 1748 (Maiuri, 1958b), ongoing systematic archaeological investigations have brought to light a large part of the city of Pompei, which thus became one of the most important archaeological sites worldwide, as well as a volcanological heritage and milestone in modern volcanology (e.g., Scandone et al., 2019; Giacomelli et al., 2021).

Di Girolamo (1968) and Sigurdsson et al. (1985), reported the occurrence of damages and victims, in some lower PDC deposits (corresponding to the S-4 and S-5 surge) and mainly in the S-6 unit.

Cioni et al. (1990; 1992) also reported the presence of a cluster of bodies in the EU4b unit, while Cioni et al. (2000) described the recognition of tiles and bricks in the EU3pf unit. According to recent experiments and numerical modelling on the pyroclastic current-building interaction (Doronzo and Dellino, 2011), the EU3pftot unit is interpreted to have reached Pompei and entered the city by overcoming its walls, without leaving any remarkable visible effects on the buildings.

Lirer et al. (1993; 1997) described findings of building fragments such as tiles and bricks at the stratigraphic height of EU4b unit.

The first systematic study about the interaction of the most destructive PDC [i.e. that emplacing the S-6 surge of Sigurdsson et al. (1985), corresponding to the EU4b of Cioni et al. (1992; 2020) and the E1 unit of Luongo et al. (2003a); see section 1.4 and Table 1] and the urban structure of Pompei, was carried out by Luongo et al., 2003a (Fig. 1.31). The authors observed that the distribution and the type of damages were not homogeneous throughout the city and some buildings were more affected than others, suggesting a non-uniform behaviour of the pyroclastic current. The northern, relatively proximal, and the southern, relatively distal, sectors of the city were indeed observed to be generally destroyed in the same way. The ground floor appeared partly intact in most of the buildings, whereas the upper floor it was almost completely demolished. In addition, the east-west oriented walls resulted by far more damaged than those striking north-south, and a channel-shaped profile was observed in many of these demolished walls. The authors reported the presence of abundant debris and tiles in the lapilli fallout deposit and recognized that most of the destruction was associated to unit E (Fig. 1.31).

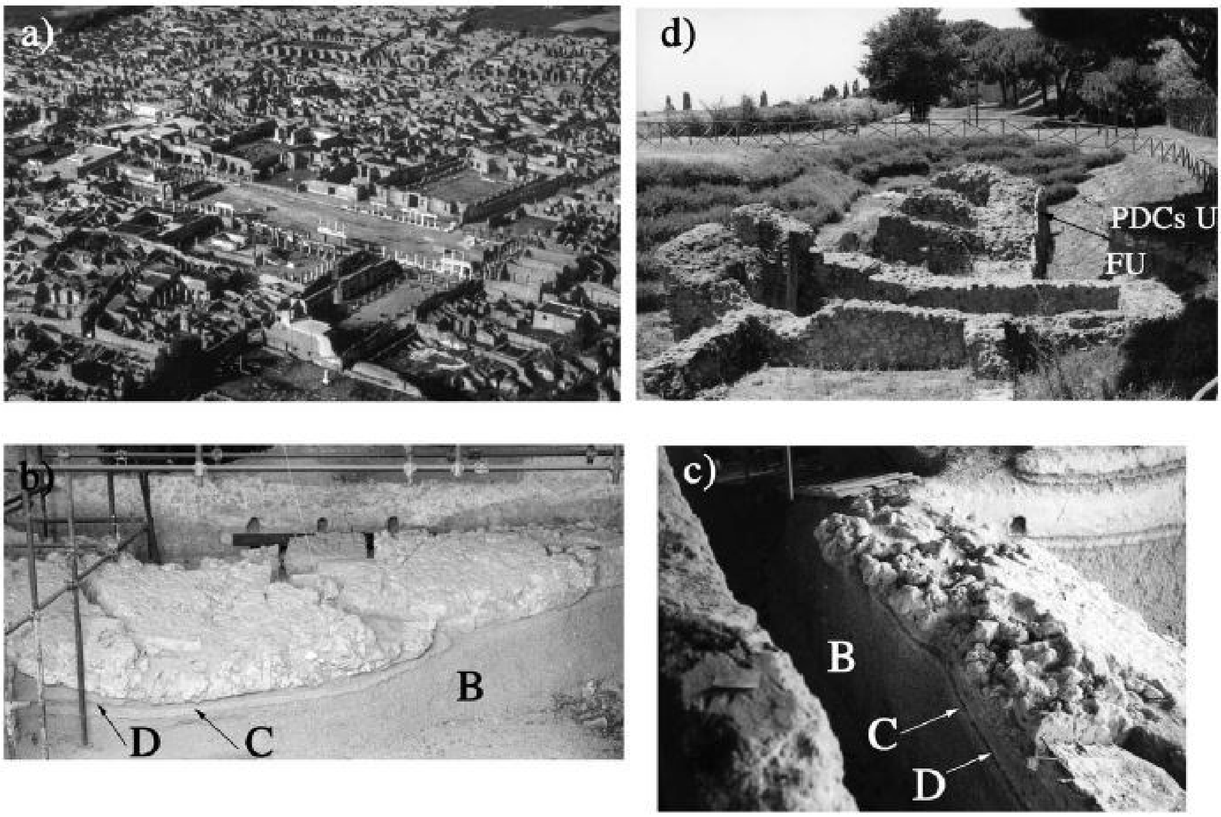

Fig. 1.31 – Field photographs showing the state of the buildings at the Pompei excavations (from Luongo et al., 2003a). The letters B, C and D refer to the stratigraphic units. a) Aerial view of the city showing that the upper floors of most buildings are missing. b) House of the Chaste Lovers: the wall, transversal to the flow direction, lies in the unit E1, with the lithic rich unit D being below the wall. c) Rear view of the same toppled wall of b): on the left is the still standing wall, while on the right is the upper part of the

wall laying above unit D. d) Section of the city walls showing a high amount of destruction in the northern, volcanic vent-facing side. The flow direction is from right to left. FU is for fallout units and PDCs U is for pyroclastic density current units. The arrow indicates the profile of the destroyed wall above the base of the PDCs deposit.

Gurioli et al. (2005a) defined the urban disturbance caused by the emplacement of the EU4pf, quantifying its flow direction at the moment of its deposition and examining the magnetic fabric of the fine matrix of the deposits (Fig. 1.32).

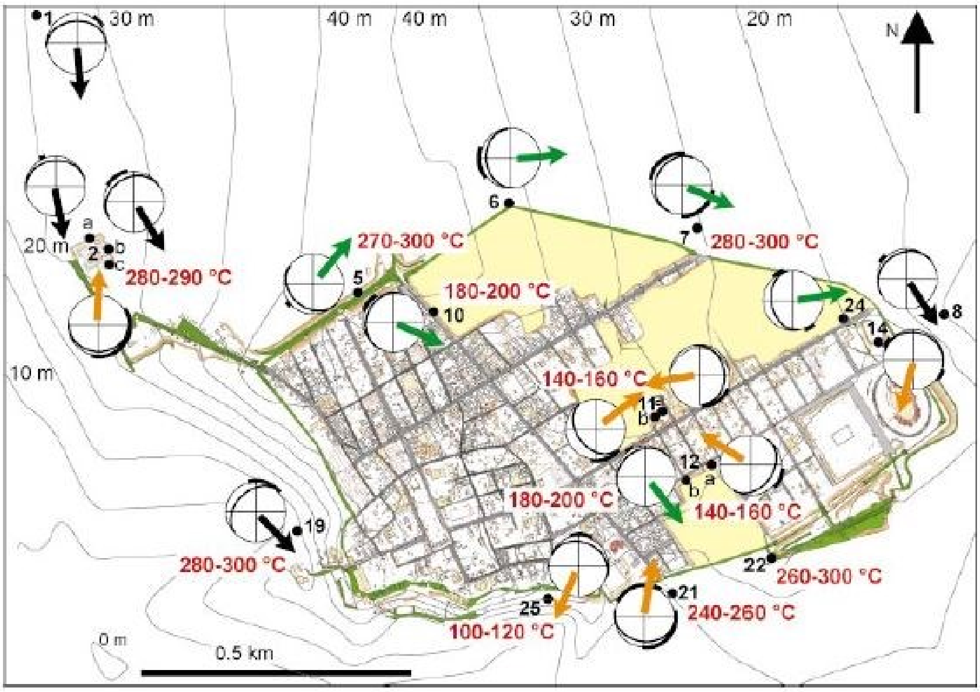

Fig. 1.32– Variations in the EU4pf unit (that corresponds to the S-6 unit of Sigurdsson et al., 1985 and E1 unit of Luongo et al., 2003a and Scarpati et al., 2020) flow direction and temperature. Dots indicate sampled sites while the black lines refer to paleocontours in metres before the AD 79 eruption. According to Gurioli et al., 2005a and the following work of Gurioli et al., 2007, the densest, lowermost portion of the EU4pf current kept its original physical characteristics, interacting with obstacles of a few metres in height and showing the most efficient interaction with the town (in agreement with the model of Luongo et al., 2003a) while the upper part of the current, above the level of the town’s structures, was completely unaffected.

A few years later, Gurioli et al. (2007) investigated the effects of both the diluted (those of EU3pf, EU7pf and EU8) and less diluted (EU4pf) AD 79 pyroclastic currents, demonstrating how building-induced roughness strongly influenced flow directions. In the case of the EU3pf, EU7pf and EU8, the interaction with the structures was minimal (no artefacts are indeed reported for these units) and the currents engulfed the city without inflicting serious damage on the structures. In contrast, the EU4pf current had a significant impact, seriously damaging many structures. The lower part of this current left deposits up to 3 m thick, which interacted with 2-to 4 m high obstacles. Due to the irregular topography of the town, the high-concentration lower part of the current EU4pf was divided into several streams, which followed the external walls of the city and filled roads. According to the authors, the most significant deviations are found in the deposits inside rooms or up-flow and downflow of localized obstacles (such as walls), where in some cases local flow direction is opposite to the main flow direction, as inferred from patterns in building damage previously reported by Luongo et al. (2003a). Inside rooms, Gurioli et al. (2007) performed rock-magnetic measurements, whose results indicate that single vortices had developed, decreasing the temperature at the base of the current (and consequently in the emplaced deposit).

The effects of the eruption on the inhabitants of Pompei, Herculaneum and the other urban settlements close to the volcano, have been the subject of several studies (Baxter, 1990; Capasso, 2000a; Mastrolorenzo et al., 2001a, b; Capasso, 2001; Petrone, 2002; De Carolis and Patricelli, 2003; Giacomelli et al., 2003; Luongo et al., 2003b; Mastrolorenzo et al., 2004, 2010; Petrone, 2011a; De Carolis and Patricelli, 2013; Petrone et al., 2018; Dellino et al., 2021; Doronzo et al., 2022).

At Pompei, the first victim of the AD 79 eruption was found in 1766. The discovery aroused considerable sensation and was followed by the finding of 34 bodies brought to light two years later (De Carolis et al., 1998). The features of a human body were first set in a plaster cast in 1863, a new technique adopted in Pompei by Giuseppe Fiorelli, archaeologist and director of the excavations (Stefani, 2010). Since then, at least 1300 bodies of victims have been found in the town (De Carolis et al., 1998). For at least two centuries the history of the last minutes of life and the death of the inhabitants of the cities and the villas located at the foot of Vesuvius was based on the assumption that all the residents at the time of the eruption had died of slow asphyxiation due to the inhalation of lethal gases. The main evidence for this lies in the protective attitude of the victims, as the postures of many casts seemed to testify (e.g. Maiuri, 1961; Baxter, 1990). As shown in the Table 6, 394 corpses were found in the pumice fallout deposit and 650 in PDCs deposit. Therefore, a total of 1044 victims were recovered inside 2/3 of the city of Pompei (the excavated part). Further 100 victims were estimated based on many groups of scattered bones. Most of the corpses within the pumice fallout deposit were found inside buildings (about 80%) whereas 334 out of 650 corpses recovered in the PDCs deposits were found inside buildings, the remaining 316 being found outdoor (Table 6).

Luongo et al. (2003b) stated that all human casts in the PDCs deposit lay over the well-recognisable lithic-rich unit D, enclosed within the unit E. These corpses are mostly intact and only few corpses are partially or totally dismembered. Most of the casts lie prone in the attempt to shelter their face, while in some places human casts show the head and the bust supported by arms, with this raised part of the body at higher stratigraphic level within E1 unit.

	Victims in the Fall deposit		Victims in the PDC deposit		
	Indoor areas (a)	Outdoor places (b)	Indoor areas (a)	Outdoor places (b)	Total
External areas	17	17	49	70	153
Regio I	66	9	86	41	202
Regio II	12	7	26	73	118
Regio III	9			4	13
Regio IV	1	1			2
Regio V	40		11	16	67
Regio VI	41	2	39	35	117
Regio VII	59	5	33	14	111
Regio VIII	21	5	43	51	120
Regio IX	69	1	43	7	120
Unknown location	10	2	4	5	21
Subtotal	345 (88%)	49 (12%)	334 (51%)	316 (49%)	
Total	394 (38%)		650 (62%)		1044

Table 6 – Summary of the corpses found in the pumice fallout deposit and in the stratified PDC sequence at Pompei, inside buildings or in outdoor places (from Giacomelli et al., 2003).

Sigurdsson et al. (1985) described the products of the AD 79 pumice lapilli fallout as a “relatively innocuous” Plinian fallout phase when compared to the later PDCs deposits and reported that the most of the victims lay above it.

Luongo et al. (2003b) demonstrated that during the first phase of the eruption, a huge quantity of pumice lapilli fell on Pompei, burying the city under 3 m of pyroclastic material. During this phase, 38% of the victims were killed mainly because of roofs and walls collapsing under the increasing weight of the deposit (De Carolis and Patricelli, 2003, 2013). During the second phase of the eruption, 49% of the total victims were on the roadways and 51% inside buildings. All of them were killed by an unanticipated PDC. According to the authors, casts of some excavated corpses lie above the basal part of the PDC unit E (Fig. 1.33), testifying that some of the inhabitants survived the first pyroclastic current that deposited layer C. On the other hand, the most destructive current depositing unit E1 likely caused the victims to die quite rapidly by ash asphyxiation (in agreement with Maiuri, 1961; Giacomelli et al., 2003; De Carolis and Patricelli, 2003).

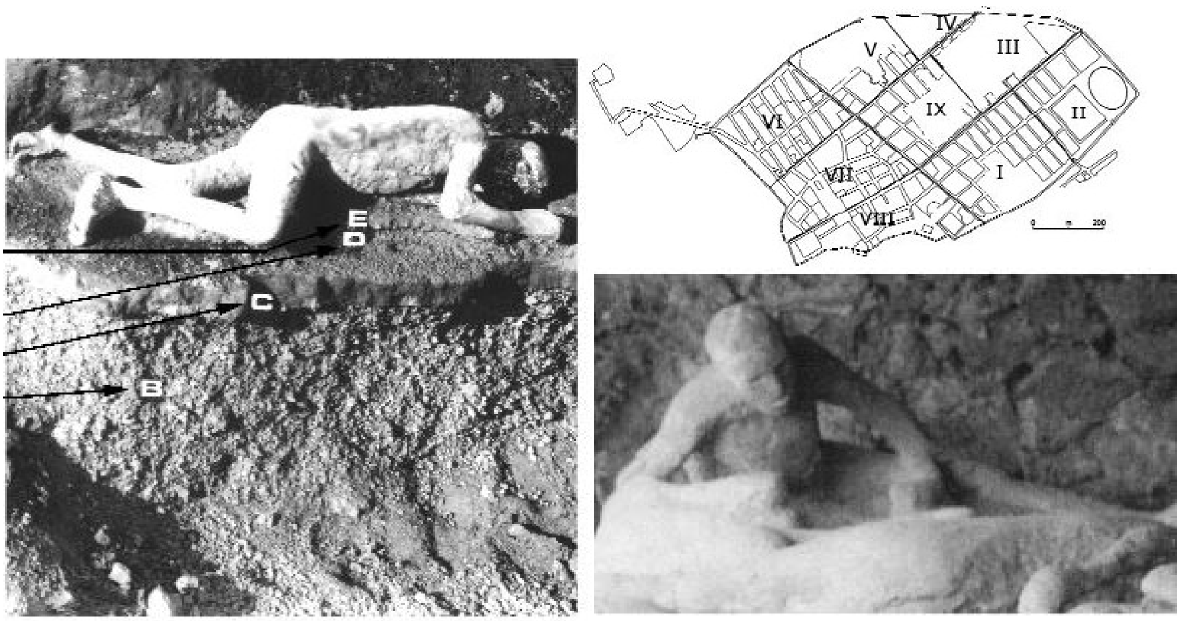

Fig. 1.33 – On the left, a human cast lying above a well-exposed sequence from the unit B to the unit E according to the stratigraphy of Luongo et al. (2003a) and Scarpati et al. (2020). On the lower right, a human cast attempting to support himself from the aggrading deposit. On the upper right, a map of Pompei excavations: the roman numbers are referred to the regions of the city.

Mastrolorenzo et al. (2010) developed a numerical model for the PDC depositing the EU4pf in which the current crossed Pompei as a dilute poorly energetic dusty gas cloud, with temperatures between 250 and 600 °C. The authors suggested that neither asphyxia nor impact force, but rather heat was the main cause of death of the people of Pompei.

Dellino et al. (2021) estimated the duration of the flow of the PDCs entering the town using a numerical method and concluded that the PDCs had low strength and low temperature, as suggested by the absence of signs of trauma on the victims (e.g. bone dislocations or fractures). Under such conditions, survival could have been possible if the current lasted just a few minutes or less. The authors calculated a flow duration of 17 min, long enough to make the breathing of ash suspended in the current, lethal.

Unlike Pompei, Herculaneum was mostly out of the main dispersal region of the Plinian fallout, and therefore no destruction was caused during the first hours of the eruption. The city was instead buried beneath 20 metres of pyroclastic flow deposits (e.g., Sheridan et al., 1981; Sigurdsson et al., 1985; Gurioli et al., 2002). Stratigraphy and paleotemperature determinations have shown that pyroclastic surge and flows reached the town with discrete pulses (Sigurdsson et al., 1985; Gurioli et al., 2002; Caricchi et al., 2014; Giordano et al., 2018). Early arrivals severely damaged buildings and were mixed with debris and surface water, leading to highly variable local conditions of emplacement, and temperatures up to about 500

°C. Later pyroclastic flow deposits buried the town at lower temperatures of about 350 °C on average (Caricchi et al., 2014; Giordano et al., 2018).

A detailed systematic study on the interaction of the main PDCs with the urban structure of the city of Herculaneum was carried out by Gurioli et al. (2002), who suggested that the behaviour of pyroclastic currents entering the city was affected by even small local irregularities of the urbane substratum such as the presence of buildings and steps. The density stratified flow that emplaced the EU4b deposit experienced clear disturbances when its dense and viscous basal layer crossed small obstacles and steps, leading to the development of a reversely graded coarse ash layer. In the model proposed by Gurioli et al. (2002), the interaction with the town structures is different for the pyroclastic currents of the phreatomagmatic activity. In fact, the dense basal underflow that characterized the currents succeeded in generating local turbulence at a small jump, probably because of the generally finer grain size of the transported material. On the other hand, the presence of buildings perpendicular to the main flow, probably broke and splitted the currents into secondary arms flowing along the main Roman streets.

At Herculaneum, the first discovery of human victims of the eruption dates back to the early Bourbon excavations reported by the Spanish military engineer Alcubierre, just one year after the exploration of Herculaneum by tunnels, and is dated 18 November 1739 (Ruggiero, 1885). In 1831 the first victim was discovered in open-air excavations, in a room on the first floor of the House of the Skeleton (Ruggiero, 1885), followed, in 1932, by six victims found in the apodyterium of the men's sector of the Central Baths (Pagano, 2003b). The excavations carried out during the 18th century uncovered 12 victims, followed by seven other corpses found in the open pit excavations of the following century, and 19 recovered around the half of the 20th century, during investigations led by Amedeo Maiuri (De Carolis and Patricelli, 2013). A new campaign of excavations started at the beginning of the 1980s (Pagano, 2003a; Guidobaldi, 2007), bringing to light some 350 human skeletons, the skeletons of two horses and a dog, a boat, dozens of coins, and gold, silver, bronze and glass personal objects in about two decades (Franchi Dell'Orto, 1993; Pagano, 2000; D'Ambrosio et al., 2003).

As the case of Pompei, several interpretations have been proposed for the main cause of death for the people of Herculaneum. Some hypothesized a gradient of heat-induced effects, while recently most studies agree on the instant death of people discovered in the seashore area (Petrone, 2011a; Shmidt et al., 2015; Petrone et al., 2018). In fact, even if almost every skeleton bears some evidence of bone thermal exposure (such as changes in colours, charring, fracturing; Capasso 2001; Mastrolorenzo et al., 2001a; Shmidt et al., 2015; Petrone et al., 2018), the few victims found on the beach appear to show greater thermal effects compared to those sheltering inside the chambers (Capasso, 2000a; Shmidt et al., 2015). It was also proposed that death was instantaneous only for people found on the beach, while those taking refuge in the chambers would have died of asphyxiation (Capasso, 2000a; 2001). In contrast to this hypothesis, Petrone et al. (2018) suggested that the emplacement of the first surge caused the instant death of the 80 people found in the chambers due to a fulminant shock. These individuals did not suffer by mechanical impact, since their corpsed do not display evidence of voluntary self-protective reaction or agony contortions (Fig. 1.34), indicating that the activity of their vital organs must have stopped within a shorter time than the conscious reaction time.

Fig. 1.34 – Victims found in the arcades of the beach of Herculaneum (photo by Scandone et al., 2019). Note the different positions of the corpses. According to Petrone et al. (2018), the observed flexion of the hands and feet, together with the “pugilistic attitude” is only apparent for some of the victims at Herculaneum. The signs of bone carbonization and the preservation of joint connections indicate that most soft body tissues were destroyed by the intense heat and then replaced rapidly by ash.

In addition to Pompei and Herculaneum, several other areas have been excavated around the Vesuvius.

In 1967, a large Roman villa was discovered in Torre Annunziata (Nunziante et al., 2007), the ancient city of Oplonti. About 0.5 km farther east, other excavation unearthed a compound of more buildings, in more recent time known as “Villa Crassius Tertius”. A third archaeological site was found at Via Marconi, in the Torre Annunziata city. At Oplonti and Via Marconi, damages and destroyed vegetation are reported in the S-1 and S-5 surge deposits (Sigurdsson et al., 1985), and the city of Oplonti is thought to have been completely buried by the deposition of the S-6 surge. Sigurdsson et al. (1985) reported the finding of two Roman buildings at 7 km W and NW respectively, of Oplonti, completely buried under a 4 m thick pumice-rich, massive flow deposit, which the authors correlated with the F-5 or F-6 units at Oplonti.

In 1977, during the excavations for the foundations of a building in Boscoreale, Villa Regina was brought to light (Sigurdsson et al., 1985). This rustic villa consists of several rooms arranged on three sides of an open courtyard. The most famous finding is represented by a curved “tree”, obtained by the method of casting, which provided a complete set of information about the pyroclastic flows, especially in terms of shear strength and timing of the main events of the eruption. The geometry of the tree and the increasing upward bending indeed show how the pyroclastic material made up of pumice clasts and coarse ash, filled the open space where the tree was located during the main Plinian fallout phase. Subsequent, more energetic pyroclastic flows started to overrun the whole area, bending gradually the tree and charring it.

In the spring of 1981, a new Roman rustic villa was discovered in a large quarry south of Terzigno, only 6 km east of the crater of Vesuvius, shortly followed by the discovery of another rustic villa in an adjacent quarry, 1 km to the north. In the latter, evidence from the excavations suggests that the A-1 fine ash layer (Sigurdsson et al., 1985) lay in the doorway and courtyard of the villa where skeletons were found. Furthermore, the main Plinian fallout was interrupted by the emplacement of the first surge S-2 (Sigurdsson et al., 1985) that partially damaged both the *villae rusticae* as evidenced by the occurrence of minor building fragments in the deposit.

Moving away from the Vesuvius (15 km toward the south), another archaeological site of great interest is represented by the Roman villas of “San Marco” and “Arianna”, in the city of Castellammare di Stabia. The archaeological site is located on the Varano plateau, a volcanic and alluvial terrace lying at an altitude of 50 metres a.s.l. (Ruffo, 2011). Villa San Marco was the first Roman villa to be explored in the Bourbons period between 1750 and 1754. Based on the recognition of the typical characteristics of city domus and luxurious holiday homes, it is regarded to as an urban residential villa. The occurrence of fragments of walls and ceiling decorations inside some flow deposits, together with the finding of truncated columns and walls, suggest an impact associated with the pyroclastic currents, still acting at such great distances from the vent.

CONCLUSIONS

The dynamic of the AD 79 PDCs generating during the very initial phase of the eruption and by the following partial and total collapsing eruptive column has been reconstructed on the basis of a detailed field work and laboratory analysis.

The field work was aimed at the reconstruction of the entire depositional architecture of the ignimbrite deposits through the study of numerous sections located around Vesuvius, in the Campanian Plain and on the Lattari Mts. A total of 75 stratigraphic sections studied in 23 localities at distances between 3 and 25 km from the vent, allowed an accurate reconstruction of the complex internal stratigraphy of the AD 79 PDC deposits.

The field work has revealed that the vertical AD 79 sequence is never uniform and based upon internal sedimentary structures, grainsize and lithology, fourteen main lithofacies were recognized: (1) massive lapilli tuff (mLT), (2) massive tuff (mT), (3) massive lithic Breccia (mlBr), (4) pumice Lapilli Tuff (pLT), (5) lithic massive Lapilli Tuff (lmLT), (6) lithic massive Tuff, (7) diffuse stratified Lapilli Tuff (dsLT), (8) diffuse-stratified Tuff (dsT), (9) lenses of pumice and lithic bedded Lapilli (lenspL and lenslL), (10) stratified Lapilli Tuff (dsLT), (11) stratified Tuff (sT), (12) cross-stratified Tuff (xsT), (13) plane-parallel thin bedded Tuff (//bT), (14) accretionary lapilli Tuff (accT), reflecting several processes and conditions in the flow boundary zone of the AD 79 PDCs.

The 344 granulometric analyses and 264 component analyses allowed to define the lithological and sedimentological parameters of the AD 79 PDC deposits by quantifying, in terms of grainsize, types and amounts of components, the character of each lithofacies. All these results have provided insights to a full understanding of the sedimentological and compositional relationships between the deposits and the paleotopography, contributing to better define the areal extent of each stratigraphic units. In fact, the stratigraphy and the distribution of the facies of the AD 79 PDC sequence has shown sectorial variations around the source and longitudinal changes with the distance from the vent. In order to ascertain the stratigraphic position of each identified PDC unit, distinctive interstratified Plinian and post-Plinian marker fallout layers have been used to correlate the AD 79 PDC deposits. In the upwind sector of the Vesuvius (from NW to NE sector), outside the dispersal area of the fallout deposits, relative proportions of components, together with detailed stratigraphic and lithological studies, has provided a fundamental contribution to the correlations of the AD 79 PDC deposits.

27 individual PDC stratigraphic units from the opening to the intra- and post-Plinian phases of the eruption have been documented for the first time with this research, emplaced by 16 PDCs. Quantitative parameters such as bulk volume and invaded area have been calculated for each identified PDC unit and a tentatively new classification of the AD 79 PDC deposits has been proposed following the more recent classification criteria for the ignimbrite deposits (Giordano

et al., 2021). Among the several identified PDC units, some show significative lateral and vertical facies variations indicating spatial and temporal changes of the dominant physical flow processes acting in the flow boundary zone (e.g., Branney and Kokelaar, 2002; Brown and Branney, 2004) such as the i-PDC unit C4 and C8 and the p-PDC units C11, E1, γ; while other PDC units deposits with a limited dispersion and thickness (e.g. the opening PDC unit C1, the i-PDC units C2, C3, C5, C6, C9, C10 and p-PDC units F, G2, H, L, O) consist of a single facies, indicating significant steadiness and uniformity in transport and emplacement conditions with episodes of diachronic deposition for the i-PDC unit C2 and C3.

The topography and the increasing distance from the vent also affect the behaviour of the parental AD 79 PDCs, some of which (such as PDC 8, PDC 11, PDC12 that emplaced the i-PDC unit C8, p-PDC unit C11 and the p-PDC units E1, E2 and F) show a depositional system very sensitive to the variations of the substrate both at local and regional scale. A new reconstruction of the behaviour of the AD 79 PDCs has been established through the merging of all the available data. The very initial phase of the eruption is marked by the formation of a small-volume, slow-moving, ground-hugging ash flow with a limited areal distribution. For the first time, nine partial Plinian column collapses are documented representing a purely magmatic phase of the eruption. These partial column collapses determined the formation of relatively small-volume, sectoral distributed, restricted to relatively widespread dispersal turbulent, stratified PDCs (PDC2, PDC3 PDC 5, PDC 6, PDC 7, PDC9 and PDC 10) with some more energetic pulses represented by the sustained, strongly unsteady and non-uniform i-PDCs C4 and C8 that strongly interacted with the pre-existing paleotopography. The PDC 11 represents a sustained and first radially-moving, turbulent, stratified PDC recording the total Plinian column collapse. A gradual change in the eruptive dynamics led to the formation of the p-PDC 12 representing the most powerful and turbulent AD 79 PDC, even capable to overcome the barrier ridge represented by the Lattari Mountains. With time this PDC has shown a significant transition from a waxing to waning to another waxing pulse (that emplaced the p-PDC unit E1, E2 and F, respectively) with a gradual transition from a magmatic to phreatomagmatic eruptive style. The p-PDC 13 records the total collapse of a short-lived eruptive column while a further change in the eruptive dynamics is marked by the PDC 14 associated with a phase of the incremental caldera collapse. The ash-rich PDC 15 and 16 are diluted, turbulent, not affected by either topography or distance from the vent and represent the final phreatomagmatic stages of the AD 79 eruption.

The results of the petrochemical analysis add new information on the geochemical composition of the AD 79 PDC deposits, representing a significant contribution to the overall petrochemical dataset for the eruption. The white pumice clasts occurring in the i-PDC and p-PDC deposits do not represent actual juvenile clasts. Rather, they should represent “recycled clasts”, i.e., clasts from the Plinian White pumice lapilli fallout deposits eroded by the pyroclastic currents and then re-deposited and incorporated in the i-PDC and p-PDC deposits as accidental cognate lithic clasts. I suggest that also some grey pumice clasts from the i-PDC and p-PDC deposits might include “recycled clasts”, scraped off from the Plinian Grey pumice lapilli fallout deposits by the advancing PDCs. Furthermore, while the presence of such recycled component does not allow investigating in detail the dynamics of magma withdrawal during the emplacement of the PDC deposits, some interesting insights on the feeding reservoir can be retrieved from the composition of the juvenile fraction of the basal C1 deposits. In fact, the simultaneously occurrence of white and grey pumice clasts possibly records a major event of injection of less evolved (near-primitive?) magma, which likely triggered the eruption. At that stage, the magma reservoir had already developed its stratified structure, which allowed both the “white” and the “grey” portions to be tapped when the replenishment event produced a major destabilisation of the reservoir. This possibly occurred as some aliquots of the “grey” magma rose up to the surface, breaking the white/grey interface and dragging some “white” magma batches in their route to the surface, which should have been extremely rapid to prevent substantial mixing of the two.

Finally, the detailed and well constrained stratigraphy of the AD 79 PDC deposits has been a useful tool to define the exact timing of the destruction during the intra-Plinian and post-Plinian phases of the eruption. The first PDC reaching the city of Pompei (PDC 8, from 4:01 to 6:13 am of the 24 October or August) was harmless and penetrated the town by about 200 m. Also the following PDCs 9 and 11 reached the city (from 4:01 to 6:13 am and from 6:13 to 7:00 am, respectively) and did not cause relevant damages. The following PDC12 reached the city at about 7:00 am with the greater destructive power, flattening most of the walls in its north-south pattern and completely burying the Roman city. The frontal part of the PDC was diluted enough to allow the inhabitants to walk on the aggrading deposit and breathe for a few minutes before being suffocated. Furthermore, the currents associated with the final phreatomagmatic phase of the eruption (such as the PDC 14) not simply mantled the towns, but also interacted with the Roman towns of Pompei and Stabia. Of course, if compared with the impact of the PDC 12, seriously damaging many structures, the PDC 14 engulfed the cities without inflicting serious damages on the structures.

REFERENCES

Alegret, L., Arenillas, I., Arz, J.A., Diaz, C., Grajales-Nishimura, J.M., Meléndez, A., Molina, E., Rojas, R., Soria, A.R. (2005). Cretaceous-Paleogene boundary deposits at Loma Capiro, central Cuba: Evidence for the Chicxulub impact: Geology, v. 33, 721–724.

Allen, J.R.L. (1984). Sedimentary structures. Their character and physical basis, Vol II. Developments in sedimentology 30B. Elsevier, Amsterdam, 1-663.

Andronico, D., Calderoni, G., Cioni, R., Sbrana, A., Sulpizio, R., Santacroce, R. (1995). Geological map of Somma−Vesuvius Volcano. Periodico di Mineralogia 64: 77–78

Andronico, D., Cioni, R. (2002). Contrasting styles of Mount Vesuvius activity in the period between the Avellino and Pompeii Plinian eruptions, and some implications for assessment of future hazards. Bulletin of Volcanology 64: 372–391.

Aravena, A., Cioni, R., de' Michieli Vitturi, M., Neri, A. (2019). The lithic component of pyroclastic deposits as a proxy for the reconstruction of the syneruptive evolution of volcanic conduits: The CE 79 eruption of Vesuvius. Journal of Geophysical Research: Solid Earth 124: 11022– 11037.

Arnò, V., Principe, C., Rosi, M., Santacroce, R., Sbrana, A., Sheridan, M.F. (1987). Eruptive history. In: Santacroce, R. (ed), Somma−Vesuvius, CNR, Quaderni de La ricerca Scientifica. CNR Roma, 114: 5−103.

Arnott, R.W.C., Hand, B.M. (1989). Bedforms, primary structures and grain fabric in the presence of suspended sediment rain. J Sediment Petrol 59:1062–1069

Ayuso, R.A., De Vivo, B., Rolandi, G., Seal II, R.R., Paone, A. (1998). Geochemical and isotopic (Nd−Pb−Sr−O) variations bearing on the genesis of volcanic rocks from Vesuvius, Italy. J. Volcanol. Geotherm. Res., 82: 53−78.

Baer, E.M., Fisher, R.V., Fuller, M., Valentine, G. (1997). Turbulent transport and deposition of the Ito pyroclastic flow: determinations using anisotropy of magnetic susceptibility. Journal of Geophysical Research: Solid Earth 102 (B10), 22565–22586.

Balcone−Boissard, H., Boudon, G., Villemant, B. (2011). Textural and geochemical constraints on eruptive style of the 79AD eruption at Vesuvius. Bulletin of Volcanology 73: 279−294

Balcone−Boissard, H., Villemant, B., Boudon, G., Michel, A. (2008). Non−volatile vs volatile behaviours of halogens during the AD 79 Plinian eruption of Mt. Vesuvius, Italy. Earth and Planetary Science Letters 269, 66–79.

Barberi, F., Bizouard, H., Clocchiatti, R., Metrich, N., Santacroce, R., Sbrana, A. (1981). The Somma−Vesuvius magma chamber: a petrological and volcanological approach. Bull. Volcanol. 44, 295−315.

Barberi, F., Cioni, R., Rosi, M., Santacroce, R., Sbrana, A., Vecci, R. (1989). Magmatic and phreatomagmatic phases in explosive eruptions of Vesuvius as deduced by grain−size and compositional analysis of pyroclastic deposits. J. Volcanol. Geotherm. Res. 38, 287−307.

Barberi, F., Leoni, L. (1980). Metamorphic Carbonate Ejecta from Vesuvius Plinian Eruptions. Evidence of the occurrence of shallow magma chambers. Bull. Volcanol. 43-1, 107-120.

Baxter, P.J. (1990). Medical effects of volcanic eruptions, I. Main causes of death and Injury. Bull. Volcanol. 52: 532–544.

Baxter, P.J., Aspinall, W., Neri, A. et al. (2008). Emergency planning and mitigation at Vesuvius: a new evidence−based approach. J. Volcanol. Geotherm. Res. 178: 454–73.

Baxter, P.J., Boyle, R., Cole, P., Neri, A., Spence, R., Zuccaro, G. (2005). The impacts of pyroclastic surges on buildings at the eruption of the Soufrière Hills volcano, Montserrat. Bull. Volcanol. 67: 292–313.

Baxter, P.J., Neri, A., Todesco, M. (1998). Physical modelling and human survival in pyroclastic flows. Nat. Hazards 17, 163–176.

Bertagnini, A., Cioni, R., Guidoboni, E., Rosi, M., Neri, A., Boschi, E. (2006). Eruption early warning at Vesuvius: The A.D. 1631 lesson. Geophysical Research Letters.

Bertagnini, A., Landi, P., Rosi, M., Vigliargio, A. (1998). The Pomici di Base Plinian eruption of Somma−Vesuvius. J Volcanol Geotherm Res 83: 219–239.

Best, M.G., Christiansen, E.H., Deino, A.L., Gromme, S., Hart, G.L., and Tingey, D.G. (2013). The 36– 18 Ma Indian Peak–Caliente ignimbrite field and calderas, southeastern Great Basin, USA: Multicyclic super-eruptions: Geosphere, v. 9, p. 964– 950.

Bevilacqua, A., Neri, A., Bisson, M., Esposti Ongaro, T., Flandoli, F., Isaia, R., Rosi, M., Vitale, S. (2017). The effects of vent location, event scale, and time forecasts on pyroclastic density current hazard maps at Campi Flegrei caldera (Italy). Front Earth Sci 5:72.

Blackburn, E., Wilson, L., Sparks, R.S.J. (1976). Mechanisms and dynamics of strombolian activity. J. Geol. Soc. Lond. 132, 429-440.

Blott, S.J., Pye, K. (2001). Gradistat: a grain size distribution and statistics package for the analysis of unconsolidated sediments. Earth Surf. Process. Landforms vol. 26, pp. 1237–1248.

Brand, B.D., Bendaña, S., Self, S. Pollock, N. (2016). Topographic controls on pyroclastic density current dynamics: Insight from 18 May 1980 deposits at Mount St. Helens, Washington (USA). J. Volcanol. Geoth. Res. 321, 1-17.

Branney, M.J., Kokelaar, B.P. (1992). A reappraisal of ignimbrite emplacement: progressive aggradation and changes from particulate to non−particulate flow during emplacement of high−grade ignimbrite. Bull. Volcanol. 54: 504–520.

Branney, M.J., Kokelaar, B.P. (2002). Pyroclastic density currents and the sedimentation of ignimbrites, Geol. Soc. Lond. Mem. 27, 51–58.

Brocchini, D., Principe, C., Castradori, D., Laurenzi, M. A., Gorla, L. (2001). Quaternary evolution of the southern sector of the Campanian Plain and early Somma−Vesuvius activity: Insights from the Trecase 1 well. Mineralogy and Petrology 73, 67–91.

Brown, R.J., Branney, M.J. (2004). Event−stratigraphy of a calderaforming ignimbrite eruption on Tenerife: the 273 ka Poris Formation. Bull. Volcanol. 66: 392–416.

Brown, R.J., Branney, M. (2013). Internal flow variations and diachronous sedimentation within extensive, sustained, density-stratified pyroclastic density currents flowing down gentle slopes, as revealed by the internal architectures of ignimbrites on Tenerife. Bull. Volcanol. 75, 727.

Brown R.J., Branney M.J., Maher C., Dávila-Harris P. (2010). Origin of accretionary lapilli within ground-hugging density currents: Evidence from pyroclastic couplets on Tenerife. Bull. Geol. Soc. Am. 122:305–320.

Brown, R.J., Kokelaar, B.P., Branney, M.J. (2007). Widespread transport of pyroclastic density currents from a large silicic tuff ring: the Glaramara tuff, Scafell caldera, English Lake District, UK. Sedimentology 54, 1163–1189.

Bullard, F.M. (1978). Volcanoes of the Earth. University of Texas Press, Austin, 1–579.

Burgissier, A., Bergantz, G.W. (2002). Reconciling pyroclastic flow and surge: the multiphase physics of pyroclastic density currents. Earth Planet Sci Lett 202:405–418

Bursik, M., Woods, A. (1996). The dynamics and thermodynamics of large ash flows. Bull Volcanol 58, 175–193.

Calder, E.S., Sparks, R.S.J., Gardeweg, M.C. (2000). Erosion, transport and segregation of pumice and lithic clasts in pyroclastic flows inferred from ignimbrite at Lascar Volcano, Chile, Journal of Volcanology and Geothermal Research, Volume 104, Issues 1–4.

Capasso, L. (2000a). Herculaneum victims of the volcanic eruptions of Vesuvius in 79 AD. The Lancet 356: 1344–1346.

Capasso, L. (2001). I fuggiaschi di Ercolano. Paleobiologia delle vittime dell'eruzione vesuviana del 79 d.C. L'Erma di Bretschneider, Roma.

Carey, S., Sigurdsson, H. (1987). Temporal variations in column height and magma discharge rate during the 79 A.D. eruption of Vesuvius. Geol. Soc. Am. Bull. 99, 303-314.

Carey, S.N. (1991). Transport and deposition of tephra by pyroclastic flows and surges. In Fisher R.V. and Smith G.A. (Eds). Sedimentation in volcanic settings, SEPM, Special Publications, p.45.

Caricchi, C., Vona, A., Corrado, S. et al. (2014). AD 79 Vesuvius PDC deposits' temperatures inferred from optical analysis on woods charred in−situ in the Villa dei Papiri at Herculaneum (Italy). J. Volcanol. Geotherm. Res., 289: 14–25.

Carrasco-Núñez, G., Branney, M. (2005). Progressive assembly of a massive layer of ignimbrite with a normal-to-reverse compositional zoning: The Zaragoza ignimbrite of central Mexico. Bulletin of Volcanology. 68. 3-20.

Cas, R.A.F., Wright, J.V. (1987). Volcanic Successions: Ancient and Modern. Allen and Unin, London.

Cas, R.A.F., Wright, H.M.N., Folkes, C.B., Lesti, C., Porreca, M., Giordano, G., Viramonte, J.G. (2011). The flow dynamics of an extremely large volume pyroclastic flow, the 2.08 Ma Cerro Galán Ignimbrite, NW Argentina, and comparison with other flow types. Bull. Volcanol. 73, 1585–1609.

Castruccio, A., Diez, M., Gho, R. (2017). The influence of plumbing system structure on volcano dimensions and topography. J Geophys Res Solid Earth 122:8839–8859.

Chiominto, G. (2023). Plinian eruption ands and their impact in urban contexts: dynamics and effects on the territory of the fall phases of the 79 AD Vesuvian eruption. PhD Thesis.

Choux, C.M., Druitt, T.H. (2002). Analogue study of particle segregation in PDCs, with implications for the emplacement mechanisms of large ignimbrites. Sedimentology 49:907–928

Cioni, R., Bertagnini, A., Santacroce, R., Andronico, D. (2008). Explosive activity and eruption scenarios at Somma−Vesuvius (Italy): Towards a new classification scheme. Journal of Volcanology and Geothermal Research, 178, 331–346.

Cioni, R., Civetta, L., Marianelli, P., Metrich, N., Santacroce, R., Sbrana, A. (1995). Compositional layering and syneruptive mixing of a periodically refilled magma chamber: the A.D. 79 Plinian eruption of Vesuvius. J. Petrol., 36, 739–776.

Cioni, R., D'Oriano, C., Bertagnini, A., Andronico, D. (2013). The 2nd to 4th century explosive activity of Vesuvius: New data on the timing of the upward migration of the post−AD 79 magma chamber. Annals of Geophysics, 56(4), S0438–S0417.

Cioni, R., Gurioli, L., Lanza, R., Zanella, E. (2004). Temperatures of the A.D. 79 pyroclastic density current deposits (Vesuvius, Italy). J Geophys Res 109:B02207.

Cioni, R., Gurioli, L., Sbrana, A., Vougioukalakis, G. (2000b). Precursory phenomena and destructive events related to the Late Bronze Age Minoan (Thera, Greece) and A.D. 79 (Vesuvius, Italy) plinianeruptions: inferences from the stratigraphy in the archaeological areas. In: McGuire, W.G. et al (eds). The archaeology of geological catastrophes. Geol Soc Spec Pub 171:123–141.

Cioni, R., Longo, A., Macedonio, G., Santacroce, R., Sbrana, A., Sulpizio, R., Andronico, D. (2003). Assessing pyroclastic fall hazard through field data and numerical simulations: example from Vesuvius. J Geophys Res 108:2063.

Cioni, R., Marianelli, P., Santacroce, R. (1998). Thermal and compositional evolution of the shallow magma chambers of Vesuvius: evidence from pyroxene phenocrysts and melt inclusions. J. Geophys. Res., 103, 18277−18294

Cioni, R., Marianelli, P., Sbrana, A. (1990). L'eruzione del 79 d.C.: stratigrafia dei depositi ed impatto sugli insediamenti romani nel settore orientale e meridionale del Somma-Vesuvio. Rivista di Studi Pompeiani IV: 179-198.

Cioni, R., Marianelli, P., Sbrana, A. (1992). Dynamics of the A.D. 79 eruption: stratigraphic sedimentological and geochemical data on the successions from the Somma–Vesuvius southern and eastern sectors. Acta Vulcanol 2:109–124

Cioni, R., Santacroce, R., Sbrana, A. (1999). Pyroclastic deposits as a guide for reconstructing the multi−stage evolution of the Somma−Vesuvius caldera. Bulletin of Volcanology, 61, 207–222.

Cioni, R., Sbrana, A., Gurioli, L. (1996). The deposits of AD 79 eruption, in R. Santacroce et al. (ed.) Vesuvius decade Volcano Workshop Handbook, Cons. Nac. Ric., Rome, Italy, pp. E1–E31.

Cioni, R., Tadini, A., Gurioli, L., Bertagnini, A., Mulas, M., Bevilacqua, A., Neri, A. (2020). Estimating eruptive parameters and related uncertainties for pyroclastic density currents deposits: worked examples from Somma−Vesuvius (Italy). Bull. Volcanol. 82, 65.

Civetta, L., Galati, R., Santacroce, R. (1991). Magma mixing and convective compositional layering within the Vesuvius magma chamber. Bull. Volcanol., 53, 287–300.

Civetta, L., Santacroce, R. (1992). Steady state magma supply in the last 3400 years of Vesuvius activity. Acta Vulcanol. 2, 147−159.

Cole, P.D., Calder, E.S., Sparks, R.S.J., Druitt, T.H., Young, S.R., Herd R., Harford, C., Norton, G., Robertson, R. (2002). Pyroclastic flow deposits formed during the 1996–99 eruption of Soufriere Hills Volcano, Montserrat, W. I. In: Druitt TH, Kokelaar BP (eds) The eruption of Soufriere Hills Volcano, Montserrat, from 1995 to 1999. Mem Geol Soc London 21, 231–262.

Cole, P.D., Neri, A., Baxter, P.J. (2015). Chapter 54 – Hazards from pyroclastic density currents. In: Sigurdsson H. (ed.), The Encyclopedia of Volcanoes (Second Edition). Academic Press, Amsterdam, pp. 943–956.

Cole, P.D., Scarpati, C. (1993). A facies interpretation of the eruption and emplacement mechanisms of the upper part of the Neapolitan Yellow Tuff, Campi Flegrei, southern Italy. Bull. Volcanol. 55(5): 311−326.

Cole, P.D., Scarpati, C. (2010). The 1944 eruption of Vesuvius, Italy: combining contemporary accounts and field studies for a new volcanological reconstruction. Geol. Mag. 147 (3), 391–415.

Colella, A., Hiscott, R.N. (1997). Pyroclastic surges of the Pleistocene Monte Guardia sequence (Lipari Island, Italy): depositional processes. Sedimentology, 44: 47-66.

Cornell, W., Sigurdsson, H. (1984). Modeling of trace element gradients in the Vesuvius 79 A.D. reservoir. Eor:65, 1128.

Cornell, W., Sigurdsson, H. (1987). Compositional zoning in the Pompei 79 A.D. pumice deposit: magma mixing and observed trends. Eos:68, 434.

D'Ambrosio, A., Guzzo, P. G., Mastroroberto, M. (2003). Storie da un'eruzione. Pompei, Ercolano, Oplontis. Mondadori Electa, Milano.

Dade, W.B., Huppert, H.E. (1996). Emplacement of the Taupo ignimbrite by a dilute turbulent flow. Nature 381 (6582), 509–512.

De Carolis, E., Patricelli, G. (2013). Rinvenimenti di corpi umani nel suburbio pompeiano e nei siti di Ercolano e Stabia. Rivista di Studi Pompeiani, 24: 11–32.

De Carolis, E., Patricelli, G., Ciarallo, A. (1998). Rinvenimenti di corpi umani nell'area urbana di Pompei. Rivista di Studi Pompeiani, 9: 75–123.

De Carolis, E., Patricelli, G. (2003). Le vittime dell'eruzione. In A. d'Ambrosio, P.G. Guzzo & M. Mastroroberto (eds): Storie da un'eruzione. Pompei Ercolano Oplontis, pp. 56–72. Milano.

De Vivo, B., Rolandi, G., Gans, P. B., Calvert, A., Bohrson, W. A., Spera, F. J., & Belkin, H. E. (2001). New constraints on the pyroclastic eruptive history of the Campanian volcanic plain (Italy). Mineralogy and Petrology 73, 47–65.

Delibrias, G., Di Paola, G.M., Rosi, M., Santacroce, R. (1979). La storia eruttiva del complesso vulcanico Somma-Vesuvio ricostruita dalle successioni piroclastiche del Somma. Rend. Soc. It. Mineral. Petrol. 35, 411-438.

Dellino, P.F., Dioguardi, F., Isaia, R., Sulpizio, R., Mele, D. (2021). The impact of pyroclastic density currents duration on humans; the case of the AD 79 eruption of Vesuvius. Sci. Rep. 11, 4959.

Di Girolamo, P. (1963). La serie piroclastica dell'eruzione di Pompei. Studio chimico – petrografico, mineralogico e stratigrafico dell'eruzione del 79 d.C. e dei prodotti ottavianitici del Somma−Vesuvio. Annali dell'Osservatorio Vesuviano 5, 1−69.

Di Girolamo, P. (1968). Petrografia del Somma−Vesuvio: le serie piroclastiche. Rend. Soc. Acc. Sci. FF. MM. Soc. Naz. Sci. Lett. Napoli 35, 5−68.

Doronzo, D.M., Dellino, P. (2011). Interaction between pyroclastic density currents and buildings: Numerical simulation and first experiments. Earth Planet. Sci. Lett. 310, 286–292.

Doronzo, M., Di Vito, M.A., Arienzo, I., Bini, M., Calusi, B., Cerminara, M., Corradini, S., De Vita, S., Giaccio, B., Gurioli, L., Mannella, G., Ricciardi, G.P., Rucco, I., Sparice, D., Tedesco, M., Trasatti, E., Zanchetta, G., (2022). The 79 CE eruption of Vesuvius: a lesson from the past and the need of multidisciplinary approach for developments in volcanology. Earth Sci. Rev. 231, 104072.

Douillet, G.A., Bernard, B., Bouysson, M., Chaffaut, Q., Dingwell, D.B., Gegg, L., Hoelscher, I., Kueppers, U., Mato, C., Ritz, V.A., Schlunegger, F. (2019). Pyroclastic dune bedforms: macroscale structures and lateral variations. Examples from the 2006 pyroclastic currents at Tungurahua (Ecuador). Sedimentology, 66(5), 1531–1559.

Douillet, G.A., Tsang−Hin−Sun, È., Kueppers, U., et al (2013). Sedimentology and geomorphology of the deposits from the August 2006 pyroclastic density currents at Tungurahua volcano, Ecuador. Bull Volcanol 75(765): 1–21.

Druitt, T.H. (1992). Emplacement of May 18, 1980, lateral blast ENE of Mount St. Helens, Washington. Bull. Volcanol. 54: 544−572.

Druitt, T.H. (1998). Pyroclastic density currents. In: Gilbert, J.S. and Sparks, R.S.J. (Eds). The Physics of Explosive Volcanin Eruptions. Geological Society, London, Special Pubblications, Vol. 145, pp 145−182.

Esposti Ongaro, T., Clarke, A.B., Voight, B., Neri, A., Widiwijayanti, C. (2012). Multiphase flow dynamics of pyroclastic density currents during the May 18, 1980 lateral blast of Mount St. Helens J Geophys Res: Solid Earth (1978–2012)117

Esposti, Ongaro, T., Orsucci, S., Cornolti, F. (2016). A fast, calibrated model for pyroclastic density currents kinematics and hazard. J Volcanol Geotherm Res.

Esposti, Ongaro T., Neri, A., Menconi, G., de'Michieli Vitturi, M., Marianelli, P., Cavazzoni, C., Erbacci, G., Baxter, P.J. (2008). Transient 3D numerical simulations of column collapse and pyroclastic density current scenarios at Vesuvius. J Volcanol Geotherm Res 178: 378–396.

Esposti, Ongaro T., Neri, A., Todesco, M., Macedonio, G. (2002). Pyroclastic flow hazard assessment at Vesuvius (Italy) by using numerical modeling. II. Analysis of flow variables. Bull. Volcanol. 64, 178–191.

Fedele, L., Scarpati, C., Lamphere, M., Melluso, L., Morra, V., Perrotta, A., Ricci, G. (2008). The Breccia Museo formation, Campi Flegrei, southern Italy: geochronology, chemostratigraphy and relationship with the Campanian Ignimbrite eruption. Bull. Volcanol., 70(10): 1189 – 1219.

Fedele, L., Scarpati, C., Sparice, D., Perrotta, A. and Laiena, F. (2016). A chemiostratigraphic study of the Campanian Ignimbrite eruption (Campi Flegrei, Italy): Insight on magma chamber withdrawal and deposit accumulation as revealed by compositionally zoned stratigraphic and facies framework. Journal of Volcanology and Geothermal Research, 324, pp 105−117.

Fierstein, J., Hildreth, W. (1992). The Plinian eruptions of 1912 at Novarupta, Katmai National Park, Alaska. Bull Volcanol 54: 646–684

Fisher, R.V. (1966). Mechanism of deposition from pyroclastic flows. Am. J. Sci. 264 (5), 350–363.

Fisher, R.V., Schmincke, J.−U. (1984). Pyroclastic Rocks. Springer−Verlag, Berlin.

Folk, R.L., Ward, W.C. (1957). A Study in the Significance of Grain-Size Parameters. Journal of Sedimentary Petrology 27, 3-26.

Franchi Dell'Orto, L. (1993). Ercolano 1738− 1988: 250 anni di ricerca archeologica. Atti del Convegno internazionale (Ravello − Ercolano − Napoli − Pompei, 30 ottobre − 5 novembre 1988), 6 Monografie, Sopr. Archeologica di Pompei. L'Erma di Bretschneider, Roma.

Francis, P.; Oppenheimer, C. (2004). Volcanoes, 2nd ed.; Oxford University Press: Oxford, UK; p. 521.

Freundt, A., Bursik, M. (1998). Pyroclastic flow transport mechanisms. In: Freundt, A., Rosi, M. (Eds.), From Magma to Tephra, Modeling Physical Processes of Explosive Volcanic Eruptions, Vol. 4. Elsevier Science, Amsterdam, 173-231.

Freundt, A., Schmincke, H.U. (1986). Emplacement of small−volume pyroclastic flows at Lacher See (East Eifel, Germany). Bull. Volcanol., 48, 39−59.

Freundt, A., Wilson, C.J.N., Carey, S.N. (2000). Ignimbrites and block−and−ash flow deposits. In: Sigurdsson, et al. (Eds.), Encyclopedia of Volcanoes. Academic Press.

Fulignati, P., Kamenetsky, V.S., Marianelli, P., Sbrana, A., Meffre, S. (2011). First insights on the metallogenic signature of magmatic fluids exsolved from the active magma chamber of Vesuvius (AD 79 "Pompei" eruption). Journal of Volcanology and Geothermal Research 200, 223–233

Fulignati, P., Marianelli, P., Santacroce, R., Sbrana, A. (2004). Probing the Vesuvius magma chamber–host rock interface through xenoliths. Geological Magazine 141, 417−428

Giacomelli, L., Perrotta, A., Scandone, R. et al. (2003). The eruption of Vesuvius of 79 AD and its impact on human environment in Pompeii. Episodes, 26: 234–237.

Giacomelli, L., Scandone, R., Rosi, M. (2021). The loss of geological memory of past catastrophes: the case of Pompeii. Ann. Geophys. 64, V0547.

Gigante, M. (1989). Il Fungo sul Vesuvio secondo Plinio il Giovane. Lucarini Ed. 38.

Gilbert J.S., Lane S.J. (1994). The origin of accretionary lapilli. Bull Volcanol 56: 398–411.

Giordano, G., Cas, R.A.F. (2021). Classification of ignimbrites and their eruptions: Earth-Science Reviews, v. 220.

Giordano, G., Zanella, E., Trolese, M. et al. (2018). Thermal interactions of the AD79 Vesuvius pyroclastic density currents and their deposits at Villa dei Papiri (Herculaneum archaeological site, Italy). Earth Plan. Sci. Let., 490: 180–192.

Graup, G., (1981). Terrestrial chondrules, glass and accretionary lapilli from the suevite, Ries Crater, Germany: Earth and Planetary Science Letters, v. 55, 407–418. doi: 10.1016/0012-821X(81)90168-0.

Grosse, P., van Wyk de Vries, B., Petrinovic, I.A. et al. (2009). Morphometry and evolution of arc volcanoes. Geology 37:651–654.

Guidobaldi, M.P. (2007). Ercolano. Guida agli scavi. Electa, Napoli.

Gurioli, L. (2000). Pyroclastic flow: classification, transport and emplacement mechanisms. Plinius 23:84–89.

Gurioli, L., Cioni, R., Bertagna, C., (1999). I depositi di flusso piroclastico dell'eruzione del 79 d.C: caratterizzazione stratigrafica, sedimentologica e modelli di trasporto e deposizione. Procedings Società Toscana Science Naturali, Memorie, Ser. A, 106, 61−72.

Gurioli, L., Cioni, R., Sbrana, A., Zanella, E. (2002). Transport and deposition from pyroclastic flows over densely inhabited areas: Herculaneum (Italy). Sedimentology 46:929–953.

Gurioli, L., Houghton, B., Cashman, K., Cioni, R. (2005a). Complex changes in eruption dynamics and the transition between Plinian and phreatomagmatic activity during the 79 AD eruption of Vesuvius. Bull Volcanol 67:144–159.

Gurioli, L., Pareschi, M.T., Zanella, E., Lanza, R., Deluca, E., Bisson, M. (2005b). Interaction of pyroclastic currents with human settlements: evidences from ancient Pompeii. Geology 33:441–444

Gurioli, L., Sulpizio, R., Cioni, R., Sbrana, A., Luperini, W., Santacroce, R., Andronico, D. (2010). Pyroclastic flow hazard assessment at Somma−Vesuvius based on the geological record. Bull. Volcanol. 72 (9), 1021–1038.

Gurioli, L., Zanella, E., Pareschi, M.T., Lanza, R. (2007). Influences of urban fabric on pyroclastic density currents at Pompeii (Italy): Flow direction and deposition. J Geophys Res Solid Earth, 112:B05213.

Ippolito, F. (1950). Sul meccanismo del seppellimento di Pompei e di Ercolano. Pompeiana 1950: 387−395.

Johnston Lavis, H.J. (1884). The geology of the Mt. Somma and Vesuvius: being a study of volcanology. Q J Geol Soc Lond 40:35–149.

Jolis, E.M., Troll, V.R., Harris, C., Freda, C., Gaeta, M., Orsi, G., Siebe, C. (2015). Skarn xenolith record crustal CO2 liberation during Pompeii and Pollena eruptions, Vesuvius volcanic system, central Italy. Chemical Geology 415, 17−36.

Joron, J.L., Metrich, N., Rosi, M., Santacroce, R., Sbrana, A. (1987). Chemistry and petrography, In Santacroce, R (ed) Somma-Vesuvius. Quaderni de la ricerca scientifica, CNR, Roma 8:105- 171.

Kneller, B., McCaffrey, W. (1999). Depositional effects of flow nonuniformity and stratification within turbidity currents approaching a bounding slope: deflection, reflection, and facies variation. J Sed Res 69:980–991

Kneller, B.C., Branney, M.J. (1995). Sustained high-density turbidity currents and the deposition of thick massive sands. Sedimentology 42:607–616.

Kokelaar, P., Raine, P., Branney, M.J. (2007). Incursion of a large-volume, spatter-bearing pyroclastic density current into a caldera lake: Pavey Ark ignimbrite, Scafell caldera, England. Bull Volcanol **70**, 23–54.

Krumbein, W. C. (1936). Application of logarithmic moments to size frequencies distribution of sediments. Journal Sedimentology & Petrography 6, 35–47.

Lacroix, A. (1908). Les dernies jours d'Herculaneum et de Pompei interpretes a l'aide de quelques phenomenes recents du volcanisme. Bullettin de la Societè de Geographie: 18: 5.

Lajoie, J., Lanzafame, G., Rossi, P.L., Tranne, C.A. (1992). Lateral facies variations in hydromagmatic pyroclastic deposits at Linosa, Italy, Journal of Volcanology and Geothermal Research, Volume 54, Issues 1–2, Pages 135-143.

Le Maitre, R.W. (2002). Igneous Rocks: A Classification and Glossary of Terms. Recommendations of the International Union of Geological Sciences Subcommission on the Systematics of Igneous Rocks. Cambridge University Press, Cambridge, UK, 256 pp.

Lesti, C., Porreca, M., Giordano, G., Mattei, M., Cas, R.A., Wright, H.M., Viramonte, J. (2011). High-temperature emplacement of the Cerro Gal´an and Toconquis Group ignimbrites (Puna plateau, NW Argentina) determined by TRM analyses. Bull. Volcanol. 73 (10), 1535–1565.

Linde, N., Ricci, T., Baron, L., Shakas, A. and Berrino, G. (2017). The 3−D structure of the Somma Vesuvius volcanic complex (Italy) inferred from new and historic gravimetric data. Sci Rep 7, 8434.

Lirer, L., Pescatore, T. (1968). Studio sedimentologico delle piroclastici del Somma−Vesuvio: Accad. Sci. Fis. e Mat. (Soc. Naz. Sci. Lettere ed Arti Napoli) Rend., ser. 3a, v. 7.

Lirer, L., Munno, R., Petrosino, P., Vinci, A. (1993). Tephrostratigraphy of the AD 79 pyroclastic deposits in perivolcanic areas of Mt. Vesuvio (Italy). J Volcanol Geotherm Res 58:133–139.

Lirer, L., Munno, R., Postiglione, I., Vinci, A., Vitelli, L. (1997). The A.D. 79 eruption as a future explosive scenario in the Vesuvian area: evaluation of associated risk. Bull. Volcanol. 59, 112-124.

Lirer, L., Pescatore, T., Booth, B. and Walker, G.P.L. (1973). "Two Plinian pumice−fall deposits from Somma−Vesuvius, Italy", Geological Society American Bullettin, 84, pp. 759−772.

Lirer, L., Petrosino, P., Alberico, I., Postiglione, I. (2001). Long−term volcanic hazard forecasts based on Somma−Vesuvio past eruptive activity. Bull Volcanol 63:45–60.

Lucchi, F. (2013). Stratigraphic methodology for the geological mapping of volcanic areas: insights from the Aeolian archipelago (southern Italy). Geological Society, London, Memoirs 37, 37–55.

Luongo, G., Perrotta, A., Scarpati, C. (2003a). Impact of AD 79 explosive eruption on Pompeii I: relations amongst the depositional mechanism of the pyroclastic products, the framework of the buildings and the associated destructive events. J. Volcanol. Geotherm. Res. 126, 201−223.

Luongo, G., Perrotta, A., Scarpati, C., De Carolis, E., Patricelli, G., Ciarallo, A. (2003b). Impact of the AD 79 explosive eruption on Pompeii II: causes of death of the inhabitants inferred by stratigraphical and areal distribution of the human corpses. J. Volcanol. Geotherm. Res. 126, 169−200.

Macdonald, G.A. (1972). Volcanoes. Prentice−Hall, New Jersey pp 1–503.

Maiuri, A. (1958b). Pompeii. Sci. Am., 198: 70.

Maiuri, A. (1961). Last moments of the Pompeians. Nat. Geo., 120: 651–669.

Marianelli, P., Métrich, N., Santacroce, R., Sbrana, A. (1995). Mafic magma batches at Vesuvius: a glass inclusion approach to the modalities of feeding stratovolcanoes. Mineralogy and Petrology, 120, 159-165.

Mastrolorenzo, G., Petrone, P., Pagano, M., Incoronato, A., Baxter, B.J., Canzanella, A., Fattore L. (2001a). Herculaneum victims of Vesuvius in AD 79. Nature, 410: 769–770.

Mastrolorenzo, G., Petrone, P., Pappalardo, L., Guarino, F.M. (2010). Lethal Thermal Impact at Periphery of Pyroclastic Surges: Evidences at Pompeii. PLoS One, 5: 1–12.

Mauro, A., Di Vito, Zanella, E., Gurioli, L., Lanza, R., Sulpizio, R., Bishop, J., Tema, E., Boenzi, G., Laforgia, E. (2009). The Afragola settlement near Vesuvius, Italy: The destruction and abandonment of a Bronze Age village revealed by archaeology, volcanology and rock-magnetism, Earth and Planetary Science Letters, Volume 277, Issues 3–4, Pages 408-421.

McBirney, A.R. (1973). Factors governing the intensity of explosive andesitic eruptions. Bull. Volcanol. 37, 443-453.

Mele, D., Sulpizio, R., Dellino, P., & La Volpe, L. (2011). Stratigraphy and eruptive dynamics of a pulsating Plinian eruption of Somma−Vesuvius: The Pomici di Mercato (8900 years B.P.). Bull. Volcanol., 73, 257–278.

Melluso, L., Scarpati, C., Zanetti, A., Sparice, D. (2022). The petrogenesis of chemically zoned, phonolitic Plinian and sub−Plinian eruptions of Somma−Vesuvius, Italy: role of accessory phase removal, independently filled magma reservoirs with time, and transition from slightly to highly silica undersaturated magmatic series in an ultrapotassic stratovolcano. Lithos 430−431, 106854.

Merrill, E.T. (1918). Notes on the eruption of Vesuvius in 79 AD. American Journal of Archaeology 22: 304−309

Merrill, E.T. (1920). Further note on the eruption of Vesiuvius in 79 AD. American Journal of Archaeology 24: 262−268.

Milia, A., Mirabile, L., Torrente, M.M., Dvorak, J.J. (1998). Volcanism offshore of Vesuvius volcano in Naples Bay. Bull Volcanol 50:404–413

Milner, D.M., Cole, J.W., Wood, C.P. (2003). Mamaku Ignimbrite: a caldera-forming ignimbrite erupted from a compositionally zoned magma chamber in Taupo Volcanic Zone, New Zealand. J. Volcanol. Geotherm. Res. 122 (3–4), 243–264.

Montanaro, A. (2019). La sequenza piroclastica del 79 d.C. all'interno dell'area archeologica di Pompei. Master's Thesis.

Morgan, D.J., Blake, S., Rogers, N.W., De Vivo, B., Rolandi, G., Davidson, J.P. (2006). Magma chamber recharge at Vesuvius in the century prior to the eruption of A.D. 79. Geology 34, 845−848.

Mues−Schumacher, U. (1994). Chemical variations of the A.D. 79 pumice deposits of Vesuvius. European Journal of Mineralogy 6, 387−395

Nairn, I.A., Self, S. (1978). Explosive eruptions and pyroclastic avalanches from Ngauruhoe in February 1975. J. Volcanol. Geoth. Res. 3, 39-60.

Nazzaro, A. (1997). Il Vesuvio. Storia eruttiva e teorie vulcanologiche. Liguori, Napoli, pp 1–362

Nunziante, L., Lucibello, E., Perrella, G., Petrosino, P., Fraldi, M., Fergola, L., Lirer, L. (2007). La distruzione di Oplontis: relazione fra le fasi dell'eruzione del 79 d.C. e i danni rilevati nella villa di Poppea. Quaderno di studi Pompeiani.

Osanna, M., Santaniello, E., De Nicola, V., Camardo, D., Notomista, M. (2017). Rivista di Studi Pompeiani, XXVIII, Interventi di manutenzione e messa in sicurezza del complesso archeologico di Villa Sora (NA), Roma, «L'ERMA» di BRETSCHNEIDER. 161−163.

Pagano, M. (2000). Gli antichi ercolanesi. Antropologia, società, economia. Guida alla mostra. Electa, Milano.

Pagano, M. (2003a). Gli scheletri dei fuggiaschi: l'indagine archeologica dalle prime scoperte alle indagini interdisciplinari sui fornici 4 e 12. In A. d'Ambrosio, Guzzo, P.G. & Mastroroberto, M. (eds): Storie da un'eruzione. Pompei, Ercolano, Oplontis, pp. 124−126. Mondadori Electa, Milano.

Pagano, M. (2003b). L'apodyterium delle Terme del Foro, settore maschile. In d'Ambrosio, A., Guzzo, P.G., & Mastroroberto, M. (eds): Storie da un'eruzione. Pompei, Ercolano, Oplontis, pp. 120−121. Mondadori Electa, Milano.

Paolillo, A. et al. (2016). Volcanology of the Southwestern sector of Vesuvius volcano, Italy. Journal of Maps 12, 425–440.

Pearce, J.A. (1996). A users guide to basalt discrimination diagrams. In: Wyman, D.A. (ed), Trace Element Geochemistry of Volcanic Rocks: Applications for Massive Sulphide Exploration. Geological Association of Canada, Short Course Notes 12, 79−113.

Peccerillo, A. (2017). Cenozoic volcanism in the Tyrrhenian Sea region. Advances in Volcanology Vol. 399. Springer, Heidelberg, 399 pp.

Pensa A., Cas R., Giordano G., Porreca M., Wallenstein N. (2015). Transition from steady to unsteady Plinian eruption column: the VEI 5, 4.6 ka Fogo A Plinian eruption, São Miguel, Azores. J. of Volcanol. Geother. Res., 305, 1-18.

Perrotta, A., Scarpati, C. (2003). Volume partition between the Plinian and co−ignimbrite air fall deposits of the Campanian Ignimbrite eruption. Miner. Petrol. 79, 67–78.

Perrotta, A., Scarpati, C., Giacomelli, L., Capozzi, A.R. (1996). Proximal depositional facies from a caldera forming eruption: The Parata Grande Tuff at Ventotene island (Italy). J. Volcanol. Geotherm. Res., 71: 207−228.

Petrone, P. (2002). Le vittime dell'eruzione. In Petrone P., & Fedele F. (eds): Vesuvio 79 A.D. Vita e morte ad Ercolano, pp. 35–45. Fridericiana Editrice Universitaria, Napoli.

Petrone, P. (2011a). Human corpses as time capsules: new perspectives in the study of past mass disasters. J. Anthropol. Sci., 89: 1–4.

Petrone, P., Giordano, G., Vezzoli, E., Pensa, A., Castaldo, G., Graziano, V., Sirano, F., Capasso, E., Quaremba, E., Vona, A., Miano, M.G., Savino, S., Niola, M. (2020). Preservation of neurons in an AD 79 vitrified human brain. Plos One 15(10): e0240017.

Petrone, P., Pucci, P., Vergara, A., Amoresano, A., Birolo, L., Pane, F., Sirano, F., Niola, M., Buccelli, C., Graziano, V. (2018). A hypothesis of sudden body fluid vaporization in the 79 AD victims of Vesuvius. PLoS One 13(9): e0203210.

Pittari, A., Cas, R.A.F., Edgar, C.J., Nichols, H.J., Wolff, J.A., Marti, J. (2006). The influence of palaeotopography on facies architecture and pyroclastic flow processes of a lithic-rich ignimbrite in a high gradient setting: the Abrigo ignimbrite, Tenerife, Canary Islands. J. Volcanol. Geotherm. Res. 152:273–315

Potapov, A.V., Campbell, C.S. (1997). Computer simulation of shear-induced particle attrition. Powder Technol. 94, 109–122.

Rittmann, A. (1950). L'eruzione Vesuviana del 79, studio magmatologico e vulcanologico. Pompeiana, 1950: 456−474.

Rittmann, A. (1964). Vulkanismus und Tektonik des Ätna. Geologische Rundschau 53: 788-800.

Rittmann, A. (1967). I vulcani e la loro attività. Cappelli, Firenze, 1–359.

Roche, O., Azzaoui, N., Guillin, A. (2021). Discharge rate of explosive volcanic eruption controls runout distance of pyroclastic density currents. Earth Planet Sci Lett 568:117017.

Rolandi, G., Barrella, A.M., Borrelli, A. (1993c). The 1631 eruption of Vesuvius. J. Volcanol Geotherm. Res. 58, 183–201.

Rolandi, G., Petrosino, P., McGeehin, J. (1998). The interplinian activity at Somma-Vesuvius in the last 3500 years. J. Volcanol. Geotherm. Res. 82, 19–52.

Rolandi, G., Munno, R., e Postiglione, I. (2003). "The A.D. 472 eruption of the Somma volcano", Journal of Volcanology and Geothermal Research, vol. 129, 291 – 319.

Rosi, M., Sbrana, A. (Eds.). (1987). Phlegrean fields (Vol. 9). CNR, Quad. Ric. Sci., 114 (9), 175 pp.

Rosi, M., Principe, C., Vecci, R. (1993). The 1631 Vesuvius eruption. A reconstruction based on historical and stratigraphical data. Journal of Volcanology and Geothermal Research, 58(1–4), 151–182.

Ruffo, F. (2011). L'insula sud−occidentale del cosiddetto 'impianto urbano' di Stabiae. Nuovi dati dalla recente campagna di scavo (2009). Oebalus. Studi sulla Campania nell'antichità, 177−239

Ruggiero, M. (1885). Storia degli scavi di Ercolano ricomposta su' documenti superstiti. Napoli.

Rutarindwa, R., Spiller, E.T., Bevilacqua, A., Bursik, M.I., Patra, A.K. (2019). Dynamic probabilistic hazard mapping in the Long Valley Volcanic Region CA: integrating vent opening maps and statistical surrogates of physical models of pyroclastic density currents J. Geophys. Res. Solid Earth, 124, 9600-9621.

Santacroce, R. (1987). Somma Vesuvius. CNR, Quad. Ric. Sci., 114 (8), 220 pp.

Santacroce, R., Cioni, R., Marianelli, P., Sbrana, A., Sulpizio, R., Zanchetta, G., Joron, J. L. (2008). Age and whole rock–glass compositions of proximal pyroclastics from the major explosive eruptions of Somma−Vesuvius: A review as a tool for distal tephrostratigraphy. Journal of Volcanology and Geothermal Research, 177, 1–18.

Santacroce, R., Sbrana, A. (2003). Carta geologica del Vesuvio. Scala 1:15,000. Progetto CARG. Servizio Geologico Nazionale – Consiglio Nazionale delle Ricerche. Firenze. S.E.L.C.A.

Sbrana, A., Cioni, R., Marianelli, P., Sulpizio, R., Andronico, D., Pasquini, G. (2020). Volcanic evolution of the Somma−Vesuvius Complex (Italy). Journal of Maps:1–11.

Sbrana, A., Marianelli, P., & Pasquini, G. (2018). Volcanology of Ischia (Italy). Journal of Maps, 14(2), 494–503.

Scaillet, B., Pinchvant, M., Cioni, R. (2008). Upward migration of Vesuvius magma chamber over the past 20,000 years. Nature, 455, 216−220

Scandone, R. (1990). Chaotic collapse of calderas. J Volcanol Geotherm Res 42 :285–302

Scandone, R., Giacomelli, L., Rosi, M. (2019). Death, survival and damage during the 79 AD eruption of Vesuvius which destroyed Pompeii and Herculaneum. J. Res. and Didact in Geogr., 5−30.

Scarpati, C., Perrotta, A., 2021. Report to PAP.

Scarpati, C., Perrotta, A., De Simone, G. F. (2016). "Impact of explosive volcanic eruptions around Vesuvius: a story of resilience in Roman time", Bulletin of Volcanology, vol. 78, 21.

Scarpati, C., Perrotta, A., Martellone, A., Osanna, M. (2020). Pompeian hiatuses: new stratigraphic data highlight pauses in the course of the AD 79 eruption at Pompeii. Geol. Mag. 157, 695−700.

Scarpati, C., Sparice, D., Perrotta, A. (2014). A crystal concentration method for calculating ignimbrite volume from distal ash−fall deposits and a reappraisal of the magnitude of the Campanian Ignimbrite. Journal of Volcanology and Geothermal Research 280, 67−75.

Scott, W.E., Hoblitt, R.P., Torres, R.C., Self, S., Martinez, M.L., Nillos, T.J. (1996). Pyroclastic flows of the June 15 1991, climactic eruption of Mount Pinatubo. In: Newhall, C.G., Punongbayan, S. (eds) Fire and mud: eruptions of Pinatubo, Philippines. Philippine Institute of Volcanology and Seismology, Quenzen City. University of Washington Press, Seattle, pp 545–570

Self, S., Sparks, R.S.J. (1978). Characteristics of widespread pyroclastic deposits formed by the interaction of silicic magma and water. Bull. Volcanol. 41, 196-212.

Sevink, J., Bergen, M., Plicht, J., Feiken, H., Anastasia, C., & Huizinga, A. (2011). Robust date for the Bronze Age Avellino eruption (Somma−Vesuvius): 3945±10 calBP (1995±10 calBC). Quaternary Science Reviews, 30.

Shea, T., Gurioli, L., Houghton, B. F., Cioni, R. & Cashman, K. V. (2011). Column collapse and generation of pyroclastic density currents during the A.D. 79 eruption of Vesuvius: The role of pyroclast density. Geology 39, 695-698.

Shea, T., Hellebrand, E., Gurioli, L., Tuffen, H. (2014). Conduit− to Localized−scale Degassing during Plinian Eruptions: Insights from Major Element and Volatile (Cl and H2O) Analyses within Vesuvius AD 79 Pumice. Journal of Petrology 55, 315−344.

Shea, T., Larsen, J.F., Gurioli, L., Hammer, J.E., Houghton, B.F., Cioni, R. (2009). Leucite crystals: Surviving witnesses of magmatic processes preceding the 79 AD eruption at Vesuvius, Italy. Earth and Planetary Science Letters 281, 88−89.

Sheridan, M.F., Barberi, F., Rosi, M. and Santacroce, R. (1981). A model for Plinian eruption of Vesuvius. Nature 289: 282−285.

Sheridan, M.F., Updike, R.G. (1975). Sugarloaf Mountain Tephra – A Pleistocene rhyolitic deposit of base−surge origin in northern Arizona. Geol. Soc Am. Bull., 86: 571−581.

Sheridan, M.F., Wohletz, K.H. (1981). Hydrovolcanic explosions: the systematics of water-tephra equilibration. Science 212: 1387-1389.

Shmidt, C.W., Oakley, E., D'Anastasio, R., Brower, R., Remy, A., Viciano, J. (2015). Herculaneum In: Schmidt, C.W., Symes, S.A. editors. The analysis of burned human remains. Academic Press; pp. 149–161.

Sigurdsson, H., Carey, S., Cornell, W., Pescatore, T. (1985). The eruption of Vesuvius in 79 AD**.** Nat. Geo. Res., 1, 332−387.

Sigurdsson, H., Cashdollar, S., Sparks, R.S.J. (1982). The eruption of Vesuvius in AD 79: Reconstruction from historical and volcanological evidence, Am. J. Archaeol., 86, 39– 51.

Sigurdsson, H., Cornell, W., Carey, S. (1987). Dynamics of magma withdrawal during the 79 A.D. eruption of Vesuvius. EOS 68, 16:434.

Sigurdsson, H., Cornell, W., Carey, S. (1990). Influence of magma withdrawal on compositional gradients during the 79 A.D. Vesuvius eruption. Nature, 345, 519-521.

Silleni, A., Giordano, G., Isaia, R., Ort, M.H. (2020). Magnitude of the 39.8 ka Campanian Ignimbrite Eruption, Italy: method, uncertainties and errors. Front. Earth Sci. 8, 444.

Smith, C. M., Thompson, G., Reader, S., Behnke, S. A., McNutt, S. R., Thomas, R., & Edens, H. (2020). Examining the statistical relationships between volcanic seismic, infrasound, and electrical signals: A case study of Sakurajima volcano, 2015. Journal of Volcanology and Geothermal Research, 402, 16996.

Sohn, Y.K., Chough, S.K. (1989). Depositional processes of the Suwolbong tuff ring, Cheju Island (Korea). Sedimentology 37:1115−1135.

Sparice, D., Scarpati, C., Mazzeo, C.F., Petrosino, P., Arienzo, I., Gisbert, G., Petrelli, M. (2017). New proximal tephras at Somma−Vesuvius: evidence of a pre−caldera, large (?), explosive eruption. Journal of volcanology and Geothermal Research 335, 71−81.

Sparks, R.S.J., Gardeweg, M.C., Calder, E.S., Matthews, S. J. (1997). Erosion by pyroclastic flows on Lascar volcano. Chile. Bull. Volcanol. 58, 557−565.

Sparks, R.S.J., Self, S., Walker, G.P.L. (1973). Products of ignimbrite eruptions. Geology 1:115−118.

Sparks, R.S.J., Sigurdsson, H., Wilson, L. (1977). Magma mixing: a mechanism of triggering acid explosive eruptions. Nature 267, 315-318.

Sparks, R.S.J., Walker, G.P.L. (1973). The ground surge deposit: a third type of pyroclastic rock. Nature 241: 62−64.

Sparks, R.S.J., Walker, G.P.L. (1977). The significance of vitric−enriched air−fall ashes associated with crystal−enriched ignimbrites. J. Volcanol. Geotherm. Res. 2, 329–341.

Sparks, R.S.J., Wilson, G.P.L. (1976). A model for the formation of ignimbrite by gravitational column collapse. J. Geol. Soc. Lond. 132, 441-452.

Spiller, E.T., Bayarri, M.J., Berger, J.O., Calder, E.S., Patra, A.K., Pitman, E.B., Wolpert, R.L. (2014). Automating emulator construction for geophysical hazard maps SIAM/ASA. J Uncertain Quantif 2:126–152.

Stefani, G. (2010). Uno alla volta. 3. I calchi, pp. 1–16. Mondadori Electa S.p.A., Milano.

Stothers, R. B., & Rampino, M. R. (1983). Volcanic eruptions in the Mediterranean before A.D. 630 from written and archaeological sources. Journal of Geophysical Research 88(B8), 6357–6371.

Streck, M.J., Grunder, A.L. (1995). Crystallization and welding variations in a widespread ignimbrite sheet; the Rattlesnake Tuff, eastern Oregon, USA. Bull. Volcanol. 57 (3), 151–169.

Sulpizio, R., Bonasia, R., Dellino, P., Mele, D., Di Vito, M. A., & La Volpe, L. (2010a). The Pomici di Avellino eruption of Somma−Vesuvius (3.9 ka BP). Part II: Sedimentology and physical volcanology of pyroclastic density current deposits. Bulletin of Volcanology, 72, 559–577.

Sulpizio, R., Cioni, R., Di Vito, M. A., Mele, D., Bonasia, R., & Dellino, P. (2010b). The Pomici di Avellino eruption of Somma−Vesuvius (3.9 ka BP). Part I: Stratigraphy, compositional variability and eruptive dynamics. Bulletin of Volcanology, 72, 539–558.

Sulpizio, R., Dellino, P. (2008). Sedimentology, depositional mechanisms and pulsating behaviour of pyroclastic density currents. In: Gottsman, J., Marti, J. (eds). Calderas volcanism: analysis, modelling and response. Devel Volcanol 10: 57–96.

Sulpizio, R., Dellino, P., Doronzo, D.M., Sarocchi, D. (2014). Pyroclastic density currents: state of the art and perspectives. J. Volcanol. Geotherm. Res. 283, 36–65.

Sulpizio, R., De Rosa, R., Donato, P., (2008a). The influence of variable topography on the depositional behaviour of pyroclastic density currents: the examples of the Upper Pollara eruption (the island of Salina, southern Italy). Journal of Volcanology and Geothermal Research 175, 367–385.

Sulpizio, R., Mele, D., Dellino, P., La Volpe, L. (2005). A complex, subplinian−type eruption from low−viscosity, phonolitic to tephri−phonolitic magma: The AD 472 (Pollena) eruption of Somma−Vesuvius, Italy. Bulletin of Volcanology, 67, 743–767.

Sulpizio, R., Mele, D., Dellino, P., La Volpe, L. (2007). Deposits and physical properties of pyroclastic density currents during complex subplinian eruptions: the AD 472 (Pollena) eruption of Somma–Vesuvius, Italy. Sedimentology 54:607–635.

Tadini, A., Bevilacqua, A., Neri, A., Cioni, R., Biagioli, G., de' Michieli Vitturi, M., and Esposti Ongaro, T. (2021). Reproducing pyroclastic density current deposits of the 79 CE eruption of the Somma–Vesuvius volcano using the box-model approach, Solid Earth, 12, 119–139.

Talbot, J.P., Self, S. & Wilson, C.J.N. (1994). Dilute gravity current and rain-flushed ash deposits in the 1.8 ka Hatepe Plinian deposit, Taupo, New Zealand. Bull Volcanol **56**, 538–551.

Todesco, M., Neri, A., Esposti, Ongaro T., Papale, P., Macedonio, G., Santacroce, R., Longo, A. (2002). Pyroclastic flow hazard assessment at Vesuvius (Italy) by using numerical models. I. Large−scale dynamics. Bull. Volcanol. 64, 155–177.

Toniolo, L., Amoretti, V., Gravina, E., Martinelli, R., Scala, P., Sparice, D. (2021). Da Mumia alle ultime vittime di Pompei: nuove ricerche nella villa di Civita Giuliana. Rivist. Studi Pomp. XXXII, 123–130.

Valente, F., Cruz, J.V., Pimentel, A., Coutinho, R., Andrade, C., Nemésio, J., Cordeiro, S. (2022). Evaluating the Impact of Explosive Volcanic Eruptions on a Groundwater−Fed Water Supply System: An Exploratory Study in Ponta Delgada, São Miguel (Azores, Portugal). Water, 14, 1022.

Valentine, G.A. (1987). Stratified flow in pyroclastic surges. Bull Volcanol 49:616–630.

Vrolijk, P.J., Southard, J.B. (1998). Experiments on rapid deposition of sand from high-velocity flows. Geosci Can 24:45–54

Walker, G.P.L. (1971). "Grain−size characteristics of pyroclastic deposits", Journal of Geology 79, 696 – 714.

Walker, G.P.L. (1972). Crystal concentration in ignimbrites. Contrib. Mineral. Petrol. 36, 135–146.

Walker, G.P.L. (1973). Explosive volcanic eruptions —a new classification scheme. Geol. Rundsch. 62, 431–446.

Walker, G.P.L. (1983). Ignimbrite types and ignimbrite problems. J. Volcanol. Geotherm. Res. 17 (1–4), 65–88.

Walker, G.P.L. (1984). Downsag calderas, ring faults, caldera sizes and incremental caldera growth. J Geophys Res 89:8407–8416.

Walker, G.P.L. (1985). Origin of coarse lithic breccias near ignimbrite source vents. J Volcanol Geotherm Res 25:157–171

Walker, G.P.L., Heming, R.F., Wilson, C.J.N. (1980). Low−aspect ratio ignimbrites. Nature 283 (5744), 286–287.

Walker, G.P.L., Wilson, C.J.N., Froggatt, P.C. (1981b). An ignimbrite veneer deposit: the trail−marker of a pyroclastic flow. J. Volcanol. Geotherm. Res., 9(4): 409−421.

Warme, J.E., Morgan, M., Kuehner, H.-C. (2002). Impact-generated carbonate accretionary lapilli in the Late Devonian Alamo Breccia, in Koeberl, C., and Macleod, K.G., eds., Catastrophic Events and Mass Extinctions: Impacts and Beyond: Geological Society of America Special Paper 356, 489–504.

Williams, H., McBirney, A.R. (1979). Volcanology. Freeman, San Francisco, 1–396.

Wilson, C.J.N. & Hildreth, W. (1997). The Bishop Tuff: new insights from eruptive stratigraphy. Journal of Geology 105, 407-439.

Wilson, C.J.N., Walker, G.P.L. (1982). Ignimbrite depositional facies: the anatomy of a pyroclastic flow. J. Geol. Soc. Lond. 139 (5), 581–592.

Wilson, C.J.N., Walker, G.P.L. (1985). The Taupo eruption, New Zealand: II. The Taupo Ignimbrite. Phil Trans Roy Soc London, Series A—Math Phys Eng Sci 314:229–310

Wilson, L. (1976). Explosive volcanic eruptions – III. Plinian eruption columns. J. Geophys. Res. Astr. Soc. 45, 543-556.

Wilson, L., Sparks, R.S.J., Huang, T.C., Watkins, N.D. (1978). The control of eruption column heights by eruption energetics and dynamics. J. Geophys. Res. 83, 1829-1836.

Wilson, L., Sparks, R.S.J., Walker, G.P. (1980). Explosive volcanic eruptions—IV. The control of magma properties and conduit geometry on eruption column behaviour. Geophys. J. Int. 63 (1), 117–148.

Wohletz, K., Sheridan, M.F. (1979). A model for pyroclastic surge. Geol. Soc. Am., Special Paper 180.

Wolff, J.A., Storey, M. (1984). Zoning in highly alkaline magma bodies. Geol Mag 121:563-575.

Zanella, E., Gurioli, L., Pareschi, M.T., Lanza, R. (2007). Influences of urban fabric on pyroclastic density currents at Pompeii (Italy), part II: temperature of the deposits and hazard implications. J.Geophys. Res. 112:B05214.

ACKNOWLEDGEMENTS

This PhD thesis would not have been possible without the unwavering help, advice and support of many people from my colleagues, family, partner and friends to different institutions participating and cooperating in my PhD, making it a reality. Firstly, I would like to thank you my supervisor Claudio Scarpati and co-supervisor Lorenzo Fedele, for believing in me and supporting me throughout the past three years. I could learn so much from both of them as inspirational scientists and mentors. I extend a huge thank you to the volcanologist Annamaria Perrotta who highly helped with her enthusiasm and dedication to achieve the results shown in this research. I thank you both the reviewers who provided useful suggestions and constructive comments to improve the quality of the work, making the thesis more enjoyable for readers. I thank you the volcanologists and professors Paul Cole and Mike Branney for their interest in the present research. What great and inspiring conversations with the professor Mike Branney!

I am so grateful for the fieldwork opportunities. Thanks to the DiSTAR-PAP agreement to study volcanological aspects of new Pompei excavations, with special thanks to PAP staff and all the archaeologists involved in the recent excavations from Torre del Greco to Civita Giuliana to Pompei to the Roman villae of Stabia, who we shared the thrill of unearthing amazing findings. A special thank to the current director of the archaeological park of Pompeii, Gabriel Zuchtriegel and Massimo Osanna (director of the park until 2020). I also thank Stefano Donati, the director of the Vesuvius National Park, its president Agostino Casillo and the thecnical office Pasquale Giugliano, for his logistic help to access to some quarries around the volcano. It is worth of note the fundamental contribution of all the people that kindly allowed us to study the AD 79 eruption on their private property, making accessible, available and sharable spectacular pyroclastic sequences of this eruption and enabling us to fieldwork even for several days in their properties: Ferdinando, owner of some hectares of land within the inactive Pollena Quarry, Gennaro, the owner of Villa Elena at Ottaviano site, Eugenio Carraturo, owner of the horse riding centre at Ottaviano site, Ranieri and Vitiello, owners of the Ranieri quarry and Pozzelle quarry, respectively at Terzigno, Sorrentino's family, owner of the large vineyard at Boscotrecase site.

Huge thanks to everyone at the DiSTAR who made the department such a good place to be and helped me throughout the PhD with special thanks to Enrico di Clemente, Mauro la Manna, Carlo Donadio, Luigi Franciosi for their support with laboratory facilities and sedimentological analyses. I am so grateful for the bachelor thesis students Alessia Palombella, Luigi Rea and Roberta Coccorese together with bachelor trainee students Domenico Imparato and Vittorio di

Giovanni who worked with me during their bachelor and undergraduate studies, respectively, contributing valuable data and discussion to my project.